D i s s e r t a t i o n

Improving the Nutritional Quality of Food and Feed by Manipulation of Iron Storage in Plants

zur Erlangung des akademischen Grades

d o c t o r r e r u m n a t u r a l i u m

(Dr. rer. nat.)

im Fach Biologie eingereicht an der

Lebenswissenschaftlichen Fakultät
der Humboldt-Universität zu Berlin

von

M.Sc. Zahra Ghalamkari

Dekan der Lebenswissenschaftlichen Fakultät
Prof. Dr. Bernhard Grimm

Gutachter/innen: 1. Prof. Dr. Thomas J Buckhout
2. Prof. Dr. Simonetta Santi
3. Prof. Dr. Kurt Zoglauer

Tag der Einreichung: 08.02.2019
Tag der mündlichen Prüfung: 16.08.2019

Zusammenfassung

Eisen (Fe) liegt an vierter Stelle in der Fülle von Elementen in der Erdkruste, aber Fe-Mangel ist ein weit verbreitetes Problem bei Pflanzen und Tieren, da die Fe-Oxide unlöslich sind. Fe-Mangel führt zu einer Verringerung der Pflanzenproduktivität und am deutlichsten zu einer erhöhten Fe-induzierten Anämie beim Menschen. Es wurde angenommen, dass die Biofortifizierung von Fe ein praktischer Ansatz zur Verbesserung der Nährstoffqualität in Pflanzen und damit auch in Lebensmitteln oder Tierfutter ist. In dieser Arbeit wurden neue Strategien zur Erhöhung des Fe-Gehalts in der Modellpflanze Arabidopsis getestet. Vakuoläre Fe-Transportgene der *VTL*-Familie (*VIT1*-like) wurden in Kombination mit dem neu entdeckten Fe-Regulierungsprotein IMA1 (IronMan1) oder dem Fe-Bindungspeptid NAS3 überexprimiert. Die Überexpression jedes der fünf *VTL*-Gene (*VTL1 - 5*) führte in Arabidopsis-Samen zu einem 2- bis 3-fach erhöhten Fe-Gehalt. Der Fe-Gehalt in anderen Organen war jedoch nicht signifikant verändert. Eine Expressionsanalyse von Genen, die an der Fe-Aufnahme und -Homöostase beteiligt sind, zeigte eine erhöhte Expression in Keimlingen von optimal mit Eisen versorgten Pflanzen und eine verringerte Expression in Pflanzen unter Eisenmangel. Diese Ergebnisse wurden als Hinweis auf eine Resistenz gegen Fe-Mangel in Fe-defizienten Pflanzen und eine erhöhte Sinkstärke für Fe in ausreichend mit Fe versorgten Pflanzen interpretiert. Fe wurde durch Perls-Färbung sichtbar gemacht und es wurde festgestellt, dass es um die provaskulären Bündel im Embryo herum lokalisiert war. Es wurde bereits von anderen Forschenden nachgewiesen, dass *VIT1*, ein zusätzlicher vakuolärer Fe-Transporter, Fe in die provaskuläre Region des Embryos leitet. Daher wurde der prinzipielle Ort für die Fe-Speicherung im Embryo auch nach *VTL*-Überexpression durch das VIT1-Protein bestimmt.

IMA1 wurde stark unter Fe-Mangel induziert (Buckhout et al., 2009). Die Überexpression von *IMA*1 führte auch in optimal mit Fe versorgten Pflanzen zu einer Fe-Mangelreaktion. Der Fe-Gehalt war in Saatgut, Blättern, Wurzeln und Keimlingen von Arabidopsis um das Dreifache erhöht. Die Expression von Fe-Aufnahme- und Homöostase-Genen wurde unabhängig vom Fe-Angebot im Vergleich zum Wildtyp in überexprimierenden Pflanzen stark induziert. Diese Ergebnisse bestätigen die kürzlich veröffentlichten Ergebnisse von Gillet et al. (2018) und Hirayama et al. (2018). Die doppelte Überexpression jedes *VTL*-Gens mit *IMA1* führte zu erhöhtem Eisengehalt im Samen. Es wurde jedoch kein synergistischer Effekt auf den Fe-Gehalt beobachtet. Die Überexpression von *IMA1* korrelierte auch mit einer erhöhten Expression der *VTL*-Gene. Der Mangel an Synergien bei der Fe-Akkumulation zwischen IMA1 und den VTL-Genen war daher höchstwahrscheinlich auf die Induktion der *VTL*-Gene durch

IMA1 zurückzuführen. Der weitere Anstieg des Fe-Gehalts über den in den einzelnen überexprimierenden Linien bestimmten Wert wurde durch andere Faktoren begrenzt, die die Verfügbarkeit von Fe einschränkten.

Analysen von *NAS3* überexprimierenden Pflanzen zeigten, dass der Fe-Gehalt im Saatgut im Vergleich zum Wildtyp ungefähr um das Zweifache anstieg. In transgener Arabidopsis war unter der Doppelüberexprimierung von *NAS3* und *VTL5* der Fe-Gehalt im Samen im Vergleich zum Wildtyp erhöht. Es wurde jedoch kein synergistischer Effekt auf die Fe-Akkumulation zwischen den doppelt überexprimierenden Pflanzen beobachtet. Obwohl in den doppelt überexprimierenden Linien sowohl *VTL5* als auch *NAS3* stark überexprimiert waren, erhöhte sich der Nikotianamingehalt in Blättern im Vergleich zum Wildtyp nicht signifikant.

Zusammenfassend wurde gezeigt, dass die Überexpression von *VTL1*, *2*, *3*, *4* oder *5*, *IMA1* oder *NAS3* mit erhöhtem Eisengehalt im Samen korreliert. Die Expression der Gene für die Aufnahme von Fe und die Homöostase bestätigten den erhöhten Fe-Gehalt in diesen überexprimierenden Pflanzen. Die doppelte Überexpression der *VTL*-Gene in Kombination mit *IMA1* oder *NAS3* führte zu keinem weiteren Anstieg des Fe-Gehaltes, der wahrscheinlich durch die Regulation der *VTL*-Gene durch *IMA1*-Expression und den Mangel an erhöhtem Nicotianamin im Fall von *VTL5* / *NAS3*-Überexpressionpflanzen verursacht würde.

Zukünftige Forschung sollte der Übertragbarkeit dieser Ergebnisse auf Kulturpflanzen gewidmet sein.

Summary

Iron (Fe) ranks fourth in abundance of elements in the Earth's crust, but Fe deficiency is a widespread problem in plants and animals because of the insolubility of Fe oxides. Fe deficiency leads to reduce plant productivity and most significantly to enhanced Fe-induced anemia in humans. Fe biofortification has been suggested to be a practical approach for improving the nutritional quality in plants for food or fodder. In this work, we have tested new strategies for increasing Fe content in the model plant Arabidopsis. Vacuolar Fe transport genes of the VTL family (*VIT1*-like) were over-expressed in combination with the newly discovered Fe regulatory protein IMA1 (IronMan1) or the Fe-binding peptide NAS3. Over-expression of each of the five VTL genes (*VTL1 – 5*) led to an increased Fe content by 2- to 3-fold in Arabidopsis seeds; although, the Fe content in other organs was not significantly altered. An expression analysis of genes involved in Fe uptake and homeostasis demonstrated increased expression in seedlings of Fe-sufficient plants and a decreased expression in Fe-deficient plants. These results were interpreted as an indication for resistance to Fe deficiency in Fe-deficient plants and an increased sink strength for Fe in Fe-sufficient plants. Fe was visualized by Perls staining and found to be localized surrounding the provascular bundles in the embryo. VIT1, an additional vacuolar Fe transporter, has been shown by others to direct Fe to the provascular region of the embryo. Therefore, the principle location for Fe storage in the embryo was determined by the VIT1 protein even in VTL over-expression plants.

IMA1 was greatly induced under Fe deficiency. Over-expression of *IMA1* resulted in an Fe deficiency response also in Fe-sufficient plants. Fe content was increase by 3-fold in seed, leaves, roots and seedlings of Arabidopsis. The expression of Fe uptake and homeostasis genes was greatly induced in over-expressing plants independent of the Fe supply compared to the wild type. These results confirm the recently published results of Gillet et al. (2018) and Hirayama et al. (2018). Double over-expression of each of the VTL genes with *IMA1* resulted in increased seed Fe; however, no synergistic effect on Fe content was observed. Over-expression of *IMA1* also correlated with an increased expression of the VTL genes. Therefore, the lack of synergy in Fe accumulation between IMA1 and the VTLs was most likely due to induction of the VTL genes by *IMA1*. The further increase in Fe content beyond that determined in the single over-expressing lines was limited by other factors restricting Fe availability.

Analyses of *NAS3* OE plants showed that Fe content in seeds was increased approximately 2-fold compared to WT. In transgenic Arabidopsis doubly over-expressing *NAS3*/*VTL5* plants, seed Fe was increased compared to the wild-type but no synergistic effect on Fe accumulation

between in the double over-expressing plants was observed. Although in the doubly over-expressing lines both *VTL5* and *NAS3* were greatly over-expressed, the nicotianamine content in leaves was not significantly increased compared to the wild type.

In conclusion, we have demonstrated that single over-expression of *VTL1*, *2*, *3*, *4* or *5*, *IMA1* or *NAS3* correlated with increased seed Fe. Expression of Fe uptake and homeostasis genes confirmed the increased Fe content in these over-expressing plants. Double over-expression of the VTL genes in combination with IMA1 or NAS3 resulted in no further increase in Fe likely caused by the regulation of the VTL genes by IMA1 expression and the lack of increased nicotianamine in the case of VTL5/NAS3 over-expressing plants. Future research should be dedicated to extending these findings to crop plants.

Table of Contents

1 Abbreviations

A, C, G, T, U	Adenine, Cytosine, Guanine, Thymine, Uracil
AS	Amino acid
BPDS	Bathophenanthroline disulfonic acid
cDNA	complementary DNA
DNA	Deoxyribonucleic acid
EDTA	Ethylenediaminetetraacetic acid
Fe	Iron
Fw	forward
g	Gravitational constant
HEDTA	N-(hydroxyethyl) ethylenediaminetetraacetic acid
MES	2-(N-morpholino) ethanesulfonic acid
mRNA	Messenger RNA
OE	Over-expressed
PCR	Polymerase Chain Reaction
Rev	Reverse
RNA	Ribonucleic acid
RT	Room Temperature
Rpm	revolutions per minute
TRIS	Tris(hydroxymethyl)-aminomethane

v/v	Volume per total volume
w/v	Weight per unit volume
WT	Wild type
NA	nicotianamine
MA	mugineic acid
SAM	S-adenosyl-methionine

2 Introduction

Fe is an abundant element in soils and plays essential roles in plant growth and development. As a redox active metal, Fe is involved in numerous biochemical reactions such as porphyrin biosynthesis, conversion of chlorophyll a to b, nitrate reduction in nitrogen assimilation, respiration and photosynthesis (Briat et al. 2015). Plants require 10^{-6} to 10^{-5} M Fe for optimal growth. According the WHO (De Benoist, World Health Organization, and Centers for Disease Control and Prevention (U.S.) 2008)) Fe deficiency is one of the most prevalent nutritional diseases in the world with about 2 billion people suffering from Fe anemia. Since plants are an important source of human food, fortification of Fe in plants can be used to provide an adequate Fe source and alleviate Fe anemia. The goal of this thesis is to discover strategies to increase available Fe by genetic manipulation of Fe storage and transport.

2.1 Response of Plants to Fe Deficiency

In calcareous and alkaline soils Fe cannot be readily absorb by plant roots because it exists predominantly as insoluble ferric hydroxides. In dicotyledons and non-grass monocotyledons, Fe is acquired through a reduction-based mechanism (strategy I) with Fe^{2+} being the form of transported Fe. Grasses (Poales) have adopted a system in which secretion of high affinity Fe chelators of the mugineic acid family, referred to as phytosiderophores (PS), precedes the uptake of a Fe^{3+}-PS complex without prior reduction (strategy II; Schmidt and Buckhout, 2011; Jeong et al., 2017; Kobayashi and Nishizawa, 2012; Römheld and Marschner, 1986). The two mechanisms of Fe uptake are summarized in Fig. 1.

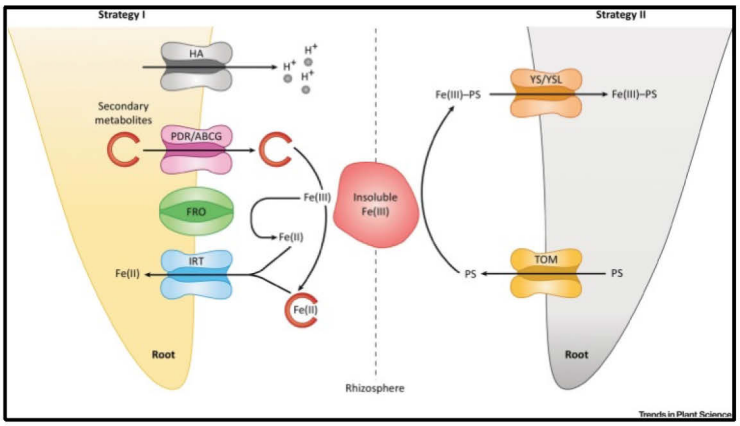

Fig. 1. Response to Fe deficiency in plants. Reduction-based Fe uptake (strategy I) is illustrated on the left of the figure and found in dicotyledon and non-grass plants. Chelate-based Fe uptake (strategy II) is found in grasses and illustrated on the right side of the figure. Adapted from Tsai and Schmidt (2017).

2.1.1 Reduction-Base Fe Uptake

Fe uptake from the rhizosphere is accomplished both by direct transport of Fe^{2+} following separation from or bound to a chelator. These two mechanisms are commonly referred to as strategy I and II, respectively. Chaney et al. (1972) provided the first demonstration that separation and absorption of Fe from Fe^{3+}-chelates required reduction prior to uptake of Fe^{2+} by the root. The reaction of strategy I plants to Fe deficiency involves four general responses: acidification of the rhizosphere, increased Fe^{3+}-chelate reduction, uptake of Fe^{2+} at the root surface and increased synthesis and secretion of phenolics. The molecular mechanisms behind these responses are well characterized. In the best-studied strategy I plant *Arabidopsis*, Fe reduction and uptake are dramatically increased in roots growing in Fe-deficient media. Ferric-chelate reduction is catalyzed by a flavocytochrome FRO2, a plasma membrane NADPH-oxidase that transports electrons across membranes (Robinson et al., 1999). The principle Fe^{2+} transporter involved is IRT1 that was discovered more than two decades ago and demonstrated to be the predominant transporter for high-affinity Fe uptake under Fe deficiency (Eide et al., 1996; Vert et al., 2002). IRT1 is the founding member of the 15-member ZIP family (ZRT, IRT-like Protein), and IRT1 and IRT3 catalyze transport of Fe^{2+} across the root plasma membrane (Lin et al., 2009; Milner et al., 2013; Socha and Guerinot, 2014; Vert et al., 2002).

Rhizosphere acidification is the result of H^+ transport *via* the plasma membrane P-type ATPase, AHA2, which leads to protonation and solubilization of Fe oxyhydrates (Dell'Orto et al., 2000; Santi and Schmidt, 2009). Rhizosphere acidification greatly increases the free Fe^{3+} activity in the vicinity of the roots. The increase in acidification is at least in part due to increased transcription of *AHA2* (Santi and Schmidt, 2009).

Most recently the role of coumarins in mobilizing Fe as a response to Fe deficiency has been elucidated (Fourcroy et al., 2014; Schmid et al., 2014; Rodríguez-Celma et al., 2013). Secretion of phenolics has long been recognized as a response to Fe deficiency; although, the role they played in Fe uptake by roots has remained controversial. In a seminal contribution to establishing the role phenolics might played in Fe nutrition, Jin et al. (2007) showed that secretion of phenolics by Fe-deficient roots improved the Fe nutritional status of *Trifolium* by enhancing utilization of external Fe. In Arabidopsis the coumarins responsible for the enhancement of Fe utilization were shown to be fraxetin and sideretin (Rajniak et al., 2018), and evidence from independent sources indicated that secretion of molecular reductants was likely widespread in strategy I plants (Clemens and Weber, 2016; Rajniak et al., 2018). These four reactions define the physiological response to strategy I plants to Fe deficiency.

2.1.2 Chelate-based Fe Uptake

Grasses respond to Fe deficiency by synthesis and secretion of phytosiderophores (PSs) of the mugineic acid (MA) family (Takemoto et al., 1978; Takagi et al., 1984). MA is synthesized from the nonproteinogenic amino acid nicotianamine (NA) that is itself synthesized from three molecules of S-adenosyl-methionine (SAM) by the enzyme NA synthase (Suzuki et al., 2006; Herbik et al., 1999). NA is found in all plants regardless of Fe uptake strategy, but the biosynthetic pathway leading to DMA formation is unique to grasses. Under Fe deficiency the expression of the genes encoding enzymes that synthesize SAM, the NA synthase and the genes encoding enzymes needed for DMA synthesis are coordinately regulated and highly induced (Koayashi et al., 2005; Kobayashi and Nishizawa, 2012).

In rice MA efflux is catalyzed by the Major Facilitator Superfamily (MFS) transporter, TOM1 with the expression of *TOM1* in roots is highest in the night preceding the peak of phytosiderophore secretion (Nozoye et al., 2011). Fe uptake in grasses is predominantly in the form of a Fe^{3+}-PS chelate. The yellow stripe mutant (*ys1*) was instrumental in the identification of the Fe^{3+}-PS transporter in maize. The *ys1* mutant synthesizes and secretes PSs but lacks Fe^{3+}-PS uptake (von Wirén et al., 1994). The uptake of Fe^{3+}-PS is catalyzed by the Yellow-Stripe1 (YS1) transporter (Curie et al., 2001), which belongs to the YS1-like (YSL) family of membrane transporters (Curie et al., 2009). In rice the Fe^{3+}-deoxymugineic acid chelate is taken up by the YSL15 oligopeptide transporter (reviewed by Connorton et al., 2017). In addition to Fe uptake, YSL transporters play a critical role in cellular and the long distance transport of Fe-, Zn- and Cu-NA chelates throughout the plant (Curie et al. 2009).

2.2 Regulators of iron homeostasis

2.2.1 The FIT and PYE Transcriptional Pathways

FIT (FER-like Iron deficiency-induced Transcription factor, AtbHLH29) is a transcriptional factor that is expressed in roots and is up-regulated in Fe-deficient Arabidopsis plants. Microarray analysis shows that the expression of 72 - 179 Fe deficiency responsive genes was depend on FIT and that all key steps in reduction-based Fe acquisition including Fe^{3+}-chelate reduction, Fe^{2+} uptake, H^+ extrusion and coumarin synthesis were regulated by FIT (Yuan et al., 2005; Colangelo and Guerinot, 2004; Ivanov et al., 2012). The regulation of these target genes required the heterodimerization of FIT to the subgroup Ib bHLH factors bHLH38, bHLH39, bHLH100 or bHLH101 (Yuan et al. 2008; Sivitz et al., 2012; Wang et al., 2013). MYB10 and MYB72 belong to the MYB family with 126 members and were shown to be up regulated in Fe-deficient plants in a FIT-dependent manner (Palmer et al., 2013). MYB72 is a

positive regulator and is required, among others, for induction of *NAS2* and *NAS4* expression in the root.

The bHLH subgroup IVc members, bHLH34, 104, 105, 115 and PYE, regulate the Fe-deficiency response. The transcription of *FIT* is activated by three of these bHLH transcription factors, bHLH34, bHLH104 and bHLH105 (ILR3) (Zhang et al. 2015; Li et al., 2016). These three transcription factors referred to as PYE-like, interact directly with POPEYE (PYE) and induce *PYE* transcription. PYE was shown to regulate a subset of genes not overlapping with the FIT regulon (Long et al., 2010; Schmidt and, Buckhout 2011). PYE was induced in roots that were grown at low Fe concentration (Long et al. 2010) and has been proposed to regulate the mobilization and translocation of Fe to the shoots (Ivanov et al., 2012). PYE is a negative regulator of *NAS4*, *FRO3* and *ZIF1* by direct interaction with the promoters of these genes. ILR3-bHLH104 dimer was shown to bind to the PYE promoter and thereby regulated Fe hemostasis (Zhang et al. 2015).

2.2.2 Sensing the Cellular Fe Concentration

BRUTUS (BTS) and HEMERYTHRIN MOTIF-CONTAINING REALLY INTERESTING NEW GENE (RING)-AND ZINC-FINGER PROTEIN1 (HRZ1) in Arabidopsis and rice, respectively, likely sensing the cytosolic Fe concentration (Selote et al., 2015; Kobayashi et al., 2013). Both BTS and HRZ contain three hemerythrin domains at the N-terminus and at the C-terminus three Zn finger domains and conserved His-xxx-Glu motifs likely acting as di-Fe centers. The C-terminal domain has 45% homology to plant and mammalian E3 ligases that target transcription factors for ubiquitination and subsequent turnover. Interestingly, BTS was found to interact with selected bHLH proteins. The abundance of PYE-like proteins but not PYE was likely regulated by the Fe-binding hemerythrin (HHE) domain-containing E3 ligase BRUTUS (BTS) in a proteasomal-dependent manner (Long et al., 2010; Selote et al., 2015; Li et al., 2016; Zhang et al. 2015).

BTS was strongly expressed in the stele in Fe-deficient plants and acted as a negative regulator of Fe homeostasis in the presence of Fe (Ivanov et al. 2012) and suppressed positive regulator transcription factors such as bHLH104, bHLH115 and ILR3 (Hindt et al., 2017a). García et al. (2018) recent demonstrated that two BTS paralogs, BTSL1 and BTSL2, were also negative regulators in Fe deficiency responses. Loss of function of this genes increased tolerance to Fe deficiency, and all Fe responsive genes were induced with the exception of *IMA1* and At3g56360, which have been shown to be important in Fe acquisition and cellular homeostasis of Fe (Grillet et al. 2018; Hindt et al., 2017b). Rice orthologues of BTS, HRZ1 and HRZ2, have

been shown to negatively regulate Fe deficiency responses via IRO2 and IRO3, the rice orthologs of bHLH38/ bHLH39 and PYE, respectively (Ogo et al., 2006; Zheng et al., 2010; Kobayashi et al., 2013; Kobayashi and Nishizawa 2012), indicating that the Fe signaling cascade was at least partly conserved among the two different strategies.

In grass plants, the cellular concentration of Fe may also be directly sense by IRON DEFICIENCY-RESPONSIVE ELEMENT-BINDING FACTOR1 (IDEF1). IDEF1 is a grass-specific transcription factor that positively regulates various genes involved in Fe uptake and translocation (Kobayashi and Nishizawa, 2012). Paradoxically, *IDEF1* transcription was not induced in response to Fe deficiency but possessed histidine-aspartate repeats and proline-rich regions that bind Fe^{2+} (Kobayashi et al., 2012). The Fe-binding regions have been shown to be essential for IDEF1 enhancement of the Fe deficiency responses. The relationship between Fe binding and the function of IDEF1 remains to be clarified.

2.2.3 Hormonal Regulation of the Fe Deficiency Response

Interactions of the Fe deficiency response with hormonal regulation of growth and development are widespread and complex. Phytohormones and effectors involved in the Fe deficiency response include ethylene (Romera et al., 2011; Lingam et al., 2011; Garcia et al. 2010), gibberellin (Matsuoka et al., 2014; Wild et al., 2016), jasmonate (Maurer et al., 2011; Kobayashi et al., 2016), cytokinin (Séguéla et al., 2008); carbon monoxide (CO) (Kong et al., 2010; Yang et al., 2016), carbon dioxide (CO_2) (Jin et al., 2009), nitric oxide (NO) (Meiser et al., 2012) and glutathione (Shanmugam et al., 2015). Only examples of some of these interactions will be presented here.

In the regulation of the Fe-deficiency response, FIT occupies a central position. Under Fe deficiency, *FIT* mRNA was increased while the FIT protein was destabilized and degraded via the 26S proteasome (Sivitz et al., 2012). Ethylene contributed to the stabilization of FIT and has a positive effect on Fe responses (Meiser et al. 2011). FIT can be stabilized by two ethylene signaling transcription factors, ETHYLENE-INSENSITIVE 3 (EIN3) and ETHYLENEINSENSITIVE 3-LIKE 1 (EIL1) (Lingam et al., 2011). As with enzyme-catalyzed processes, the effective metabolite concentration will be determined by equilibrium between the rates of synthesis and degradation. In addition, sequestration of a molecule in a bound form can further regulate its cellular activity. Under Fe-deficient conditions, proteasomal degradation of FIT is counteracted by NO, resulting in accumulation of the FIT protein (Meiser et al., 2012). Since NO positively regulates iron uptake, this effect may be achieved by altering FIT degradation. Intriguingly, the activity of FIT was not affected by cycloheximide treatment,

indicating that in the short-term FIT might be mobilized from a pool of bound FIT to initiate down-stream responses (Meiser et al., 2012).

Gibberellin (GA) was recently shown to be important for the post-translational regulation of the Fe deficiency response. GA promotes root growth by stimulating the degradation of DELLA repressors. At a physiological concentration, application of GA_4 promotes the expression of *IRT1* and *FRO2* (Matsuoka et al. 2014). This increased expression was mediated by bHLH038 and bHLH039 under Fe-sufficient conditions. Wild et al. (2016) observed that inhibition of primary root growth associated with Fe deficiency was reduced in the quadruple DELLA mutant compared to the wild-type control. DELLA was shown to bind to FIT, bHLH38 and bHLB39 and decreased the binding of FIT-bHLH38 and -bHLH39 to the E-box motifs in the promoters of *IRT1* and *FRO2*. To avoid a simultaneous inhibition of root growth and decrease in FIT heterodimer binding under Fe deficiency in epidermal cells, Fe deficiency destabilizes DELLA proteins, thereby unblocking the repression of FIT and promoting the expression of Fe uptake genes. How this asymmetric distribution of DELLA repressors was achieved was not determined. Interestingly, the rice DELLA, SLR1, destabilized IRO2, an ortholog of bHLH38/39, indicating that this regulatory mechanism is conserved.

Jasmonic acid (JA) is rapidly synthesized in response to wounding- and pathogen-associated stress and transmits the stress to the defense reaction. JA treatment suppressed expression of *IRT1* and *FRO2* but not Fe-deficiency-induced expression (Mauer et al. 2011). JA treatment suppressed the expression of FIT and type 1b bHLH38, 39, 100 and 101 transcription factors (Cui et al., 2018). The transcription factor MYC2 has been shown to be a master regulator of JA signal-transduction. In addition to regulation of JA-responsive genes, MYC2 also regulates expression of the bHLH18, 19, 20 and 25 transcription factors. These type IVa factors interacted with FIT and modulated its degradation (Cui et al., 2018). JA regulation of the Fe deficiency responses seemed not to be of benefit for the acquisition of Fe but may have been of advantage in the JA-mediated defense against pathogens.

Based largely on physiological evidence, a role of auxin in the regulation of the Fe-deficiency responses has been frequently reported in the literature. The onset of rhizosphere acidification associated with the Fe deficiency response was delayed by treatment of plants with the auxin transport inhibitor TIBA or by removal of auxin-producing tissues (Landsberg, 1982). Fe deficiency correlated with increased auxin production (Römheld and Marschner, 1986; Li and Li, 2004; Chen et al., 2010) and Fe^{3+}-chelate reductase activity in roots (Schmidt, 1994; Landsberg, 1996). Auxin was shown to be a central component in the initiation and elongation

of lateral roots (Fukaki et al. 2007; Peret et al. 2009). Giehl et al. (2012) have shown that the local Fe supply to lateral roots induced expression of the auxin transporter AUX1. Although the molecular mechanism of Fe-induced *AUX1* expression remained undiscovered, the availability of rhizosphere Fe clearly reprogramed lateral root development to optimize Fe uptake from the soil.

2.2.4 Fe Deficiency Response and Pathogen Resistance

Induced systemic resistance (ISR) is an innate immunity response that is induced by soil rhizobacteria. MYB72 is a key transcription factor for the induction of the ISR reaction as T-DNA knockout mutations in MYB72 eliminate ISR (van der Ent et al., 2008). As mentioned above, MYB72 was strongly induced in Arabidopsis roots during Fe-deficiency (Colangelo and Guerinot, 2004; Buckhout et al., 2009). Zamioudis et al. (2014) discovered that the majority of genes that are induced in Arabidopsis roots in response to pathogen defense encoded proteins that belonged to the Fe deficiency response. One of these ISR and Fe-deficiency responsive genes was BGLU42, a β-glucosidase that converts scopolin to scopoletin, one of the major coumarins secreted by Fe-deficient Arabidopsis roots (Schmid et al., 2014; Stringlis et al., 2018). Scopoletin could then be transferred through PDR9/ABCG37 to the rhizosphere and facilitate Fe acquisition (Tsai and Schmidt, 2017). Thus, BGLU42 played a dual role in stimulation of ISR and induction of the Fe deficiency response.

2.3 Approaches Iron Fortification in Plants

Deficiency of micronutrients is a prevalent problem in developing countries. Estimates of up to 33% of the world population might be Fe deficient (Zimmermann and Hurrell, 2007). Vitamin and mineral biofortification of crop plants by biotechnological methods has been used to decrease micronutrient malnutrition by modification of metabolic pathways to increase desirable compounds or decrease undesirable ones (Blancquaert et al. 2017). Although the addition of mineral nutrients or supplements to the daily diet might seem to be an easier way to improve diets in developing countries, this approach is expensive, inefficient and unreliable. Leafy crop plants such as spinach or seed plants such as legumes are known to contain relatively high amounts of Fe, but these plants also contain oxalate and phytate, which are Fe chelators and decrease the bioavailability of Fe. Therefore biofortification of Fe in a desirable form and harvestable part of the plant is an approach that can be used with a potential commercial application (Lee et al. 2009).

In general, Fe is stored either in the vacuole or in plastids bound to ferritin (Lobreaux and Briat, 1991). There are basic 3 approaches for Fe bio-fortification in plants: decrease phytic acid

content, increase Fe storage capacity and increase Fe uptake and transport capacities. In strategy II plants, a fourth possibility is to increase the biosynthetic capacity for phytosiderphores.

2.3.1 Decrease in Phytic Acid Content

As mentioned above, phytic acid decreases the availability of Fe in plants. Approximately 65 - 85% of phosphorous in seeds is found in the vacuole in the form of inositol hexakisphosphate (i.e. phytic acid; Raboy, 2001). Phytic acid strongly binds cations including Fe, and Fe-phytate is a poor source of nutritional Fe. In developing countries, a high phytate content in the diet can be one of the main causes of Fe deficiency in humans. Due to this, researchers have investigated methods to reduce phytate content through gene manipulation. Mutations in rice genes involved in phytic acid biosynthesis have been isolated that have a low phytic acid phenotype. However, these *lpa* mutants frequently have reduced seedling growth, germination rates and poor agronomic performance (Perera et al.; 2018). Mutations in *AtIPK1 and AtIPK2β*, two kinases involved in the later steps of phytic acid biosynthesis, resulted in near total elimination of phytate with little effect on seed yield and no accumulation of phytate precursors (Stevenson-Paulik et al.; 2005). Finally, there are numerous examples in the literature for the heterologous expression of microbial phytase genes in crop plant to reduce phytate and increase mineral nutrients including Fe (reviewed in Lei et al., 2013).

2.3.2 Increasing Fe Storage Capacity

Ferritin is another candidate to enhance Fe bioavailability in plants. A ferritin molecule contains approximately 4,500 Fe^{3+} ions and can store Fe for the long term in seeds or for short-term use in chloroplasts and mitochondria. Ferritin has been recognized as a major Fe storage protein in chloroplast. The four ferritin genes, *FER1*, *2*, *3* and *4* have been characterized in jArabidopsis, and FER1, FER2 and FER3 are predicted to localize to the plastid, while FER4 is predicted to localize to the mitochondria. *FER2* is only expressed in the seeds, while the other ferritins are expressed in the shoots and flowers (Petit et al. 2001). The over-expression of ferritin genes increased Fe content 2- to nearly 4-fold in rice grains (Goto et al., 1999; Oliva et al., 2014); however, the expression of ferritin genes was not directly correlated with increased plant Fe (Qu et al., 2005; Oliva et al., 2014). In ferritin over-expressing wheat lines, Fe content was increased in vegetative tissues but not in seeds (Drakakaki et al., 2000). Therefore, approaches combining ferritin and other Fe uptake methods might hold more promise.

2.3.3 Vacuolar Fe Transport

The vacuole plays a critical role in storage and buffering of Fe in plant cells. Manipulation of vacuolar Fe transport is a potential mechanism for increasing Fe in plants; however, his

approach has not been investigated in detail. Three different types of Fe transporters have been localized to the vacuolar membrane. Initially a ferroportin homologue, AtFPN2, was identified as a vacuolar Fe transporter (Schaaf et al., 2006); however, subsequently Ni and Co were identified as the primary substrates (Morrissey et al., 2009). Fe efflux is catalyzed in Arabidopsis by two NRAMP transporters, NRAMP3 and NRAMP4 (Lanquar et al., 2005). AtNRAMP3 and AtNRAMP4 belong to the natural resistance-associated macrophage protein family. These transporters are the primary source of Fe for germinating seeds (Bastow et al., 2018), and the *nramp3/nramp4* double mutant was unable to mobilize vacuolar Fe stores (Lanquar et al., 2005). Expression of *AtNRAMP3* and *AtNRAMP4* was induced under Fe deficiency, and electron microscopy data showed depletion of Fe in embryos in WT during germination, but in the *nramp3/nramp4* mutant the presence of Fe remained consistent (Lanquar et al. 2005).

A second group of vacuolar Fe influx transports belongs to the Ccc1p family of Fe and Mn transporters. Vacuolar iron transporter1 (*AtVIT1*) was highly expressed in Arabidopsis seeds and VIT1 was shown to transport Fe into vacuoles of the provasculature parenchyma in the developing embryo (Kim et al., 2006). In rice *OsVIT1* and *OsVIT2* were expressed in flag leaf blades and sheaths, respectively (Zhang et al., 2012). In tulip TgVIT1 catalyzed Fe transport into the proximal perianth cell vacuole, which was essential for blue color development (Momonoi et al., 2009).

2.3.4 Vacuolar-Iron-Transporter-Like Proteins (VTLs)

Microarray analysis, based on a comparison of mRNA abundance in *Arabidospsis thaliana* roots isolated from plants grown under normal and Fe-deficient conditions, revealed that three genes (*AtVTL1* (At1g21140), *AtVTL2* (At1g76800) and *AtVTL5* (At3g25190)) were repressed during Fe deficiency (Buckhout et al. 2009). The putative amino acid sequences were homologous to the VIT1 transporter and thus also to the Ccc1p transporter in Sacchromyces (Li et al., 2001; Gollhofer et al., 2011). In Arabidopsis there are five VTL members, *VTL1*, *2*, *3*, *4* and *5* (Gollhofer et al., 2011 and 2014). VTLs are found in all plants, as well as the green alga *Chamydomonas* and the moss *Physcomitrella* (Gollhofer et al. 2011).

Further investigations showed that VTL1 and VTL2 were localized on the vacuolar membrane in plants. All of five AtVTL genes could complement the Δccc1 mutant in yeast (Gollhofer et al., 2009; Timofeev and Buckhout, unpublished). GFP-VTL fluorescence in *Saccharomyces* was detected on vacuole membrane and in some case in the ER/Golgi network (Timofeev and Buckhout, unpublished). Isolated vacuoles from yeast cells transformed with *VTL1*, *2* or *5* had

2- to 4-fold higher Fe content compared to the Δccc1 mutant and isolated vacuoles from yeast cells transformed with *VTL1*, *2* or *5* had 2- to 4-fold higher Fe content compared to the Δccc1 mutant (Gollhofer et al. 2014). VTL1, 2 and 5 have been proposed to be vacuolar Fe transporters (Gollhofer et al. 2014). The function of VTL3 and 4 has not been determined; although, a role in vacuolar Fe transport is likely.

Over-expression of *VTL1*, *VTL2* or *VTL5* restored the wild-type phenotype in the *nramp3/nramp4* double mutant and the *vit1-1* mutant in Arabidopsis (Gollhofer et al. 2014a), and expression analyzes with GUS reporter constructs revealed *VTL1* expression in roots especially in the xylem parenchyma, seeds and the embryo. *VTL5* was also expressed in the root. *VTL2* and *VTL3* were expressed in shoots (Gollhofer, 2015).

The physiological function of the VTLs is still unclear. Rampey et al. (2006) analyzed mutants in Arabidopsis that were resistant to IAA-conjugates. One of these mutants *ilr3* (At5g54680) was a bHLH transcription factor (bHLH105) that regulated transcription of metal transporter genes including *AtVTL1*, *2* and *5* (Rampey *et al.* 2006 and 2013). They hypothesized that the decreased transcript abundance of *AtVTL1*, *2*, and *5* in the *ilr3-1* mutant might limit a metal cofactor that was necessary for ILR1 hydrolysis of IAA-conjugates.

The Fix^- mutants in *Lotus japonicas* form morphologically normal nodules with endosymbiotic bacteria but are defective in nitrogen fixation (Hakoyama et al., 2012). In one Fix^- mutant *sen1*, nitrogen fixation was completely absent. Hakoyama et al. (2012) discovered that SEN1 encoded an integral membrane protein with sequence similarity to GmNodulin-21 and to CCC1 in yeast and thus to VIT1 and the VTLs in Arabidopsis with closest homology to Nodulin-21 and AtVTL5. VTL5 is synonymous with Nodulin-21-like (Grover et al. 1985). The authors hypothesize that SEN1 was involved in Fe transport across the symbiosomal membrane.

The molecular basis for repression of *VTL1*, *2* and *5* is not well understood. In a report by Yan et al. (2016) the transcript abundance of *VTL1* was elevated in a *wrky46-1* Arabidopsis mutant when grown under Fe-sufficient or -deficient conditions. Whereas *VTL1* expression was repressed in the WT grown under Fe deficiency, the expression of *WRKY46* was induced by Fe deficiency. Both *WRKY46* and *VTL1* were expressed in root stele and vasculature tissues in shoots (Yan et al., 2016; Gollhofer et al., 2011), indicating a similar expression pattern. Yan et al. (2016) demonstrated that expression *VTL1* was correlated with a significant increase in the Fe concentration in xylem sap of the *wrky46* mutant. Finally, they found that WRKY46 bound to the promoter of *VTL1* through specific W-boxes. Yan et al. (2016) concluded that *VTL1* was regulated by WRKY46 and played a major function in Fe translocation.

2.3.5 Increasing Fe Uptake and Transport

Nicotianamine (NA) plays an essential role in the internal transport of Fe and other transition metals in both strategy I and II plants (Pich and Scholz, 1996). NA is an effective chelator of both Fe^{2+} and Fe^{3+} and binds with an affinity constant of 12.8 and 20.6, respectively (von Wiren et al., 1999). Fe-NA complexes can be transported into organelles within the cell and throughout the plant through the phloem and are the predominant form of Fe in the phloem potentially acting as a signal molecule in shoot to root communication (Koen et al., 2013). NA-Fe^{2+} has been suggested to play a role in the Fe deficiency response in non-grass plants and as a long distance systemic signal. (Curie and Briat, 2003).

The YELLOW STRIPE1-LIKE (YSL) family of membrane proteins has been implicated in the transport of NA-Fe complexes (Conte et al., 2013). AtYSL1 and AtYSL3 were thought to translocate metals into vascular parenchyma cells and facilitate Fe loading into seeds (Waters et al., 2006) and AtYSL4 and AtYSL6 were localized by Conte et al. (2013) to the vacuolar membrane and to the endoplasmic reticulum. An additional NA transporter on the vacuolar membrane is ZINC-INDUCED FACILITATOR1 (ZIF1). The overexpression of ZIF1 in Arabidopsis increased the amount of NA in the roots and shoots and led to Fe deficiency (Haydon et al., 2012). ZIF1 was shown to be required for Zn tolerance and was hypothesized to transport NA from the cytoplasm into the vacuole (Haydon et al., 2012). ENA1 is a member of the MFS family that presumably transports NA into the vacuole in rice (Nozoye et al. 2011). AtZIF1 and 2 could potentially transport NA into the vacuole and thereby participate in metal detoxification (Nozoye et al., 2011).

Studies have reported increased Fe uptake and storage in seeds by increasing the NA concentration (Douchkov et al., 2005; Klatte et al., 2009; reviewed by Zheng et al. 2010). Furthermore, Lee et al. (2012) demonstrated that over-expression of nicotianamine synthase (*OsNAS2*) correlated with increased bioavailable iron in rice seeds; although, the positive effect of over-expression has not always been observed (Cassin et al. 2009).

2.4 Goals of the Dissertation

Compared to over-expression of single genes to enhance Fe content (see 1.3 above), strategies combining over-expression of Fe homeostasis genes might be needed to achieve a content of Fe necessary for nutritional benefit (Singh et al., 2017; Wu et al., 2018). VTLs might potentially be good candidates for Fe biofortification. The expression of *VIT1* from Arabidopsis controlled by a *PATATIN* promoter enhanced the Fe content of cassava (*Manihot esculenta*) tubers by 3- to 4-fold (Narayanan et al., 2015). Connorton et al. (2017) demonstrated that by over-expressing

TaVIT2 under the control of an endosperm-specific promoter a 2-fold increase in wheat flour Fe could be achieved. However, very few VITs have been characterized. The goal of this thesis is testing the suitability of the VTL transporters for enriching seed Fe in the model plant, Arabidopsis. In addition, a strategy will be tested combining the single over-expression of VTLs with either the over-expression of *IMA1*, a recently discovered regulatory protein in the Fe deficiency response, or *NAS4* will be investigated.

3 Materials and Methods

3.1 Plant Material and Transformation Methods

In Table 1 the transgenic lines are listed that were used in this study. For the transgenic plants produced for this study, the *Arabidopsis thaliana* WT was transformed with the appropriate gene construct by the floral dip method (Chang et al., 1994). For the overexpression, a 35S promoter was used. The resistance markers were as given in Table 1.

Table 1. Transgenic Arabidopsis lines, selection markers and plasmids used in this study.

Transgenic lines/Plasmids	Reference	Selection
WT (*Arabidopsis thaliana* (L.) HEYNH (Col-0))	-	-
vit1-1	Kim *et al.* 2006	Kanamycin
IMA1 (OE)	W. Schmidt	
VTL1 (OE)	(Gollhofer 2015b)	Basta®
VTL2 (OE)		
VTL3 (OE)		
VTL4 (OE)		
VTL5 (OE)		
NAS3 (OE)	Ghalamkari, this thesis	Basta®
VTL5-NAS3(OE)		
VTL2-IMA1(OE)	Ghalamkari, this thesis Fechler, MS Thesis 2017	Basta®
VTL3-IMA1(OE)		
VTL4-IMA1(OE)		
VTL5-IMA1(OE)		
pCAMBIA3301-n	AG Pflanzenphysiologie, Humboldt-Universität zu Berlin	Kanamycin, Basta®
GL1(Origin pGPTV)	Becker et al. 1992	Kanamycin Basta®
Pjet	Thermo Fisher Scientific	Ampicilin
pGMT	Promega	Ampicilin
Escherichia coli – DH5α	This lab	-

Transgenic lines/Plasmids	Reference	Selection
Agrobacterium tumefaciens - EAH105	This lab	Rifamicin

For transformation of Arabidopsis plants, the Agrobacterium strain (EAH105) containing an appropriate plasmid was grown in liquid YEB medium containing antibiotics as needed at 28° C to an OD_{600} of 0.8 – 1. The cells were harvested by centrifugation (5 min at 6,000 g and RT), and the pellet was re-suspended in transformation medium (2.2 g / l Muroshige & Skoog medium, 5% (w/v) sucrose and 0.05% (v/v) Silwett L-77). A drop of the cell suspension was place on young Arabidopsis flowers, and the plants were grown in the dark for 1 d. Plants were placed under long-day growth conditions, and seeds were collected when the siliques were completely dry.

3.2 Culture Media, Analytical Instruments, Solutions and Buffers

3.2.1 Plant Culture Media

Table 2. Composition of plant culture media used in this thesis.

Medium	Substance		Concentration
Soil	GS 90 *Einheitserde* mixed with Perlit		4:1 (v/v)
Hydroponic medium, Schmidt (1994) pH 6.0	KNO_3		3 mM
	$MgSO_4$ x 7 H_2O		0.5 mM
	$CaCl_2$ x 6 H_2O		1.5 mM
	K_2SO_4		0.5 mM
	NaH_2PO_4 x 2 H_2O		1.5 mM
	H_3BO_3		25 µM
	$MnCl_2$ x 4 H_2O		1 µM
	$ZnSO_4$ x 7 H_2O		0.5 µM
	$(NH_4)_6Mo_7O_{24}$		0.05 µM
	$CuSO_4$ x 5 H_2O		0.3 µM
	w/ Fe	Fe^{2+}-EDTA	40 µM
	Fe free	EDTA	1 µM
Medium Estelle & Somerville (1987) pH 5.5	KNO_3		5 mM
	$Ca(NO_3)_2$ x 4 H_2O		2 mM
	$MgSO_4$ x 7 H_2O		2 mM
	KH_2PO_4		2.5 mM
	$MnCl_2$ x 4 H_2O		14 µM

	H_3BO_3		70 µM
	$ZnSO_4$ x 7 H_2O		1 µM
	$CuSO_4$ x 5 H_2O		0.5 µM
	Na_2MoO_4 x 2 H_2O		0.2 µM
	$CoCl_2$ x 6 H_2O		0.01µM
	NaCl		10 µM
	w/ Fe	Fe-EDTA	40 µM
	Fe free	Ferrozine®	100 µM
	MES		0.1% (w/v)
	Sucrose		1.5% (w/v)
	Agarose		0.8% (w/v)

3.2.2 Microbiological Culture Media

Table 3. Composition of microbiological culture media used in this thesis.

Medium	Substance	Mass (g)
LB medium (liquid)	Tryptone/Peptone from Casein (Roth)	10
	NaCl	10
	Yeast Extract	5
	H_2O	to 1 L
LB medium (solid)	As above plus Agarose	15
YEB medium (liquid) adjust to pH 7.2 with NaOH	Yeast Extract (Roth)	1
	Tryptone/Peptone from Casein (Roth)	5
	Sucrose	5
	$MgSO_4$ x 7 H_2O	0.5
	H_2O	to 1 L
YEB (solid)	As above w/ agarose	20

3.2.3 Instruments

Table 4. Description and manufacturer of instruments used in this thesis.

Devices/Materials	Description	Company
Balance	CPA 225D	Sartorius AG, Göttingen
Gel Documentation System	UV-System	Intas Science Imaging Instruments GmbH, Göttingen
Gel Camera	Agagel Mini Biometra®	Biomedizinische Analytik GmbH, Göttingen
Growth Chamber		York International GmbH, Mannheim

	1601	Rubarth Apparate GmbH, Laatzen
Magnetic Stirrer/Heating Blocks	MR 3001	Heidolph Elektro GmbH & Co. KG, Kehlheim
PCR Cycler	C1000™ Thermal Cycler	Bio-Rad Laboratories GmbH, München
pH Meter	Lab 850	Schott Instruments Analytics GmbH, Mainz
Photometer	Novaspec® II	Pharmacia, Freiburg
	Specord 50	Analytik Jena AG, Jena
Retsch® Mill	MM400	Retsch GmbH, Haan
Stereo Microscope	SZX12	OLYMPUS
Clean Bench	Safemate 1.2	BioAir
Thermomixer	Compact 5436	Eppendorf AG, Hamburg
Incubator	T 6030	Heraeus Holding GmbH, Hanau
Vortex	G-560E	Scientific Industries Inc., Bohemia, N.Y., USA
Balance	Kern 510	Kern & Sohn GmbH, Albstadt
Centrifuge	1-15PK	Sigma-Aldrich Chemie GmbH
	3-16PK	
	HLC Biotech, Bovenden	Eppendorf AG, Hamburg
Concentrator	Concentrator plus	
Desiccator	-	-
Shaker	KS250 Basic	
Ultrasonic Bath	RK 156 BH	Sonorex
Wolfram-Carbide-Cobalt Beads	Zubehör MM400	Retsch GmbH, Haan
Glass Beads	(Ø 0,1 mm)	Roth, Karlsruhe
Cryotubes	2 ml	Roth, Karlsruhe
Centrifuge Tubes	Ultra x 89 mm	Beckmann Coulter

3.2.4 Solutions and Buffers

Table 5. Composition of solutions and buffers used in this study.

Title	Substance	Concentration	Use
Extraction solution	Acetone	80 % (v/v)	Chlorophyll-extraction
	KOH (0.1 N)	0,008 % (v/v)	
Solution I (fresh) in H_2O (Perls' Staining)	$K_4Fe(CN)_6$ x 3 H_2O	4 % (w/v)	Fe staining in Seedlings, Embryos and Leaves
	HCl (37 %)	4 % (v/v)	
Solution II (1 d before) in Methanol	NaN_3	0.01 M	
	H_2O_2	0.3 %	
Solution III (fresh), pH 7.4	NaH_2PO_4 x H_2O	100 mM	
	Na_2HPO_4 x H_2O	100 mM	

Solution IV (fresh)	NaH_2PO_4 x H_2O	100 mM	
	Na_2HPO_4 x H_2O	100 mM	
	DAB (3,3-Diaminobenzidine)	0.025 %	
	H_2O_2	0.3 %	
10 x TBE-Buffer	Tris	1 M	Agarose Gel electrophoresis (Stock solution)
	H_3BO_3	0,83 M	
	Na_2-EDTA	0,01 M	
Washing Buffer	EDTA	1 µM	Removing Fe^{2+}
	MES-KOH, pH 5,5	1 mM	
YelZol	Guanidinium-Isothiocyanate	235.85 g/L	RNA Extraction
	Tris-HCl, pH 4,5	75.28 g/L	
	Na-EDTA, pH 8,0	35.09 g/L	
	N-Lauroyl sarcosine	1.18 g/L	
	Aqua-Phenol, pH 4,0	0.5 % (v/v)	
	Isoamyl alcohol	0.02 % (v/v)	
	8-Hydroxychinoline	1 g/L	
	ß-Mercaptoethanol	0.005 % (v/v)	

3.2.5 Kits, enzymes, antibiotics and primers

Table 6. Kits, enzymes and antibiotics used in this thesis.

Product	Company
5x Taq-Buffer	Thermo Fisher Scientific
6x DNA Loading Dye	Thermo Fisher Scientific
Ampicilin	
Basta®	Bayer
DEPC-H_2O	Sigma
DNase I, RNase-free-Kit	Thermo Fisher Scientific
dNTP Set	Thermo Fisher Scientific
Ethidium bromide	Roth
FastAP Thermosensitive Alkaline Phosphatase	Fermentas
GeneRuler™ 1kb Plus DNA Ladder	Thermo Fisher Scientific
GeneRuler™ Low Range DNA Ladder	Thermo Fisher Scientific
Homemade Taq DNA Polymerase	Prof. Zoglauer AG
Isolate PCR and Gel Kit	Bioline
Mango Taq DNA Polymerase	Bioline
Phusion® High-Fidelity DNA Polymerase	Bio Lab
Restriction enzymes Fast digest	Fermentas
RevertAid™ Reverse Transcriptase	Thermo Fisher Scientific
Ribolock™RNase Inhibitor	Thermo Fisher Scientific
Rifamicine	
SensiMix™ SYBR® No-ROX Kit	Bioline

T4-DNA-Ligase	Thermo Fisher Scientific
TRIsureTM	Bioline

3.2.6 Primers

Table 7. Primers used in this thesis.

Gene	Primer	Sequenz (5'⟶3')	Comment
	NAS3fw	CCC GGG ATG GGT TGC CAA GAC G	Cloning SmaI
	NAS3 rev	CCC GGG TTA AGA CAA CTG TTC CTCC	
At1g09240	NAS3fw	CCA TGG ATG GGT TGC CAA G	Cloning PmlI
	NAS3 rev	CAC GTG TTA AGA CAA CTG TTC CTCCC	Cloning NcoI
	Actin2 fw	TGGAATCCACGAGACAACCTA	Semi qPCR: House-keeping Gene
At3g18780	Actin2 rev	TTCTGTGAACGATTCCTGGAC	
At1g47400	IMA1 fw	GCTCATCATACTTCTTGTGGC	
	IMA1rev	AGGAAACAATCACGCAGCAG	
At1g21140	VTL1 fw	TCAAATGAAGAGAGAGAACGGAGG	
	VTL1 rev	ATTCCCACGAAATAAAACAAGTCAC C	
At1g76800	VTL2 fw	GTTCGTCTCAGTTTACTCTCA	Semi qPCR: proof of OE
	VTL2 rev	GCTAACCAACCTCCAAACAAA	
At3g43630	VTL3 fw	GTGGCAGCGGTTACGTTGGC	
	VTL3 rev	GGCCATAGCTAACCATCCTCC	
At3g43660	VTL4 fw	GTCTCAACGGCTTCACTTAT	
	VTL4 rev	GCTAACCATCCTCCAATCAA	
At3g25190	VTL5 fw	GAACATAAGACATCACTATCAGCA	
	VTL5 rev	GTAAGAGCCATAGCCATCCA	
At1g09240	NAS3 fw	CCC GGG CCA TGG ATG GGT TGC CAA G	
	NAS3 rev	GAA TTC CAC GTG TTA AGA CAA CTG TTC	
At1g56430	NAS4 fw	CCC GGG ATG GGT TAT TGC CAA G	
	NAS4 rev	CCC GGG CTA GGT AAG TTG TTC TTC	
	Oligo-dT_{18}	TTTTTTTTTTTTTTTTT	cDNA Primer
-	NAS3- pCAMBIA REV	GAGGAGGTCGAACTCGAGCTTTCCG AG	Sequencing
-	35S prom primer	ATCCTTCGCAAGACCCTTCC	
-	seqNOS	TACATGCTTAACGTAATTCAACAG	

At1g09240	NAS3-qRT fw	GTTCGACCTCCTCGAACAAA	Real time quantitative PCR
	NAS3-qRT Rev	CCAGAAGAGAAGCGAGTGAG	
At3g18780	Actin2-qRT fw	GCACCCTGTTCTTCTTACCG	
	Actin2-qRT rev	GGCGACATACATAGCGGG	
At1g47400	NiG-qRT fw	ATTTGACCATGCTTCCACCG	
	NiG-qRT rev	TCATAGCCAATGTCATCGTC	
At1g21140	VTL1-qRT fw	GGCTGCGTTTGTGAAAGACT	
	VTL1-qRTrev	AAAACCCTAGCCGACGACTT	
At1g76800	VTL2-qRT fw	CTTTTGGCTGCTGCTTTTGT	
	VTL2-qRT rev	CTGCTCCTAACCATCCGAAA	
At3g43630	VTL3-qRT fw	GTGGCAGCGGTTACGTTGGC	
	VTL3-qRT rev	GGCCATAGCTAACCATCCTCC	
At3g43660	VTL4-qRT fw	CTATCGCGTCTGCATTAGCATTTAC	
	VTL4-qRT rev	CGCCACAATCACTCCAATCCTAAC	
At3g25190	VTL5-qRT fw	TGTGGTTAAGTCGAGCGTCA	
	VTL5-qRT rev	GCAGAGCCAATGAACTTGGT	
At3g18290	BTS-qRT fw	GGACTCAACACTTGATCCGAGGAG	
	BTS-qRT rev	CGGGGAACATCCAAGTTCAACATCACC	
At1g07890	APX1-qRT fw	GGTGCATGGACATCAAACCC	
	APX1-qRT fw	ACAGGGTCGTCCAATAGTGC	
At5g51720	NEET-qRT fw	TCGTTGTCACCGAGCTTTCC	
	NEET-qRT rev	ACGTCCCCGACCTCCAA	
At5g54680	ILR3-qRT fw	GCAACCTATTGGTGTTTCTTCTAACTC	
	ILR3-qRT rev	CCAGGTTCTTTGCTAGCTTCTGA	
At3g47640	PYE-qRT fw	CAGGACTTCCCATTTTCCAA	
	PYE-qRT rev	CTTGTGTCTGGGGATCAGGT	
At3g56980	bHLH39-qRT fw	GACGGTTTCTCGAAGCTTG	
	bHLH39-qRT rev	GGTGGCTGCTTAACGTAACAT	
At5g01600	FER1-qPCR fw	TCGTTGAGAGTGAATTTCTGG	
	FER1- qPCR rev	ACCCCAACATTGGTCATCTG	
At1g01580	FRO2-qPCR fw	CTTGGTCATCTCCGTGAGC	
	FRO2-qPCR rev	AAGATGTTGGAGATGGACGG	
At4g19690	IRT1-qPCRfw	CACCATTCGGAATAGCGTTAGG	
	IRT1-qPCR rev	CCAGCGGAGCATGCATTTA	
At1g56160	MYB72-qPCR fw	GACTCGAGAGGTAACCAAATCG	
	MYB72-qPCR rev	GTTGAACCACTCGTCGTACTC	

3.3 Experimental Methods

3.3.1 Arabidopsis thaliana growth conditions on soil, hydroponics and agarose

For cultivation of Arabidopsis on soil, seeds were sown on GS 90 soil (*Einheitserde* Patzer) mixed with Perlite (Knauf-Aquapanel) at a ratio of 4:1, covered with a glass or plastic hood and stratify in the dark at 4° C for two d. Seeds were then transferred for germination to the growth chamber under short-day conditions (10 h light, 36-130 $\mu E \cdot s^{-1} m^{-2}$). When seedlings reached the 2-leaf stage, the glass or plastic hood was removed, and when the 3rd and 4th leaves appeared, plants were selected with the herbicide Basta®. The seedlings were sprayed three times at intervals of two to three days with a Basta® solution (0.05-0.01%). Subsequently plants were grown for four weeks in the greenhouse under long-day conditions (15 h light, 125 $\mu E \cdot s^{-1} m^{-2}$) at 26° C and 36% humidity to enhance induction of flowering.

For cultivating Arabidopsis seedlings in hydroponic culture, seeds were first sterilized in one mL of 1.2% (w/v) sodium hypochlorite solution for 15 min and then rinsed with sterile water. The sodium hypochlorite solution was made fresh daily by mixing 5 mL of 12% (w/v) sodium hypochlorite solution with 45 mL water and the addition of one drop of Tween 20 as a wetting agent. Seeds were then soaked in sterile water for two d in the dark at 4° C.

Eppendorf Tubes® (1.5 mL) were filled with 0.25% Agarose and following solidification of the Agarose the bottom of tubes was cut off. Approximately five seeds were sown on the Agarose surface, and the tubes were then placed in trays so that the tips of the tubes were in contact with the hydroponic culture medium (Schmidt, 1994; Table 2). The boxes were covered with a glass plate for about two weeks and incubated in a growth chamber under short-day conditions (10.5 h light, 150-200 $\mu E \cdot s^{-1} m^{-2}$) at 22° C and 80% relative humidity. The nutrient solution was changed weekly, and the nutrient solution was aerated beginning on the second week (Schmidt 1994). After 3 weeks, the Agarose plug was removed by washing with water and one seedling was selected for further cultivation.

For cultivating Arabidopsis on ES solid medium (Table 2), seeds were sterilized by first rinsing with a 7% (w/v) sodium hypochlorite solution, freshly prepared by diluting 28 ml of a 12% (w/v) sodium hypochlorite with 20 mL water, then with 100% ethanol (100%) and finally three times with sterile water. Seeds were spread on the surface of the solid ES medium in Petri dishes. The Petri plates were wrapped with Parafilm® and stratified in the dark for two d at 4° C. The Petri plates were then placed upright in a growth chamber and grown under short-day conditions (10 h light, 125 $\mu E \cdot s^{-1} m^{-2}$, 22° C).

3.3.2 Cross pollination of Arabidopsis lines

For cross-pollination the sepals, petals and stamens were removed under a microscope from two unopened flower buds. On the following day, the remaining pistil was pollinated with pollen from anthers of a donor plant.

3.3.3 RNA isolation

One leaf from a four-week-old plant was harvested and placed in a 2 mL Eppendorf Safe-Lock® tube with 4-5 sterile steel beads. The tubes were immediately transferring to liquid nitrogen and the samples stored at -80° C. On the day of isolation, one ml of cooled Yelzol solution was added to each tube, and the tubes were transferred to a cooled (ca. 4º C) Retsch® mill holder. The samples were homogenized for 5 min at 30 Hz in a Retsch® mill. Subsequently, 200 µl of cooled chloroform were added, and the tubes shaken vigorously for about 15 s. After 5 min incubation at RT, the samples were centrifuged for 5 min at 12,000 *g* and 4° C. Two-hundred µl of the upper phase were then transferred to a new 1.5 ml Eppendorf Safe-Lock® tube, mixed with an equal volume of isopropanol and incubated at -20° C. Subsequently the samples were centrifuged for 20 min at 12,000 *g* at 4° C. The supernatant was discarded, the pellet washed with 1 ml of 75% ethanol made with DEPC-treated H_2O and centrifuged for 5 min at 10,000 g and 4° C. This step was repeated, but with centrifugation at 7,500 *g*. The supernatant was discarded and the pellets dried at 30° C in a Thermo mixer. Once the ethanol had evaporated, the pellet was dissolved in 25 µL of DEPC-treated H_2O. RNA samples were store at -80° C or used directly for cDNA synthesis (2.3.4).

3.3.4 cDNA Synthesis

The concentration of extracted RNA was determined using a NanoDrop 2000. For the cDNA synthesis, 2 µg of RNA from each sample were diluted with DEPC-treated H_2O to a total volume of 11 µL. For each sample, 1 µL oligo-dT_{18} primer was added and incubated for 5 min at 70° C. Seven µL of master mix (Table 8) were added to the RNA samples. This was followed by incubation for 5 min at 37° C. One µL of reverse transcriptase was then added per sample and incubated at 42° C for 60 min. Finally, to stop the synthesis reaction, the temperature was raised to 70° C for 10 min. The cDNA samples were either used directly for PCR (see 2.3.5) or stored at -20° C until needed. For controlling RNA quality, 1 µg RNA was adjust to 12 µL with DEPC-treated H_2O, applied to a 1.2% Agarose gel and separated by electrophoresis (85 V).

Table 8. Master mix for cDNA synthesis (20 µL)

Component	Volume (µL)

5 x Reaction buffer	4
10 mM dNTPs	2
RNase Inhibitor	0.5
DEPC-treated H_2O	0.5

3.3.5 Polymerase Chain Reaction (PCR)

For the semi-quantitative polymerase chain reaction, the expression of each specific gene of the different lines was tested in comparison to the WT. PCR reaction mixture (Table 9, 24 µL) was added to each PCR reaction. cDNA samples were diluted 1:10 with distilled water and 1 µL was added to each reaction solution for a final volume of 25 µL. The PCR was run and the reaction products were separated on an Agarose gel by electrophoresis. PCR products were store at -20° C until needed (Table 10).

Table 9. Composition of the master mix for PCR reactions

Component	Volume [µL]	
H_2O	12.80	x Number of samples + 1
5 x Buffer	5	
50 mM $MgCl_2$	1.5	
10 µM Fw Primer	1.5	
10 µM Rev Primer	1.5	
10 mM dNTPs	0.7	
Taq-Polymerase (homemade)	1	

Table 10. PCR Program

Step	Phase	Temperature [° C]	Time [s]	Comment
1	Denaturation	95	300	
2	Denaturation	95	30	x cycles
3	Annealing	Depending on T_m of the primers	30	
4	Elongation	72	45	
5	Extension	72	240	
6	Storage	4	∞	

3.3.6 Real-time quantitative PCR (RT-qPCR)

cDNA was diluted 1:10 with sterile ultrapure water and 1 µL was mixed with 9 µL of the master mix (Table 11). Three technical replicates were performed for each cDNA sample, and the reaction was run in a CFX96 Realtime System (BioRAD) thermal cycler (Table 12). In order to compensate for variation in the starting amount of the RNA, the housekeeping gene *Actin2* was used, and the data were evaluated with the $2^{-\Delta\Delta C(t)}$ method according to Livak and Schmittgen (2001). (see 2.3.4)

Table 11. Composition of a master mix for qPCR reactions

Component	Volume [µL]	Comment
SensiMix™ SYBR® No-ROX Kit	5	x Number of samples + 1
25 µM Fw Primer	0.3	
25 µM Rev Primer	0.3	
H_2O	3.4	

Table 12. qRT-PCR program

Step	Phase	Temperature [°C]	Time [s]	Comment
1	Polymerase activation	95	600	
2	Denaturation	95	15	x 45
3	Annealing	According to Primers' Tm	15	
4	Elongation	72	According to product size	
5	Detection			
6	Final Elongation	72	10	
7	Melting curve und Detection	65⟶90, Gradient 0,5	3	

3.3.7 DNA and RNA Agarose gel electrophoresis (Adkins & Burmeister, 1996)

The DNA or RNA were mixed with 10 × DNA loading buffer and separated in a 0.8-1% agarose gel in 0.5 × TBE buffer (Table 13) at 80-100 mV for to 30-60 min. Ethidium bromide at a concentration of 1 µg/ml was used for detection. For DNA samples, a suitable DNA size ladder was used, and the gels were visualized using an Intas UV documentation system.

Table 13. Composition of 0.5 x TBE Buffer

Chemical	Concentration
Tris	5.4 g/l
Boric acid	2.75 g/l
Na_2EDTA	1 mM

3.3.8 DNA extraction from an Agarose gel

DNA band was selected and cut from the gel with a sterile scalpel, and the mass was determined. The extraction solution was performed with the isolation Gel kit according to the manufacturer's instructions (Bioline).

3.3.9 DNA Cleavage with restriction enzymes and ligation

The DNA cleavage reactions were conducted with enzymes from Fermentas according to the manufacturer's instructions. The ligation of recombinant DNA was performed with T4 ligase at 4° C overnight or for 2 h at RT. The quantitative ratio of vector and DNA fragment was calculated according to the formula: Mass Fragment [ng] = 125 ng * Length Fragment [Bp].

3.3.10 Transformation of chemically competent Escherichia coli cells (Hanahan, 1983)

E. coli cells were placed on ice for 30 min and then 50-100 ng of plasmid DNA were added. The mixture was place on ice for 30 min, then heat-shocked for 2 min at 42° C and returned to ice for a 5 min incubation. Two hundred µL of cell suspension were mixed with 800 µl of LB medium without antibiotics, and the cells were placed on the shaker (250 rpm) for 60 min at 37° C. The mixture (150-300 µL) was plated on LB agar plates containing the antibiotic and incubated at 37 ° C. Bacterial colonies appeared after 24-48 h.

3.3.11 Isolation of plasmid DNA from Escherichia coli (mini preparation)

Two ml of an overnight culture was centrifuged (5 min, 5,000 *g* at RT). The resulting supernatant was discarded, and the pellet resuspended in 300 µL of P1 buffer (Table 14) and

vortexed. Three hundred µL of P2 buffer were added, and the suspension was gently mixed by inversion. The suspension was neutralized with 300 µL of P3 buffer. The cells were thoroughly mixed, incubated for 10 min at RT and then centrifuged at RT for 10 min at 14,000 *g*. The supernatant was removed and diluted with 0.7 volume of isopropanol and 0.1 volume of sodium acetate (3 M, pH 5.2). After a 5 min incubation on ice, cells were centrifuged at 4° C for 30 min at 14,000 g, the supernatant discarded and the pellet washed with 900 µL 70% (v/v) ethanol. The precipitate was collected by centrifugation (10 min, 14,000 *g*, 4° C) and the pellet dried at 30° C. The pellet was resuspended in 40 µL of sterile water and stored at -20° C until needed.

3.3.12 Transformation of Agrobacterium tumefaciens (Nishiguchi et al., 1987)

For transformation of *Agrobacterium tumefaciens*, cells were removed from -80° C freezer and thawed for about 20 min on ice. The desired plasmid DNA (0.5-1 µg) was added to competent cells, the mixture incubated for 5 min on ice, frozen in liquid nitrogen and thawed for 10 min at 37° C. The cells were diluted with 1 ml of YEB medium and incubated for 2-4 h at 28 ° C. Cells were then collected by centrifugation. The pellet (100 µL) was spread on YEB agar medium with the appropriate antibiotic and incubated for two to three d at 28 ° C.

Table 14. Mini-preparation Buffers

P1 (resuspension buffer)
50 mM Tris-HCl, pH 8.0
10 mM EDTA
100 µg/ml RNase A (Store at 4 ° C after addition of RNase A)
P2 (lysis buffer)
1% (w/v) SDS
200 mN NaOH
P3 (neutralization buffer)
3 M Potassium Acetate, pH 5.5

3.3.13 Histochemical and fluorometric GUS assay

Expression of the GUS reporter was directly visualized by the activity of the reporter β-glucuronidase (GUS) by *in situ* histochemical staining. Tissues or whole seedlings were incubated for 30 min to 24 h in GUS buffer (Table 15). The blue coloration was visualized and documented.

Table 15: GUS staining Buffer:

Composition
80 mM Na_2PO_4 2 H_2O, pH 7.2
0.4 mM K_3FeCN_6
0.4 mM K4FeCN6 3 H_2O
8 mM EDTA
0.05 % (v/v) Triton X 100
0.8 mg/ml X-Glc (added fresh)

The fluorometric GUS assay allowed quantitative determination of β-glucuronidase activity. Approximately 100 mg fresh mass of plant tissue was homogenized in extraction buffer (Table 16). Subsequently, the suspension was centrifuged for 5 min at 4° C and 14,000 g, for each measurement, a 50 µL extract was mixed with 0.5 mL assay buffer and incubated at 37 ° C for 30 min - 24 h. At various times, a sample was taken (100 µL) and mixed with 0.9 mL stop buffer. The activity was determined at 360 nm.

Table 16. GUS assay Buffer:

Fluorometric GUS Assay Buffers	
Extraction buffer	50 mM $NaPO_4$, pH 7.0
	10 mM DTT
	1 mM Na_2EDTA
	0.1% (w/v) Sodium lauryl sarcosine
	1% (v/v) Triton X 100
Assay Buffer	1 mM MUG (4-methyl umbelliferyl-β-D-glucuronide) in extraction buffer
Stop buffer	Na_2CO_3

3.3.14 Perls' Staining (Roschzttardtz et al. (2009)

For Perls' staining according to Roschzttardtz et al. (2009), seedlings grown on agar plates were washed with a wash solution (Table 5) before staining to remove surface Fe. Seedlings, embryos and leaves were incubated for 45 min in solution I, washed with distilled water and incubated in solution II for one h. They were then rinsed with solution III. Subsequently, samples were incubated for 10 min in solution IV, washed three times with Fe-free water and observed with a light microscope.

For Perls' staining with DAB/H_2O_2 intensification, isolated embryos or leaves were vacuum infiltrated with fixation solution containing 2% (w/v) paraformaldehyde, 1% (v/v) glutaraldehyde and 1% (w/v) caffeine in 100 mM phosphate buffer (pH 7.4) for 30 min and then incubated for 15 h in the same solution. Then samples in 100 mM phosphate buffer were dehydrated through a 50%, 70%, 90%, 95% and 100% ethanol series and then through butanol/ethanol 1:1 (v/v) and 100% butanol. Samples were embedded in the Technovit 7100 resin according manufacturer's instructions. Embedded samples were sectioned with a microtome, and the sections were incubated in 60° C overnight. Histological assays were performed with the support of Mrs. Jutta Zeller at the Naturkundemuseum (Berlin, Germany)

3.3.15 Determining nicotianamine (NA) content

NA content was determined with Ultra Pressure Liquid Chromatography (UPLC). The analyses were performed by Dr. Mohammad HajiRezaei in the laboratory of Prof. Dr. von Wiren at IPK (Gatersleben, Germany). NA was extracted according to Zierer et al. (2016) from 100- 150 mg plant powder with 1 ml 80% ethanol for 1 h at 80°C. The supernatant (0.8 ml) was transferred to a new reaction tube and concentrated in a speed vac (Christ, RVC2-33IR and Alpha1-4 LD-Plus). The resulting pellet was re-suspended in 50 µl purest water and an aliquot was used for the measurement.

For separation and detection of nicotianamine (NA), an Agilent UPLC 1290 system connected to an Agilent triple Quad MS 6490 mass spectrometer equipped with an easy Jet Spray was employed. Two microliters of sample was separated on an Acquity UPLC HSS T3 column (1.8 mm, 2.1 x 150 mm; Waters) with a flow rate of 0.4 mL min. Solvents were water (A) and acetonitrile (B), both acidified with 0.1% (v/v) formic acid. The binary gradient used was as follows: 0 to 0.5 min at 99.9: 0.1% (A:B), 0.5 to 3.1 min at 95:5%, 3.1 to 4.5 min at 30:70%, 4.5 to 4.6 at 99.9:0.1%, and 4.6 to 5 min at 99.9:0.1%. The mass spectrometer was operated in the ESI V+ mode and multiple reactions monitoring mode. The following instrument parameters were used: nitrogen gas flow = 12 l min^{-1}, ion spray voltage = 3000 V, and auxiliary gas temperature = 300° C. Dwell time for each transition was 20 ms. For accurate identification of the NA peak and to exclude sample matrix effects, different samples were spiked with purest NA and measured under the same conditions. Quantification was performed on the respective reconstructed ion traces of the protonated molecular ions using the Mass Hunter (version B.04.00).

3.3.16 Measurement of Fe concentration (Schmidt 1996)

For determination of the Fe content, samples (seeds, roots, leaves or seedlings) were placed in 2 mL Eppendorf Safe-Lock® tubes. Standard solutions for calibration (0, 0.5, 1, 2.5, 5, 10, 15, 25, 50, 75, 100 and 300 µL of 1 mM $FeSO_4$) were prepared in a total volume of 100 µL with 0.1 N HCl. A few glass beads and 75 µL nitric acid (65%) were added to all samples and standards. Seed samples and the corresponding standards were kept overnight at RT. All samples were transferred for 1 h at 95° C to a Thermo mixer with the lid open and then for 5 h with the lid closed until the samples become clear yellow. The samples were then centrifuged briefly after cooling, and 50 µL of hydrogen peroxide were added. Samples were incubated for a 2 h at 56° C following which the volume was adjusted to 200 µL with water. Twenty µL of each sample were mixed with 980 µL of Fe measurement solution (Table 12), and the samples were incubated for 5 min at RT. The absorption was determined at 535 nm. Water was used as a blank.

Table 17. Composition of the Fe measuring solution (store in the dark at 4° C)

Substance
0.48 M Hydroxylamine hydrochloride ($HONH_2$-HCl)
0.6 M Sodium Acetate
1 mM Bathophenanthroline disulphonate (BPDS)

3.3.17 Measurement of the Fe^{3+}-chelate reductase (Schmidt et al., 2000)

Arabidopsis seedlings were grown on Fe-sufficient ES solid medium for 3 weeks, and they were then transferred to Fe-deficient medium for two d. Finally, seedlings were transferred for 1 d to Fe^{3+}-chelate reductase plates (Table 18). The reaction was observed as a purple-colored Fe^{2+}-Ferrozine chelate and photographically documented.

Table 18. Fe^{3+}-chelate reductase medium

Substance
0.5 mM Calcium Sulfate
0.5 mM FeEDTA
0.5 mM Ferrozine®
0.7% (w/v) Agarose

3.3.18 Measurement of the Fe^{3+}-Chelate Reductase (Moog et al., 1995)

Plants growing 4 weeks in hydroponic culture were transferred for 2 d to Fe-deficient liquid medium. The roots of Fe-sufficient and –deficient plants were washed in Fe-free distilled water followed by washing with the washing solution (Table 5) and again with Fe-free distilled water. For the measurement of the reductase activity, plants were transferred to Petri plates with 10

mL of Fe-free hydroponic nutrient solution. The roots were immersed in the nutrient solution and 100 µL 1 M MES-KOH (pH 5.5), 300 µL 10 mM BPDS and 200 µL 10 mM Fe-HEDTA were added. Petri plates without plants were used as controls. The Fe^{3+} from Fe-HEDTA solution was reduced to Fe^{2+} by the reductase activity. After 10, 20 and 40 min, 0.4 mL of the solution was removed and added to 0.4 mL of distilled water in a cuvette. Absorbance was determined photometrically at 535 nm. Subsequently the fresh mass of the roots was measured. The concentration of Fe^{2+}-BPDS was determined using Lambert-Beer's law $A = \varepsilon \cdot c \cdot d$ where:

A = Absorbance
ε = 22,140 [L/mol·cm] (extinction coefficient of BPDS)
c = concentration
d = 1 cm (width of the cuvette).

The reduction rate was calculated by linear regression from the measured time points, and these values were normalized to root mass (nmol/min/mg).

3.3.19 Measurement of chlorophyll content (Porra et al., 1989)

Leave were harvested and placed in 2 ml Eppendorf Safe-Lock® tubes. All work was done on ice, and the samples were protected from the light. The fresh mass was determined per tube and 1 ml of extraction buffer was added (Table 5). Three steel beads were added, and the samples were homogenized in the Retsch® mill for 2 min at 30 Hz. Finally, the samples were sonicated for 10 min in an ice-cooled ultrasonic bath. They were then mixed briefly, centrifuged for 10 min at 10,000 rpm and 4° C and decanted into a new 2 mL Eppendorf Safe-Lock® tubes. Samples were vortexed and centrifuged as above. The absorption at the wavelengths 537 nm, 646.6 nm, 663.6 nm and 720 nm was measured in a UV cuvette. Acetone was used as a blank. The concentration of chlorophyll a and b was measured using the formula: Chl_a [µM] = $12.25 \cdot A_{663.6} - 2.55 \cdot A_{646.6}$ and

$$Chl_b \text{ [µM]} = 20.31 \cdot A_{646.6} - 2.55 \cdot A_{663.6}.$$

Chlorophyll content was normalized to fresh mass (FM).

$$Chl\ [nM/mg] = \frac{c\ [\mu M] \cdot V\ [mL]}{m\ FM\ [mg]}$$

3.3.20 Anthocyanin measurement (Mita et al., 1997)

The samples were placed in Eppendorf Safe-Lock® tubes, 1 mL of acidic methanol (methanol containing 1% (v/v) 37% HCL) and homogenized in the Retsch® mill for 5 min at 30 Hz. The samples were stored overnight at 4° C. The following day, the samples were centrifuged (20

min, 13,000 *g* at 4° C) and stored on ice. For measurements, 0.98 ml of the supernatant was removed and transferred into a cuvette. The relative anthocyanin concentration per fresh mass was calculated by the following formula.

-

$$C_{rel}\left[\frac{AE}{mg}\right] = \frac{A_{530nm} - (0{,}25 \cdot A_{657nm})}{FM\,[mg]}$$

3.3.21 Measurement of root length

The seeds were sterilized and placed in a row on Petri plates containing ES solid medium. After two d stratification in the dark, the Petri plates were placed in the growth chamber. After 2 weeks seedlings were transferred to plates with or without Fe. Root length, was determined after 7 and 14 d. Photographs were taken of the Petri plates, and roots were measured using the Image J program.

4 Results

Iron (Fe) is stored in seeds either in plastids bound in ferritin or concentrated in the vacuole. Because of its propensity to form free radicals in an aerobic environment, the concentration of Fe in organisms is tightly regulated. With the goal of this thesis being the testing of strategies to increase the concentration of storage Fe in plants without affecting their overall growth performance, we have investigated the effects of over-expression of the vacuolar transporters-like family (VTL) on Fe content. In addition, to improve the transport and distribution of Fe in the plant, we doubly over-expressed the *NAS3*

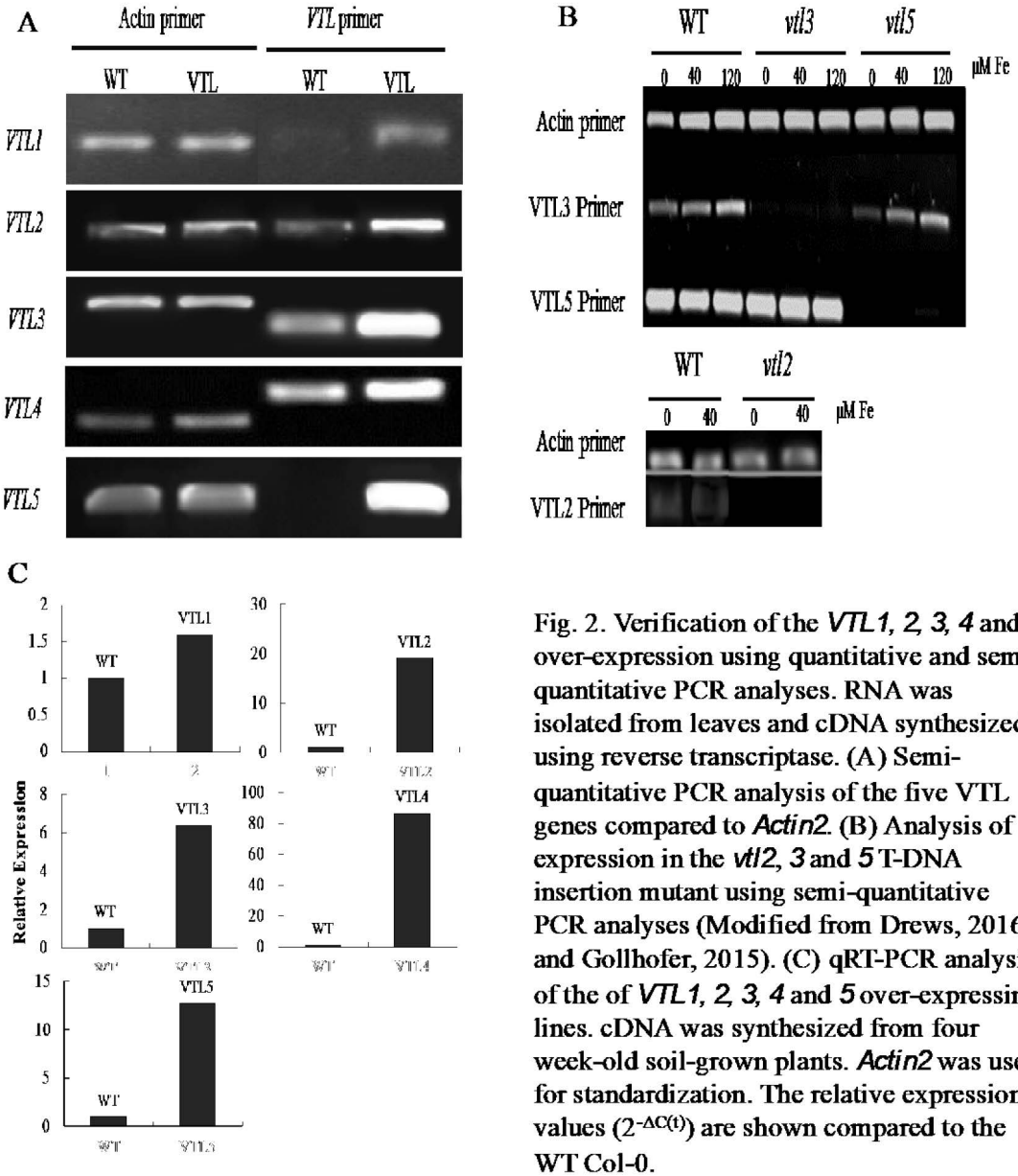

Fig. 2. Verification of the *VTL1, 2, 3, 4* and *5* over-expression using quantitative and semi-quantitative PCR analyses. RNA was isolated from leaves and cDNA synthesized using reverse transcriptase. (A) Semi-quantitative PCR analysis of the five VTL genes compared to *Actin2*. (B) Analysis of expression in the *vtl2, 3* and *5* T-DNA insertion mutant using semi-quantitative PCR analyses (Modified from Drews, 2016 and Gollhofer, 2015). (C) qRT-PCR analysis of the of *VTL1, 2, 3, 4* and *5* over-expressing lines. cDNA was synthesized from four week-old soil-grown plants. *Actin2* was used for standardization. The relative expression values ($2^{-\Delta C(t)}$) are shown compared to the WT Col-0.

(*nicotianamine synthase-3*) and *VTL5* genes. The nicotianamine synthase synthesizes the non-proteogenic amino acid nicotianamine (NA) that plays a major role in transport and distribution of Fe in plants.

4.1 Analysis of Over-Expression of *AtVTL1*, *2*, *3*, *4* and 5

At present, it is not known if the function of each of the VTL proteins is unique and essential or if they are redundant in their function. The function of these proteins is being unraveling by establishing stably over-expressing lines and determining the seed Fe content. Each VTL gene has been over-expressed under the control of a constitutive CaMV35S promoter. These over-expressing lines were made available in part from previous work in our lab (Gollhofer et al., 2014). Since there is no evidence that all the lines were homozygous, all lines were reselected 3 times with BASTA® as a resistant marker. Plants were self-pollenated to obtain a T_5

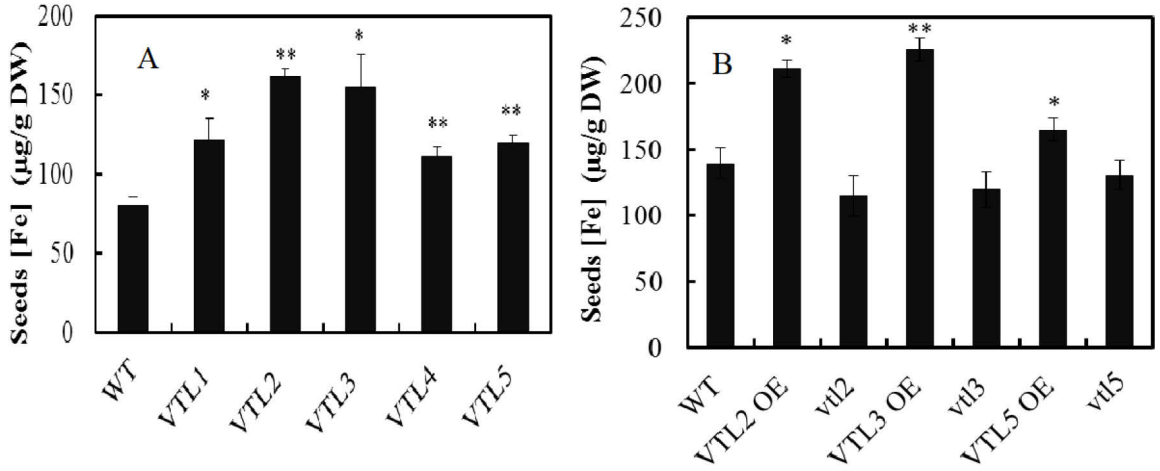

Fig. 3. Analysis of seed Fe in VTL over-expression plants. (A) Seed Fe content of soil-grown Arabidopsis plants over-expressing *VTL1, 2, 3, 4* and 5. (B) Analysis of seed Fe content in the T-DNA mutants vtl2, vtl3 and vtl5 and the corresponding over-expressing lines. * $p \leq 0.05$, ** $p \leq 0.01$. Values are an average of samples taken from at least 3 individual plants.

generation, and over-expression in these plants was confirmed by semi quantitative PCR (Fig. 2A). Expression of knockout T-DNA mutants *vtl2*, *vtl3* and *vtl5* was also determined at different Fe concentrations (Fig. 2B), confirming the lack of expression of the mutated genes. Previous results implicated the VTL proteins in regulation of Fe homeostasis in Arabidopsis, and VTL1 and 2 have been localized to the vacuolar membrane in Arabidopsis (Gollhofer et al., 2011, 2014). To understand the physiological and biological roles of the *VTL* genes, the expression of the T_5 generations of all *VTL* overexpressing lines was also analyzed by qPCR (Fig. 2C). The relative over-expression ranged from ca. 1.6-fold for *VTL1* to 80-fold for *VTL4* compared to the WT.

4.1.1 Analyzing Fe Content and Fe Localization in VTL Over-Expressing Arabidopsis

For analysis of the Fe content in seeds, plants were grown on soil in the greenhouse to maturity, seeds were harvested and their Fe content was analyzed. The seed Fe content in the over-expressing lines *VTL 1*, *2*, *3*, *4* and *5* was greater than the WT (Fig. 3A). The investigation of

the Fe content revealed that in *VTL2*, *VTL3* and *VTL5* over-expressing lines, the Fe content was highest of the five over-expression lines compared to the WT. These results were taken as evidence for a role of the VTLs in storage of seed Fe. The Fe content in the knockout mutants *vtl2*, *vtl3* and *vtl5* was also investigated. The results showed that seed Fe content was somewhat less in the mutants than in the WT, but the decrease was not statistically significant (Fig. 3B). The contribution to seed Fe storage of these three VTL proteins individually appeared to be relatively minor in the WT.

The localization of Fe in Arabidopsis embryos was visualized using Perls' staining followed by DAB intensification as indicated in Fig. 4. In the WT embryo, localization of Fe in the provascular system was clearly visible. In all VTL-OE lines the localization of Fe was indistinguishable from the WT when embryos were stained by the Perls' method without DAB intensification. However, when embryos were post-stained with DAB, the ground tissues were more heavily stained in the OE lines. This result was particularly evident in *VTL1*, *3* and *5* OE plants. In *VTL5* OE plants, staining was more intense throughout the embryo particularly at the tip of radicle compare to WT plants (Fig. 4A). Taken as a whole, these data were interpreted as evidence for a role of VTLs in seed Fe storage. In *vtl2*, *3*, *5* knockout mutants, Perls' staining showed the same intensity as the WT (Fig. 4B), thus confirming Fe measurements in seed Fe (Fig. 3B). The Fe distribution was also investigated in the *vit1-1* mutant. In this mutant, Fe was not localization to the provascular stands in the embryo but appeared to be evenly distributed throughout the embryo (Fig. 4B). These observations confirmed the results of Kim et al. (2006).

To further explore localization of seed Fe in the *VTL* over-expressing lines, longitudinal sections of embryo tissues were stained with Perls'-DAB (Roschzttardtz et al., 2009). In WT embryos, the staining was concentrated in the endoderm layer surrounding the provascular

bundle in cotyledons and hypocotyls (Fig. 4C). Fe accumulated strongly in intracellular structures most likely corresponding to vacuoles (Roschzttardtz et al., 2009). Cytoplasmic staining was also visible. In all over-expressing lines, Fe was concentrated in a single cell layer around the provascular bundle and the staining was clearly more intense than in the WT (Fig. 4C)

To determine whether *VTL* genes played a role in Fe in plants in general, Fe content in seedlings and leaves of transgenic plants was determined. WT and over-expressing lines were grown in Fe-sufficient ES medium for 3 weeks and then transferred to Fe-sufficient or deficient ES medium for 2 d. The Fe content was then analyzed. The results showed a

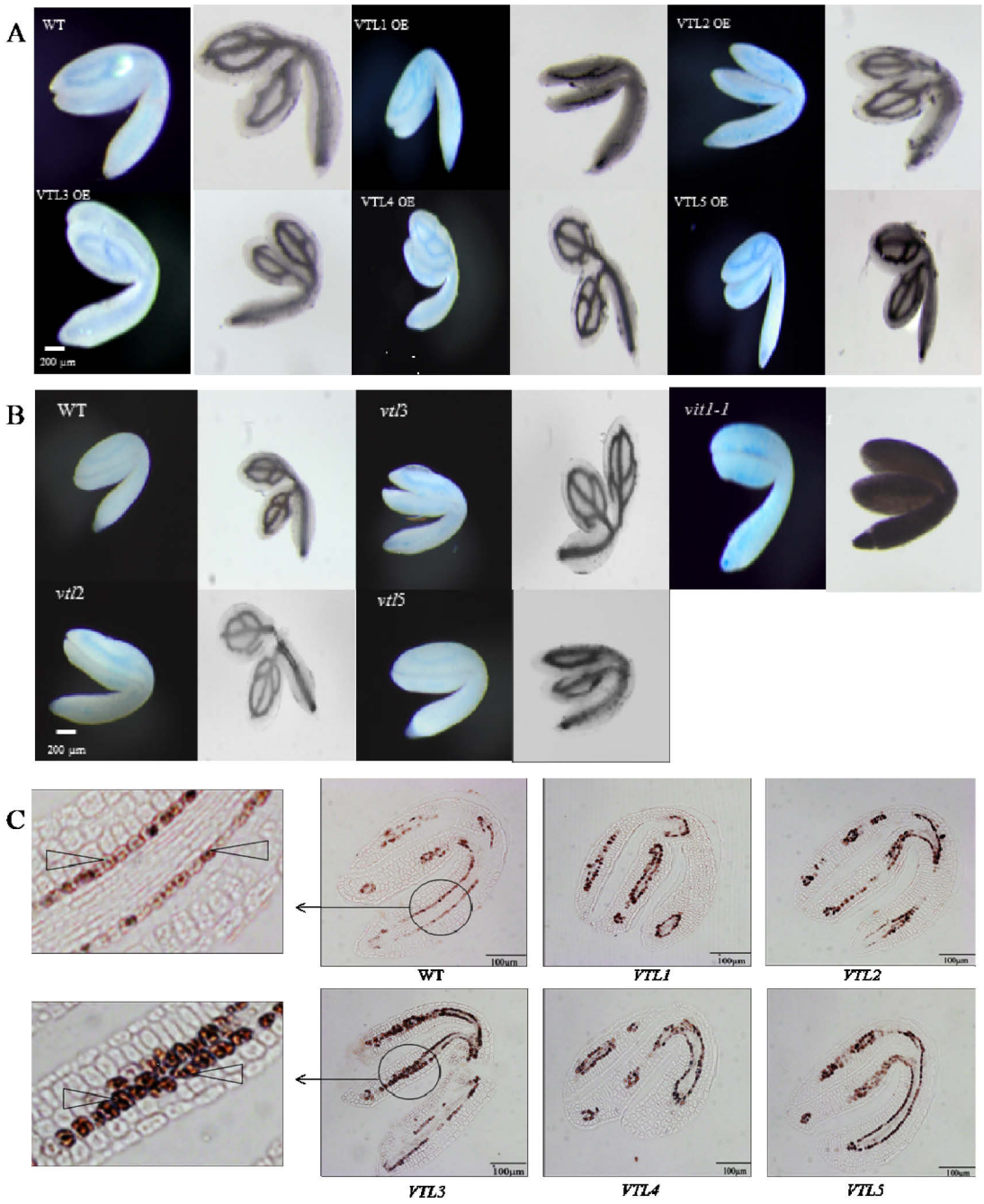

Fig. 4. Fe visualization by Perls' staining of Arabidopsis embryos. Each pair of pictures shows standard Perls' staining on the left with the DAB intensification on the right. Embryos were processed simultaneously to ensure equal staining. (A) Shown is the accumulation of Fe in the embryos for each VTL OE lines and (B) with the corresponding mutant lines *vtl2, 3, 5*. The *vit1-1* mutant is shown for comparison. (C) Longitudinal sections of Perls' stained *VTL* OE lines. The accumulation of Fe in the embryos is evident in vacuoles and the cytoplasm.

tendency for increased Fe content in seedlings in the over-expressing lines, but in nearly all cases these increases were not significant compare to WT (Fig. 5A and B). Similar to the results in seedlings, Fe content in leaves from soil-grown plants was tendentially higher in the over-expression plants but again in most cases not significantly different from the WT (Fig. 5C). An analysis of the chlorophyll a/b ratios (Fig. 5D) and the anthocyanin content (Fig. S5) as

indicators of oxidative stress showed no significant differences to the WT plants. Taken

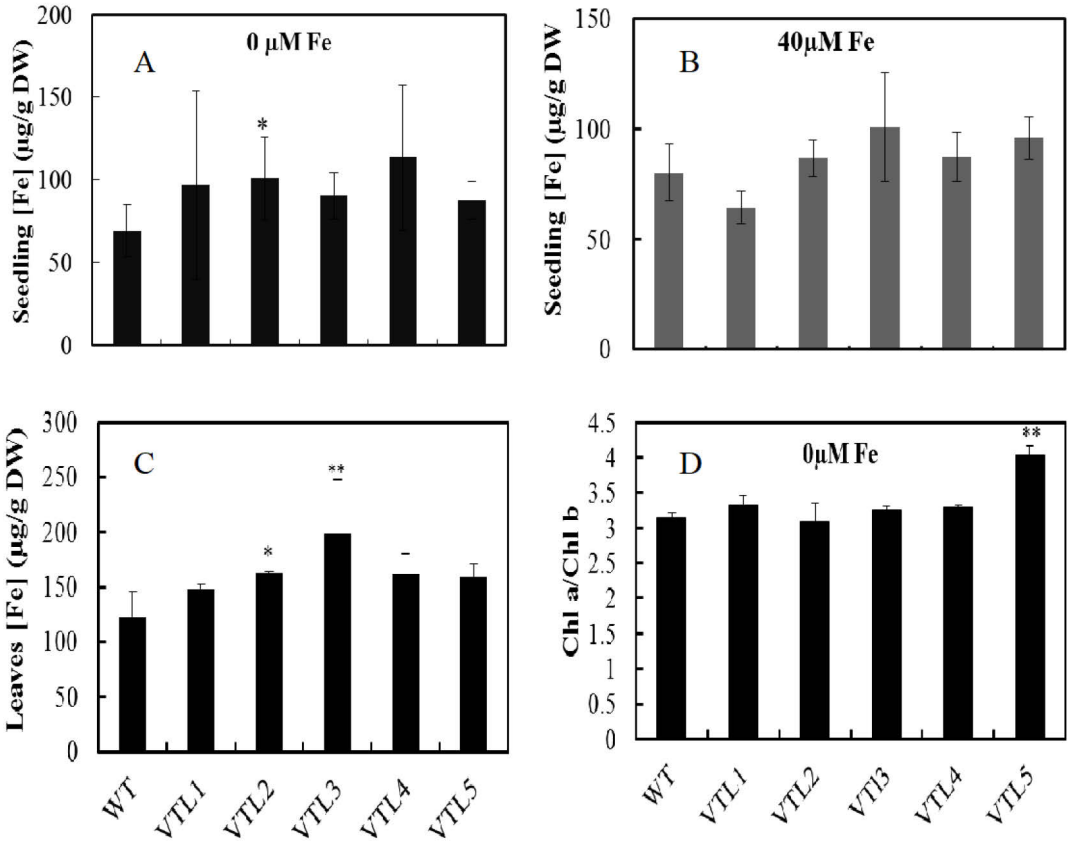

Fig. 5. Fe content and the Chl a/Chl b ratio in Arabidopsis plants over-expressing *VTL1, 2, 3, 4* and *5*. Fe was determined in seedlings from hydroponically grown plants in the presence of 0 (A) or 40 µM Fe (B) and from leaves of soil-grown plants (C). (D) The chlorophyll a/b ratio in WT and *VTL1, 2, 3, 4* and *5* over-expressed lines is shown. Statistical significance in comparison to the WT Col-0 was determined using an unpaired t-test with 3 replications (*, $p < 0.05$; **, $p < 0.01$).

together, these studies demonstrated that over-expression of the *VTL* genes led to significant increases in Fe content in seeds but that these increases were generally not found in other plant organs compared to the WT.

4.1.2 Root Growth and Fe Content in VTL1, 2, 3, 4 and 5 OE Lines

In order to identify the role played by *VTL* genes in roots, Fe content and root length were analyzed in the over-expression lines. This investigation showed that in roots of *VTL3* and *4* over-expression plants, the Fe content was greater than the WT control, while in *VTL 1, 2* and *5* over-expressing plants no change in Fe content was detected (Fig. 6A). The root length in

VTL4 and *5* over-expressing lines was shorter compared to the WT when grown both on Fe deficient and sufficient media (Fig. 6B). In contrast, primary root length was largely unchanged in *VTL1*, *2* and *3* over-expressing roots with only *VTL2* over-expressing roots showing an

increased root length in plants grown under Fe deficiency (Fig. 6B). Since the

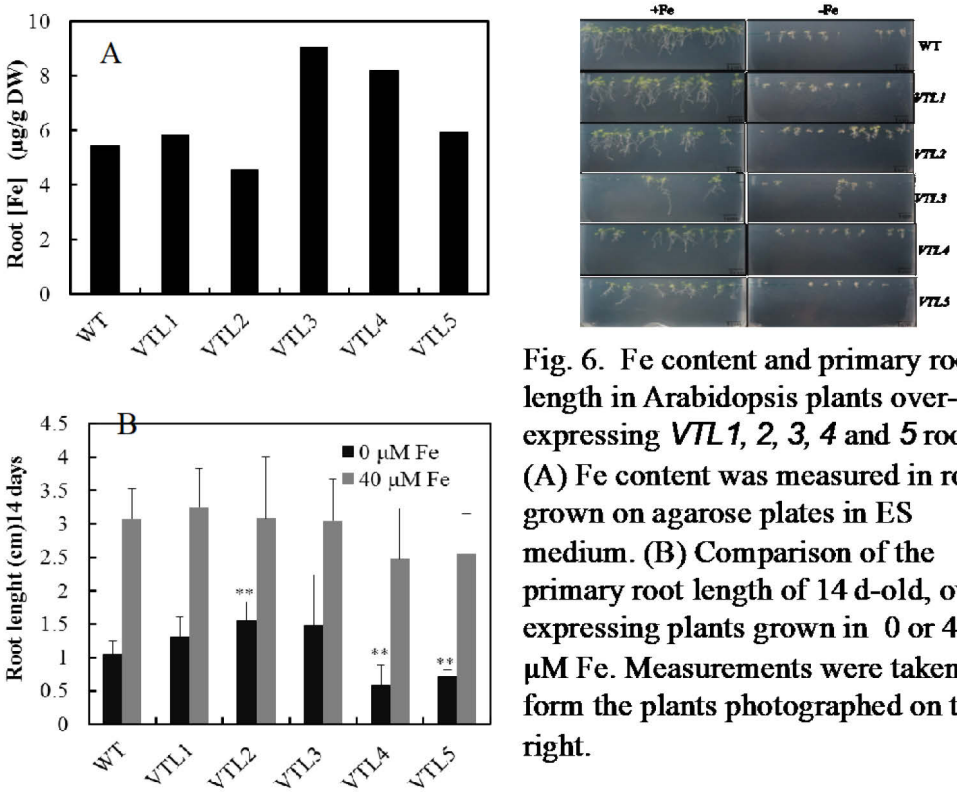

Fig. 6. Fe content and primary root length in Arabidopsis plants over-expressing *VTL 1, 2, 3, 4* and *5* roots. (A) Fe content was measured in root grown on agarose plates in ES medium. (B) Comparison of the primary root length of 14 d-old, over-expressing plants grown in 0 or 40 µM Fe. Measurements were taken form the plants photographed on the right.

changes in root growth did not correlate with Fe content, Fe content did not seem to be the direct cause of altered root growth.

4.1.3 Fe^{3+}-Chelate Reductase Activity and FRO2 and IRT1 Expression in VTL OE Lines

FRO2 belongs to an eight member gene family that encodes Fe^{3+}-chelate reductases. *FRO2* and *IRT1* play a major role in the Fe uptake mechanism in Arabidopsis and are both subjected to translational and to post-translational regulation. Over-expression of the *VTL* genes has been shown to increase Fe storage in Arabidopsis seeds (Fig. 3). To assess the effect of over-expression on Fe homeostasis, the Fe^{3+}-chelate reductase activity and the expression of *FRO2* and *IRT1* in the VTL OE lines were investigated. For measurement of the reductase activity, plants were grown for 3 weeks in Fe-sufficient medium and then for one week in 0 µM or 40 µM Fe. These experiments showed that in all VTL OE lines the Fe^{3+}-chelate reductase activity was lower under Fe deficiency than in the WT (Fig. 7A). The reductase activity in Fe-sufficient roots was relatively low and difficult to accurately measure.

The expression of *FRO2* and *IRT1* was investigated in four of the five VTL OE lines. With a greater than 2-fold change being regarded as significant, the transcript abundance of *FRO2* and *IRT1* in plants grown in 0 µM Fe was, with one exception, significantly decreased. *VTL5* transcript abundance for *FRO2* was decreased by approximately 30% compared to the WT.

Again with one expection, the expression of *FRO2* and *IRT1* in Fe-sufficient plants was higher in VTL over-expressing plants than in the WT (Fig. 7B and C). The *IRT1* expression in *VTL2* OE, Fe-sufficient plants was slightly lower than the WT (Fig. 7C). In general, it appeared that under Fe deficiency an increased Fe supply in the VTL overexpressing plants resulted in a corresponding increased resistance to Fe deficiency; whereas under Fe sufficiency the over-expression of the VTL genes increased the sink strength for Fe and thus also the expression of *FRO2* and to a less extent of *IRT1* compared to the WT (Fig 7B and C).

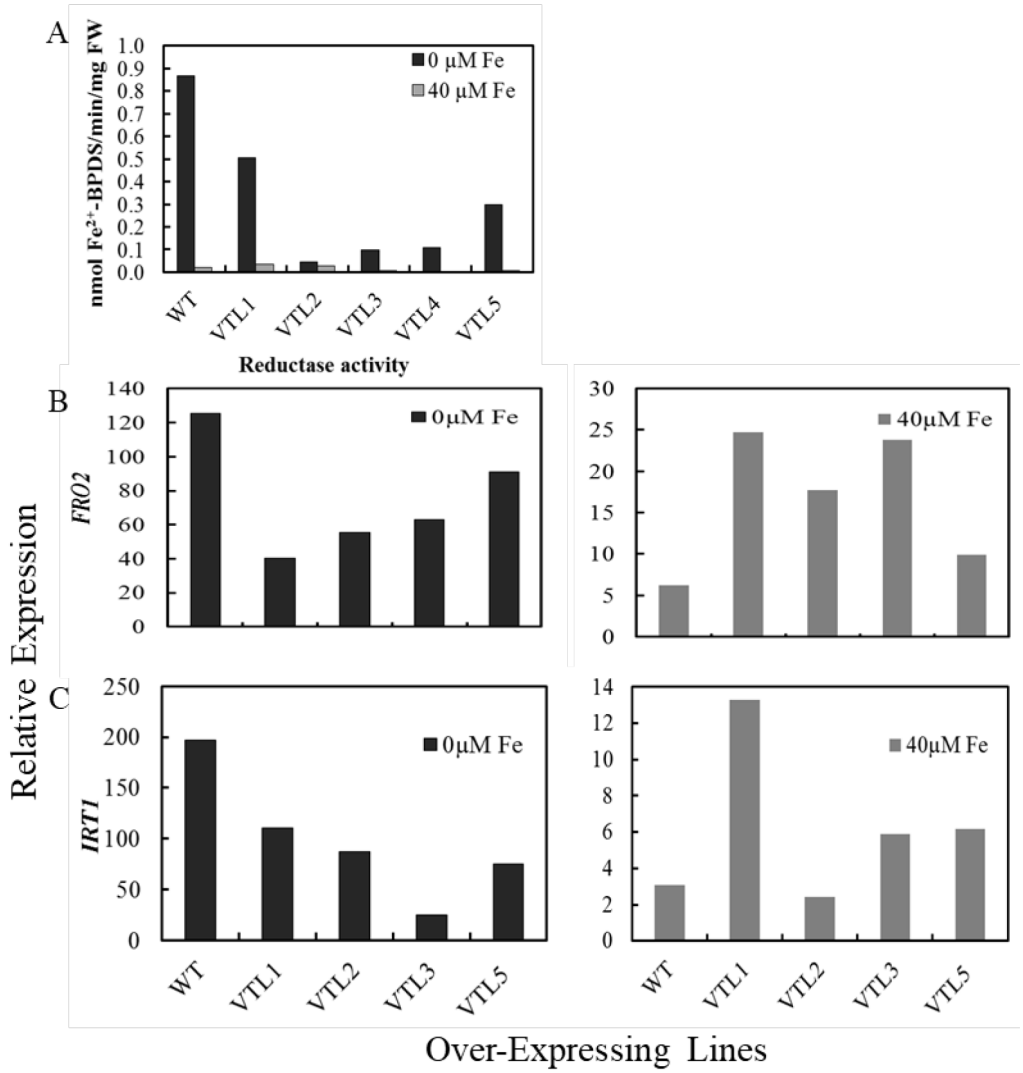

Fig. 7. Response of Fe uptake processes in *VTL1*, *2*, *3*, *4* and *5* over-expressing lines. (A) Analysis of Fe^{3+}-chelate reductase activity in the WT and *VTL1*, *2*, *3*, *4* and *5* over-expressing lines. The activity was calculated by linear regression of values taken at 10, 20 and 40 min. The Pearson correlation (r^2) coefficient was greater than 0.9 for all measurements. qRT-PCR analysis of *FRO2* (B) and *IRT1* (C) transcript abundance in the over-expressing lines. cDNA was synthesized from four week-old soil-grown plants. *Actin2* was used for standardization. The relative expression values ($2^{-\Delta C}(t)$).

4.1.4 Expression of Fe Homeostasis Genes in the VTL1, 2, 3 and 5 OE Lines

In the previous section the expression of *FRO2* and *IRT1* in the over-expressing lines indicated possible resistance to Fe deficiency and to an increased the sink strength in plants that were grown on sufficient Fe (3.1.3 and Fig. 7). To strengthen this hypothesis, gene expression was investigated by qPCR for four transcription factors known to participate in regulation of the Fe-deficiency response and a ferritin gene involved in Fe storage (Fig. 8).

Although the *VTL* genes were not regulated by the bHLH transcription factor FIT (bHLH29; Colangelo, et al, 2004; Buckhout et al., 2013), the effect of VTL over-expression was investigated in *bHLH39* and *MYB72*, a gene highly induced under Fe deficiency. *bHLH39* is one member of bHLH subgroup Ib transcription factors that along with three other members has been shown to form a heterodimer with FIT. It is the heterodimer that regulated gene expression in the so called FITome in response to Fe deficiency. The expression of MYB72 was induced by Fe deficiency in a FIT-dependent manner (Colangelo, et al, 2004). MYB72 is also required for induced systemic resistance (ISR) in Arabidopsis roots (Sagarra et al., 2009), and MYB72, along with its close paralog MYB10, is required for survival under Fe deficiency through the regulation of the nicotianamine synthase gene *NAS4* (Palmer et al., 2013).

Although the transcript abundance for both bHLH39 and MYB72 was not altered in plants grown under Fe deficiency (0 μM Fe), in the VTL over-expressing plants, their expression was significantly increased when plants were grown under an Fe sufficient supply (40 μM Fe). These data were interpreted in support of the hypothesis that over-expression of the VTL genes increased the sink strength for Fe and thus resulted in induction of *bHLH39* and *MYB72*.

A second group of bHLH transcription factors belonging to the bHLH subgroup IVc (POPEYE (PYE, bHLH047) and the PYE-like IAA-LEUCINE RESISTANT3 (ILR3,

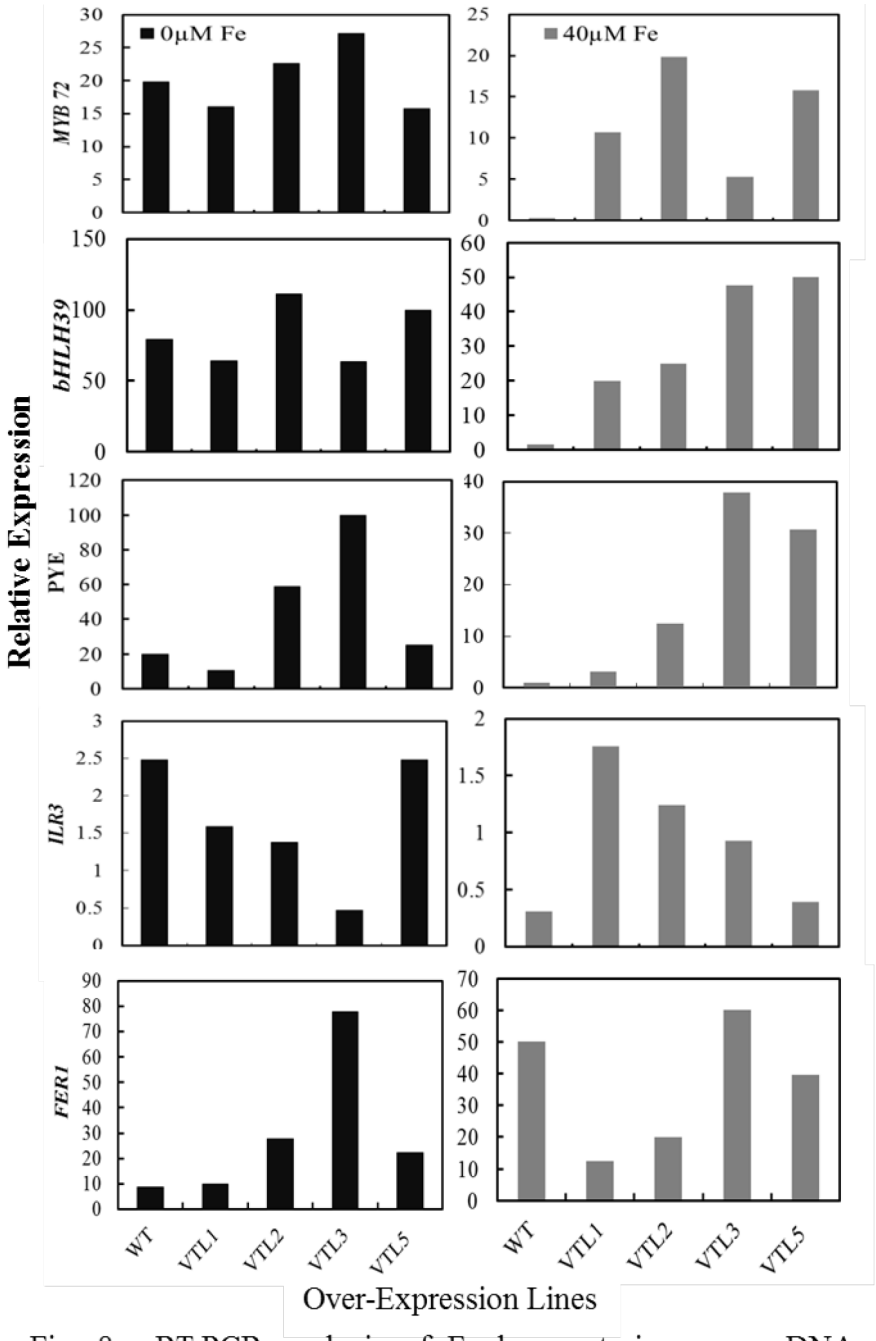

Fig. 8. qRT-PCR analysis of Fe homeostasis genes. cDNA was synthesized from four week-old soil-grown plants. *Actin2* was used for standardization. The relative expression values ($2^{-\Delta C(t)}$) are shown

bHLH105)) was investigated (Fig. 8). These transcription factors regulated aspects of the Fe deficiency response independent of FIT. PYE was shown to interact with ILR3 and two other subgroup IVc factors. The heterodimers bound to the promoters of Fe deficiency regulated genes not being regulated by FIT. Loss of function of bHLH IVc factors led to an increased

sensitivity to Fe deficiency, while over-expression caused increased Fe uptake (Long et al., 2010).

Under Fe sufficient growth the expression of *PYE* and *ILR3* was increased with one expection compared to their expression in the WT (Fig. 8). However, when grown under Fe-deficient conditions the transcriptional response was more complex. The expression of PYE was unchanged in the *VTL1* and *5* but increased in the *VTL2* and *3* OE lines compared to the WT (Fig. 8). With the exception of *VTL3* OE, which was decreased compared to the WT, expression of *ILR3* was largely unchanged. In summary, the increased expression of *PYE* and *ILR3* in the over-expressing lines grown under Fe-sufficient conditions was a result consistent with an increased sink demand for Fe.

Finally *FER1* expression, with the exception of *VTL1*, in VTL OE lines was increased in plants grown under Fe deficient conditions compared to the WT control (Fig. 8), while under Fe sufficient conditions expression was either unchanged or slightly decreased compared to the WT. In general the expression of *FER1* as with the expression of the bHLH transcription factors in the over-expression lines would support an increased sink demand for Fe in Fe-sufficient and an increased Fe supply in Fe-deficient VTL OE lines (Fig. 8).

4.1.5 Molecular and Physiological Analysis of *IronMan1* (*IMA1*)

IronMan1 (At1g47400; *IMA1)* is a small 50 amino acid peptide that is conserved in plants and is induced strongly in response to Fe deficiency (Buckhout and Schmidt., 2013). Over-expression of *IMA1* resulted in a constitutive Fe deficiency response in Arabidopsis. This observation has recently been published (Hirayama et al., 2018; Gillet et al. 2018). *IMA1* was induced under

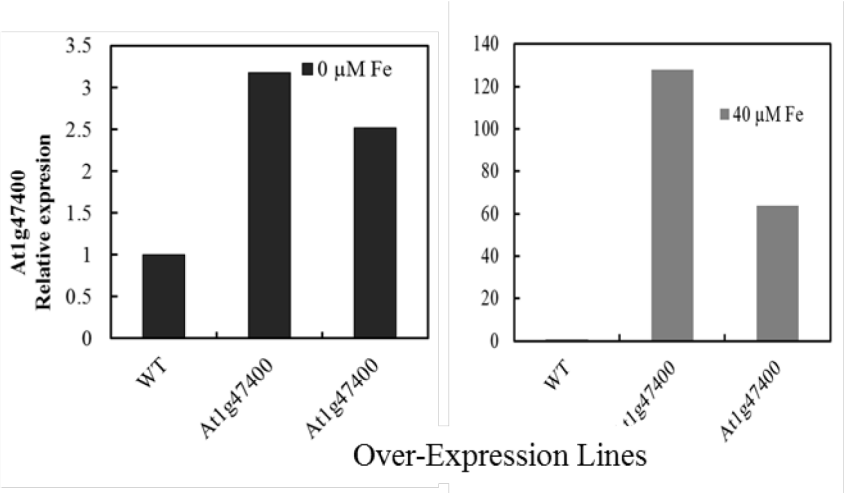

Fig. 9. qRT-PCR analysis of two At1g47400 over-expressing plants. Plants were grown hydroponically in 40 or 0 Fe medium. cDNA was synthesized from 4 week old soil-grown plants. *Actin2* was used for standardization of At1g47400. The relative expression values ($2^{-\Delta\Delta C(t)}$) of At1g47400 are shown with respect to the WT.

Fe deficiency and played a major role in Fe homeostasis by affecting Fe-deficiency-regulated genes. Seeds of an over-expressing *IMA1* line were obtained from laboratory of Prof. Wolfgang Schmidt (Grillet et al., 2018), and the over-expression was varified by qPCR in two different *IMA1* plants that were grown in the presence or absence of Fe (Fig. 9).

4.1.6 Determination of the Fe Content in IMA1 OE Lines

Under Fe deficeincy *IMA1* transcripts were enhanced in leaves and roots (Grillet et al., 2018). In the over-expressing *IMA1* line the Fe content in seeds, roots, leaves and seedlings was determined with the result that in seeds the Fe content was approximately twice that of the WT (Fig. 10A). The Fe content in *IMA1* seedlings that were grown either in 0 or 40 µM Fe was approximately triple that of the WT (Fig. 10B). Finally in leaves and roots of the IMA OE line, the Fe content was double and quadruple that found in the WT, respectively (Fig. 10C). Clearly, over-expression of *IMA1* resulted in increased Fe content in all organs tested.

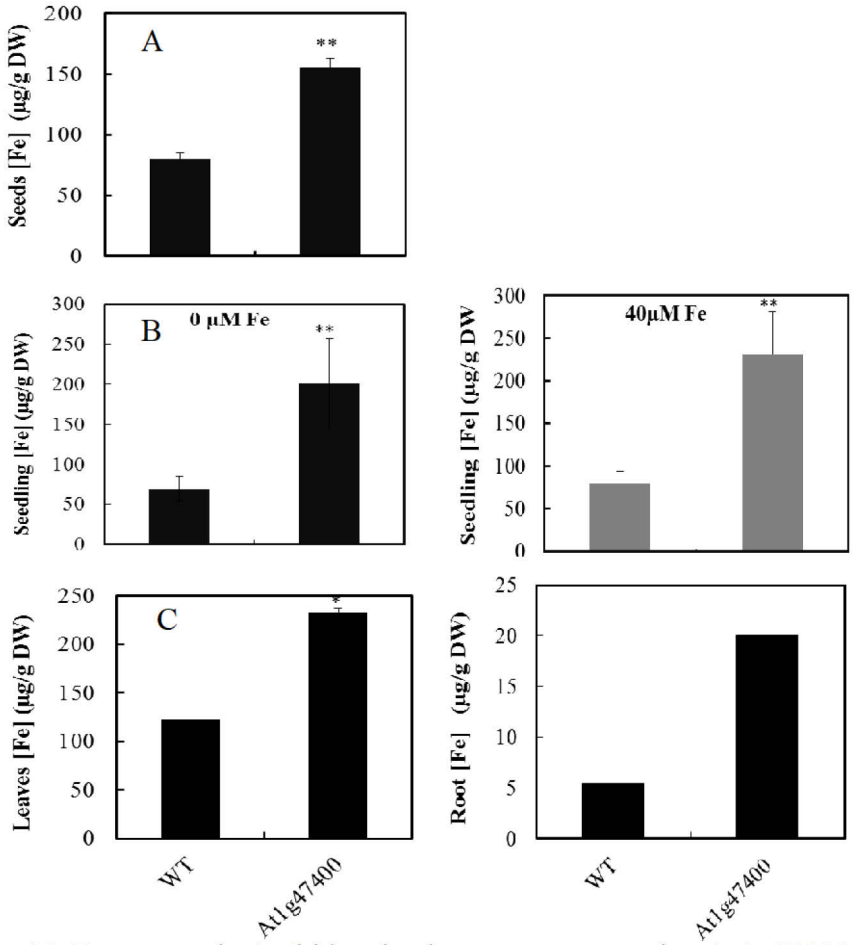

Fig. 10. Fe content in Arabidopsis plants over-expressing At1g47400 (***IMA1***). **(A) Fe was measured in seeds and (B) seedlings from hydroponically grown plants in the presence of 0 and 40 µM Fe. (C) Fe content in leaves from soil-grown plants and (D) in roots grown on ES solid medium. Statistical significance in comparison to the WT Col-0 was determined using an unpaired t-test with 3 replications (* $p < 0.05$; ** $p < 0.01$).**

4.1.7 Localization of Leaf Fe in an IMA1 Over-Expressing Plants

Fe was localized by the method of Perls with DAB intensification (Roschzttardtz et al., 2009). Three µm cross sections were made at the Naturekundemuseum Berlin. Perls – DAB staining was observed in mesophyll cells as dark blue particles located on the periphery of cells at a

location commonly occupied by chloroplasts (Fig. 11). These dot-shaped particles have been identified in association with ferritin, since they were not found in ferritin mutants (Duvol et

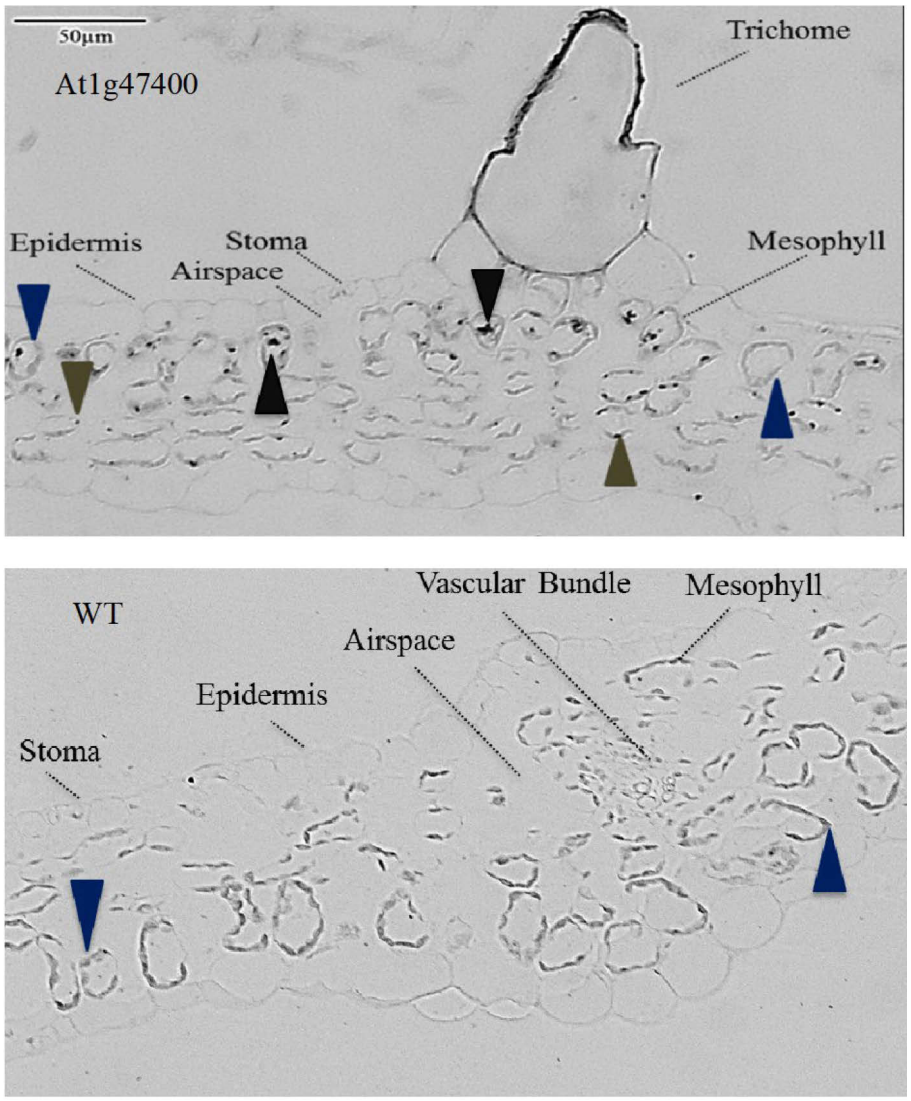

Fig. 11. Localization of Fe by Perls' staining with DAB intensification in a cross-section of an Arabidopsis At1g47400 over-expressing leaves.

al., 2013; Reyt et al., 2014). Additionally relatively large particles were centrally located in cells at a position corresponding to the vacuole. However, most cells showed no staining in the vacuolar region. In the epidermis staining was only observed in guard cells. These results are indicative of a role for IMA1 in regulating Fe storage.

Whereas severe Fe deficiency is known to inhibit root growth, mild Fe deficiency stimulated primary root growth (Gruber et al., 2013). We analyzed primary root growth in the *IMA1* over-expression plants. As expected, the root length in plants grown in the absence of Fe was decreased compared to plants grown in the presence of Fe (Fig. 12). There was no significant

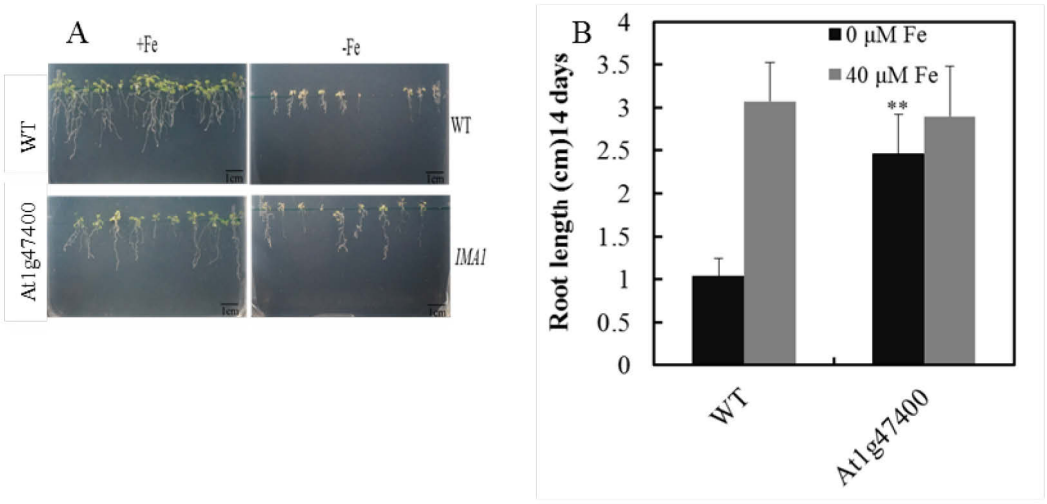

Fig. 12. Root length as affected by Fe supply of Arabidopsis WT and At1g47400 OE plants. (A) Roots grown with or without Fe on ES solid medium. (B) Root length was determined after 14 d of growth. (** $p < 0.01$)

difference in length between WT and *IMA1* over-expressing plants; however, when grown in the absence of Fe the *IMA1* over-expressing roots were significantly longer that the WT. Thus, it appeared that over-expressing plants showed increased resistance to Fe deficiency compared to the WT.

4.1.8 Response of IMA1 Over-Expressing Plants to Fe Deficiency

In all nongrass plants, Fe acquisition starts with Fe^{3+} reduction by the activity of *FRO2*-encoded Fe^{3+}-chelate reductase. The resulting Fe^{2+} is then taken up the ZIP-type transporter IRT1 (Robinson et al., 1999; Vert et al., 2002). In *IMA1* OE plants the Fe content was higher in roots, seedlings, leaves and seeds compared to the WT (Fig. 10). To understand the mechanism of this Fe increase, Fe acquisition processes were investigated by analyzing the

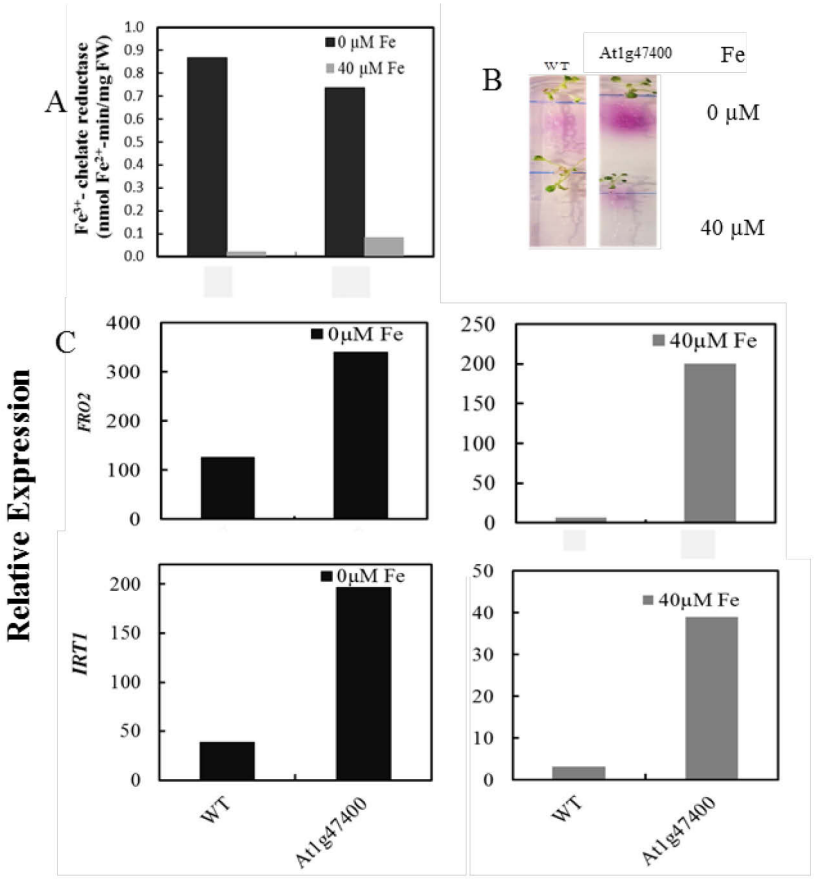

Fig. 13. Response of At1g47400 over-expression to Fe deficiency. (A) Fe^{3+}-chelate reductase activity in the WT and At1g47400 over-expressing plants was measured at 10, 20 and 40 min. The reductase rate was determined by linear regression. (B) Visualization of Fe^{3+}-chelate reductase in WT and At1g47400 plants. (C) qRT-PCR analysis of *FRO2* and *IRT1* in At1g47400 over-expression plants. The *Actin2* was used for standardization. The relative expression values were calculated as $2^{-\Delta C(t)}$.

Fe^{3+}-chelate reductase activity and the expression of *FRO2* and *IRT1*. The results showed that the effect of *IMA1* OE was most promenant in Fe sufficient plants (Fig. 13). The slope of the Fe reductase activity in *IMA1* OE plants in the presence of Fe was higher but in the absence of Fe the activity was similar to the WT (Fig. 13A). This response was also observed when Ferrozine® was used to visualize Fe^{2+} (Fig. 13B) . Similarly the expression of *FRO2* and *IRT1* in Fe sufficient plants was greatly increased with respect to the WT (Fig. 13C). In conclusion, *IMA1* OE plants showed a constitutive Fe deficiency response regardless of the Fe supply.

4.1.9 Expression of Iron Homeostasis Genes in IMA1 OE Plants

The Fe homeostasis pathway contains several genes that were regulated in response to Fe deficiency. To determine the response of this pathway in the *IMA1* OE plants, the expression

of *MYB72*, *bHLH39*, *PYE*, *ILR3* and *FER1* were investigated. These genes have been presented and discussed in a section 3.2.3 above. As was observed with *IRT1* and *FRO2*,

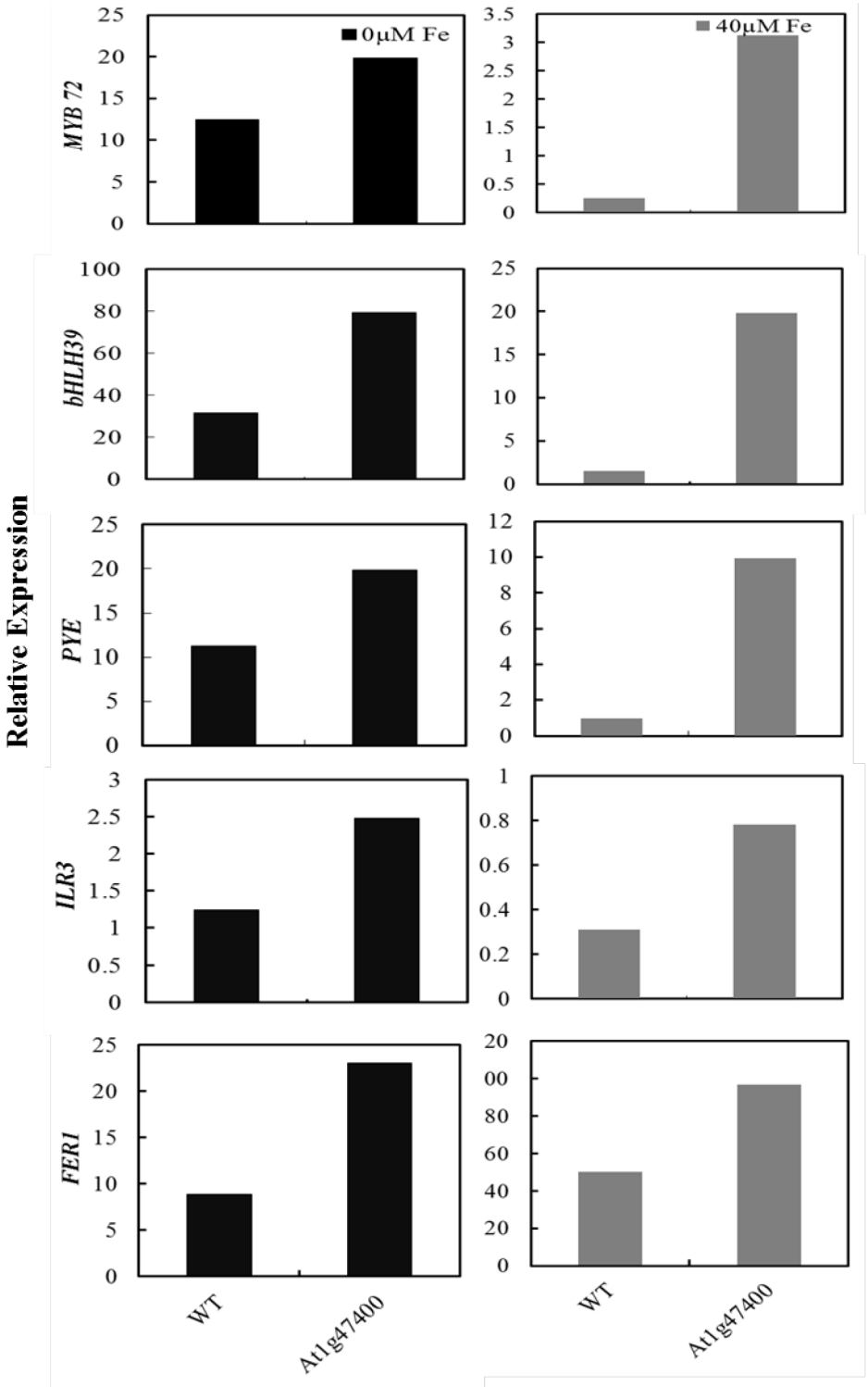

Fig. 14. Expression of Fe-responsive genes in At1g47400 over-expressing plants. cDNA was synthesized from four week-old soil-grown plants. The *Actin2* was used for standardization. The relative expression values ($2^{-\Delta C(t)}$) for *MYB72*, *bHLH39*, *PYE*, *ILR3* and *FER1* are shown.

the expression of all genes analyzed was greatly increased in the over-expressing lines compared to the WT (Fig. 14). However, with the exception of *FER1*, the fold increase of transcript abundance in *IMA1* OE plants was less in Fe-deficient compared to Fe-sufficient plants. Thus the effect of *IMA1* OE is more pronouced under Fe sufficient growth. The increased expression of *FER1* was consistent with an increased Fe content in the over-expressing plants regardless of Fe supply.

4.1.10 *VTL2*, *3*, *4* and *5* and *IMA1* Expression in Double Over-Expressing Plants

Because over-expression of both *IMA1* or the VTL genes led to an increase in Fe content in Arabidopsis (Figs. 3 and 10), we tested whether the over-expression of both genes might have a synergistic effect on the Fe content. To achive our goal of enhancing the Fe content in plants, IMA1 OE and VTL OE plants were crossed to obtain double over-expressing lines. Expression of *VTL2*, *3*, *4* and *5-IMA1* was confirmed by qPCR (Fig. 15).

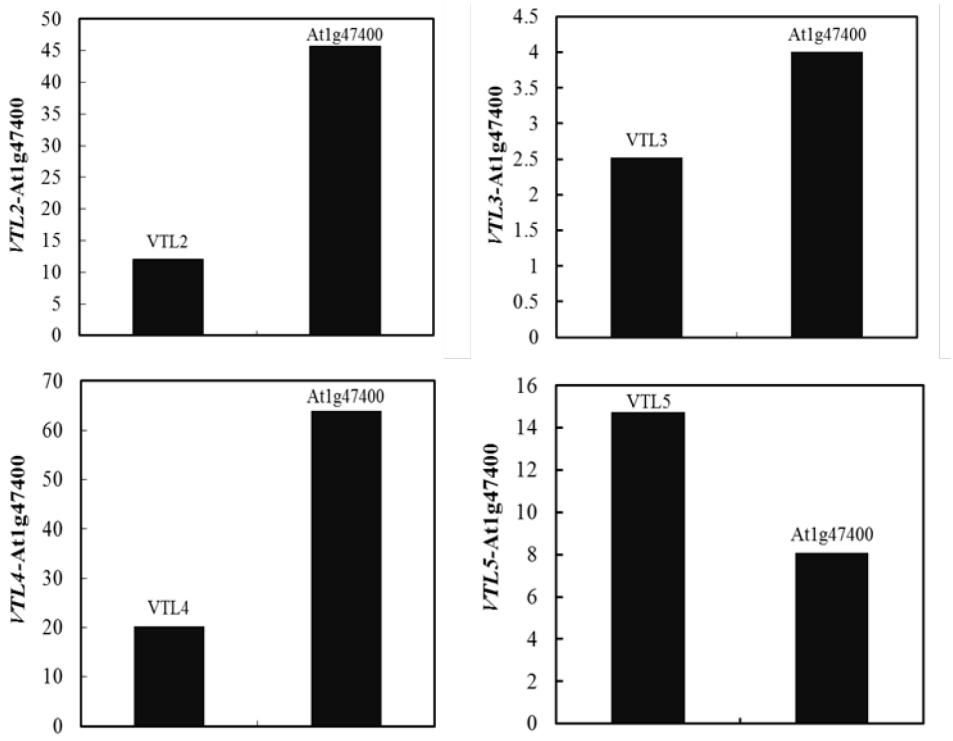

Fig. 15. Expression of *VTL2*, *3*, *4* and *5* and in At1g47400 in the double over-expressing plants. cDNA was synthesized from four week-old soil-grown plants. *Actin2* was used for standardization of in At1g47400 -*VTL2*,*3*,*4*, *5*. The relative expression values ($2^{-\Delta\Delta C(t)}$) are shown with respect to the WT Col-0.

4.1.11 Fe Content in Seeds and Seedlings of IMA1-VTL2, 3, 4 and 5 OE Lines

The Fe content of the double over-expressing lines was determined in seeds, seedlings, leaves and roots (Fig. 16). As shown previously (Figs. 3A and 10A), the seed Fe content in single over-expressing plants was significantly increased over the WT (Fig. 16A). However, double over-expression of the VTLs and *IMA1* resulted in no synergistic increase in seed Fe content (Fig. 16A). Furthermore and with the exception of *VTL2*/*IMA1*, double over-expression resulted in an insignificant increase in Fe content (Fig. 16B, C, D and E). This was the case regardless of the Fe supply or the substrate, whether hydroponics, agarose or soil, on which the plants grew. Additional physiological and molecular analyses including root length mesurments, Fe^{3+}-chelate reductase activity, chlorophyll content and expression of Fe homeostasis genes in the double over-expressing VTL-*IMA1* plants showed no synergetic effect in double over-expressing plants (Figs. S2, S3, S4 and S5).

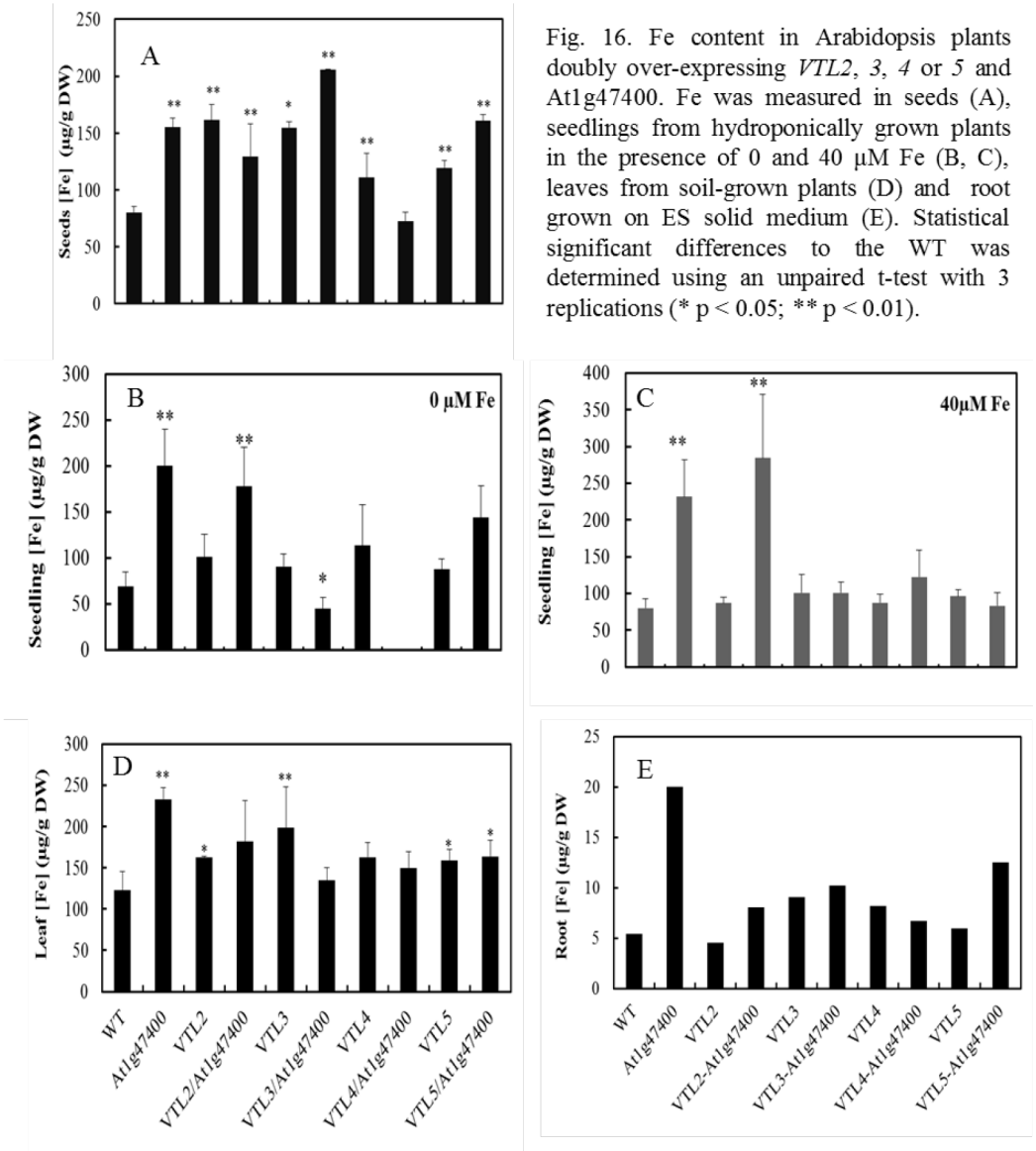

Fig. 16. Fe content in Arabidopsis plants doubly over-expressing *VTL2*, *3*, *4* or *5* and At1g47400. Fe was measured in seeds (A), seedlings from hydroponically grown plants in the presence of 0 and 40 µM Fe (B, C), leaves from soil-grown plants (D) and root grown on ES solid medium (E). Statistical significant differences to the WT was determined using an unpaired t-test with 3 replications (* $p < 0.05$; ** $p < 0.01$).

4.1.12 Expression of VTL1, 2, 3, 4 and 5 in IMA1 Over-Expressing Plants

Surprisingly to us was the observation that double over-expression of two genes that when expressed singly each increased seed Fe content, showed no synergistic effect (Fig. 16A). We

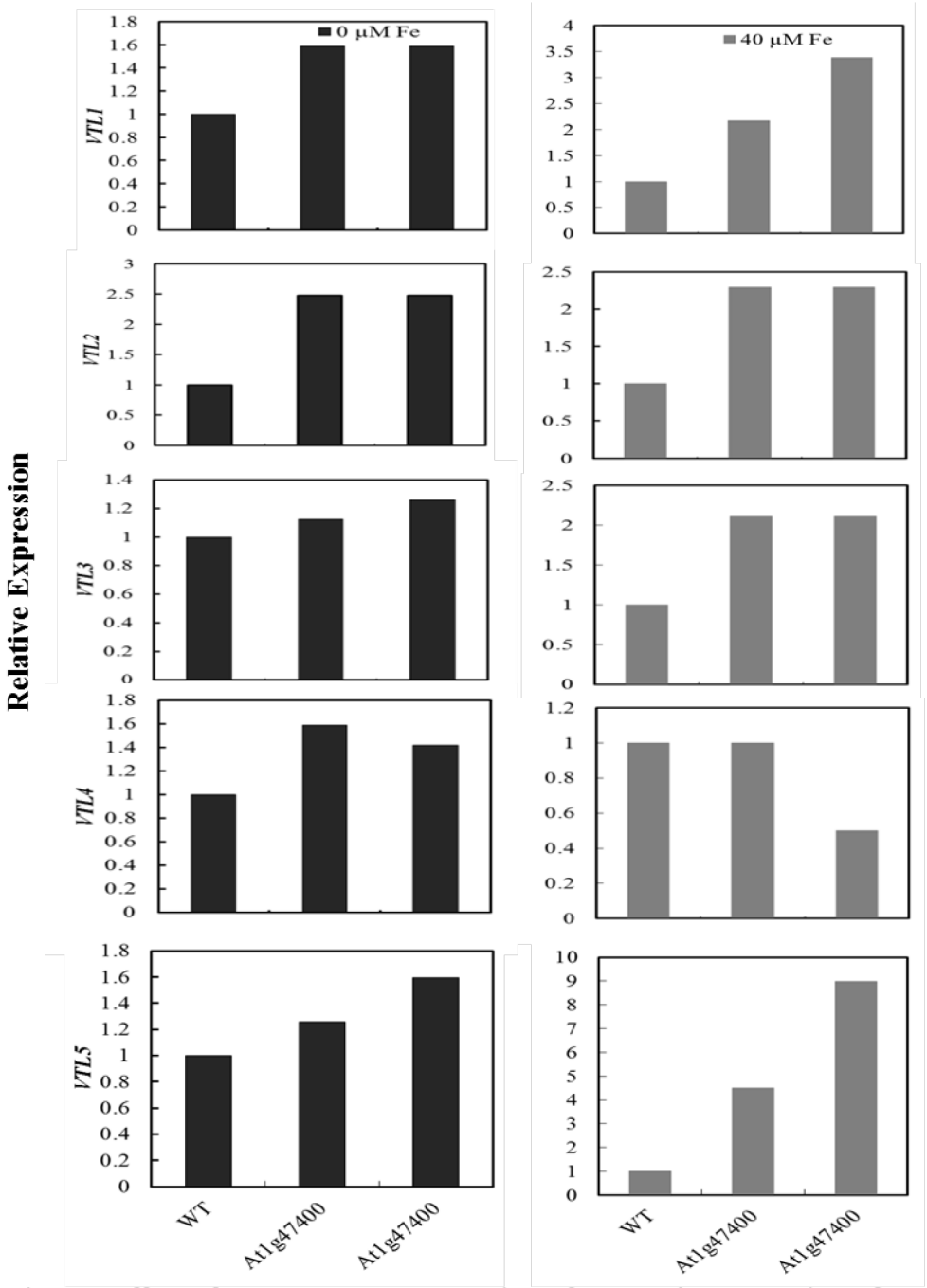

Fig. 17. Effect of At1g47400 on expression of *VTLs*. The expression of *VTL1*, *2*, *3*, *4* and *5* was determined by qRT-PCR analysis in At1g47400 over-expressing plants. cDNA was synthesized from two week-old plants grown on agarose with ES medium. *Actin2* was used for standardization. The relative expression values ($2^{-\Delta\Delta C(t)}$) are shown.

therefore investigated if the over-expression of *IMA1* affected the expression of VTL genes.

Two different *IMA1* plants were grown on agarose ES medium in 40 µM Fe and after 2 weeks seedlings were transfered to 40 or 0 µM Fe for 72 h and expression of *VTL1*, *2*, *3*, *4* and *5* in these plants was analysed.Transcription analyses of *VTL1*, *2*, *3*, *4* and *5* in both Fe sufficient and Fe deficient plants showed in general a higher expression of the VTLs in *IMA1* over-expressing plants compare to the WT (Fig. 17). Some exceptions to this generalization were observed. *VTL3* and *4* expression was unchanged in Fe-deficient plants, and VTL4 expression was unchange or even lower in Fe-sufficient plants compared to the WT (Fig. 17). These data indicated that *IMA1* expression induced the expression of the VTLs and that further over-expression of VTLs led to no further increase in Fe content.

In summary, although over-expression of the *VTL* genes or *IMA1* individually led to an increased Fe content in seeds, attempts at increasing Fe content by double over-expression were not successful. This result indicated that the Fe content in seeds was restricted by other factors not related to the expression of the genes under investigation.

4.2 Double Over-Expression of *AtVTL5* and *AtNAS3* in Arabidopsis

4.2.1 Cloning of NAS3, Expression of NAS3 and VTL5 Genes and Selection of Transgenic Plants

To clone *NAS3*, the full-length *AtNAS3* gene (At1g09240) was amplified from Arabidopsis cDNA using the polymerase chain reaction (PCR) and gene-specific primers. The PCR product was ligated into the pGEM-T vector using T/A cloning in the presence of T4 DNA ligase. The ligated vector was subsequently used to transform *E. coli* cells (DH5α). Transformed colonies were selected by blue/white screening, and colonies containing the *NAS3* insert were identified by colony PCR. Initially re-cloning of the *AtNAS3* gene into the GL1 vector was unsuccessful. Therefore, Pjet was used as a helper vector, and the gene was re-cloned using the PmlI and NcoI sites in the pCAMBIA3310-n vector (Fig. S1). The *AtNAS3* nucleotide sequence was validated by sequencing using the *nos* and *NAS3* primers (Fig. S1). The pCAMBIA3310-n vector containing *NAS3* was used to transform Agrobacterium. Arabidopsis plants were transfected using the floral-dip method (Chang et al., 1994). Seeds from transfected plants (T_0) were grown on soil under greenhouse conditions, and seeds from the T_1 generation were replanted and select with BASTA® to identify transformed plants. BASTA®-resistant plants were grown to seed, and plants over-expressing *NAS3* were identified in the T_2 generation using semi-quantitative PCR (Fig. 18A). Using quantitative real-time PCR, over-expression of *NAS3* lines was confirmed. In the *NAS3* line marked with an asterisk in Fig. 18A, expression of *NAS3* was increased greater than 35-fold compared to the WT control. This line was propagated (Fig. 18C).

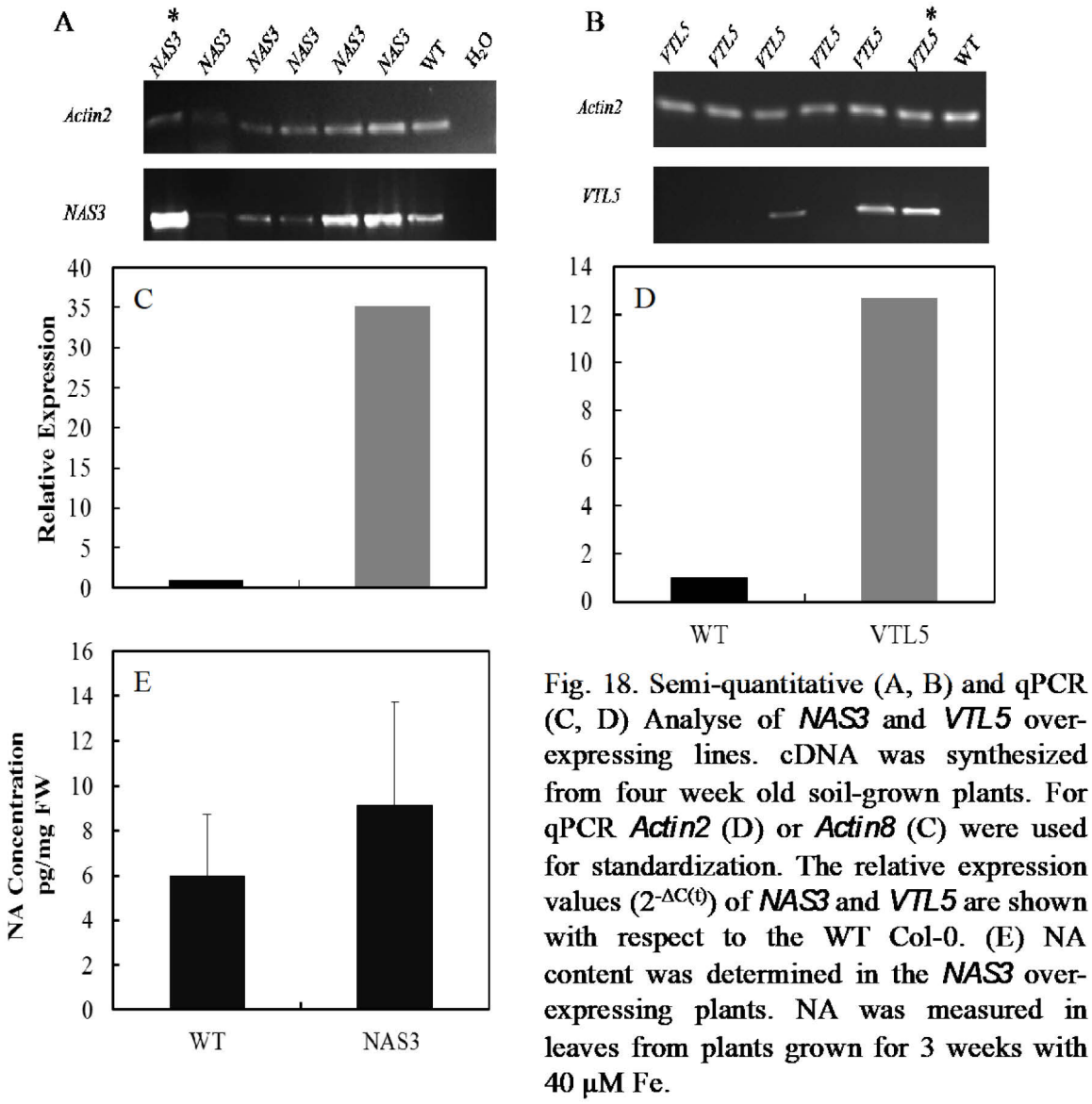

Fig. 18. Semi-quantitative (A, B) and qPCR (C, D) Analyse of *NAS3* and *VTL5* over-expressing lines. cDNA was synthesized from four week old soil-grown plants. For qPCR *Actin2* (D) or *Actin8* (C) were used for standardization. The relative expression values ($2^{-\Delta C(t)}$) of *NAS3* and *VTL5* are shown with respect to the WT Col-0. (E) NA content was determined in the *NAS3* over-expressing plants. NA was measured in leaves from plants grown for 3 weeks with 40 µM Fe.

To increase the Fe storage capacity, *VTL5* was over-expressed in Arabidopsis. The VTL family has been identified in all mono- and dicotyledon plants investigated and has been shown to participate in Fe homeostasis. Pervious investigations showed that *VTL1, 2, 5* transporters function as vacuolar Fe transporters in yeast (Gollhofer et al., 2013 and 2014; Li, 2015). *VTL5* was chosen as VTL representative because of the results from *VTL5* over-expression and Fe staining in section 3.1. The VTL5-OE line was obtained from Fechler (2017). The VTL5-OE line was re-selected for BASTA® resistance 3 times for each generation to ensure homozygosity and stable over-expression of the *VTL5* gene. Over-expression was confirmed using semi-quantitative PCR in the T_8 generation (Fig. 18B). The VTL5 line marked with an asterisk in Fig. 17B was selected and the expression confirmed by qRT-PCR (Fig. 18C and D). NA content in two different *NAS3* overexpressed plant was analyzed by UPLC at the IPK in Gatersleben.

NA content in NAS3 over-expressed plants was less than 2-fold greater than in WT plants (Fig. 18E).

4.2.2 Crossing of VTL5 (VTL5-OE) and NAS3 (NAS3-OE) Plants

To pursue the goal of increasing plant Fe, the homozygous NAS3 OE (At1g09240) and VTL5 OE (At3g25190) lines described above (3.3.1) were crossed and the first generation (T_1) was selected with BASTA®. BASTA®-resistant plants were grown to seed (T_2) and the selection repeated. Semi-quantitative PCR of the T_2 generation was employed to identify double over-expressing plants. Several double over-expressing plants were identified with the expression of *VTL5* increased between 2.5- and 33-fold and the expression of *NAS3* between 6.5- and 32-fold compared to the WT (Fig. 19). The double over-expressed lines (Fig. 19) were used for subsequent physiological and molecular analyses.

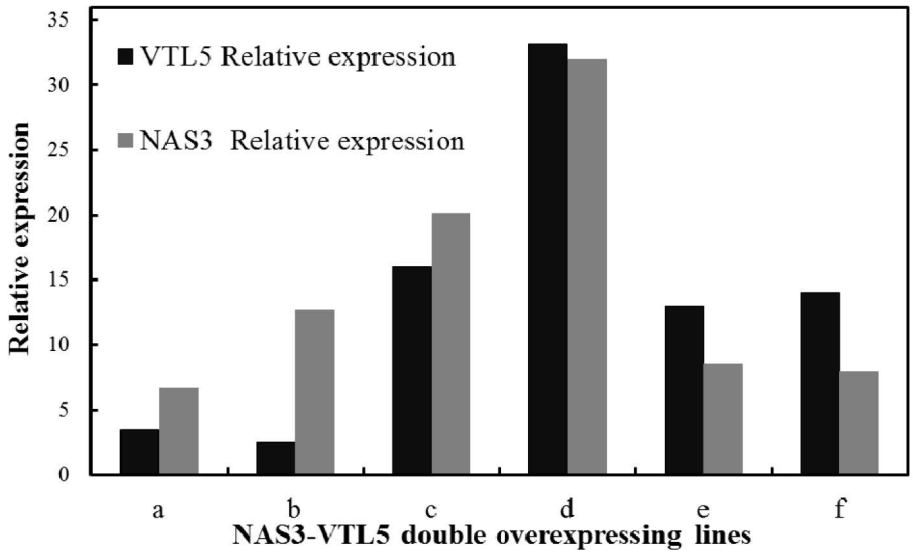

Fig. 19. qRT-PCR analysis of *VTL5-NAS3* double over-expression lines. cDNA was synthesized from four week old soil-grown plants. The *Actin2* was used for standardization. The relative expression values ($2^{-\Delta C(t)}$) of *NAS3* and *VTL5* are shown with respect to the WT.

4.3 Analysis of the *NAS3* Single and *NAS3-VTL5* Double Over-Expressing Lines

4.3.1 Determination of the Fe Content in NAS3-VTL5 Double Over-Expressed Plants

NA plays a key role in Fe homeostasis through chelation, transport and distribution of Fe in the xylem and phloem and in Fe storage in seeds (Schuler et al., 2012). *VTL5* is a putative vacuolar Fe transporter and over-expression of *VTL5* has been shown to increase Fe content in Arabidopsis seeds (Fig. 3). To discover the effect of simultaneously increasing NA and VTL5, we determined the Fe content in seeds of single and double over-expressing plants. For these studies, plants were grown under short-day conditions (8 h light, 16 h dark) in a growth chamber

to maintain plants in the vegetative state. Plants were transferred to the greenhouse and grown under long-day conditions to initiate reproductive growth. Seeds were harvested and the Fe content of different lines was determined. The Fe content in seeds of the *NAS3* OE lines was 129 µg/g DW in seeds of the *VTL5* OE line 108.4 µg/g DW. For both the *NAS3* OE and *VTL5* OE lines, the Fe content was significantly higher than WT ($p < 0.05$). However, the double over-expression of *NAS3* and *VTL5* did not improve the seed Fe content above the single over-expressing lines (Fig. 20A).

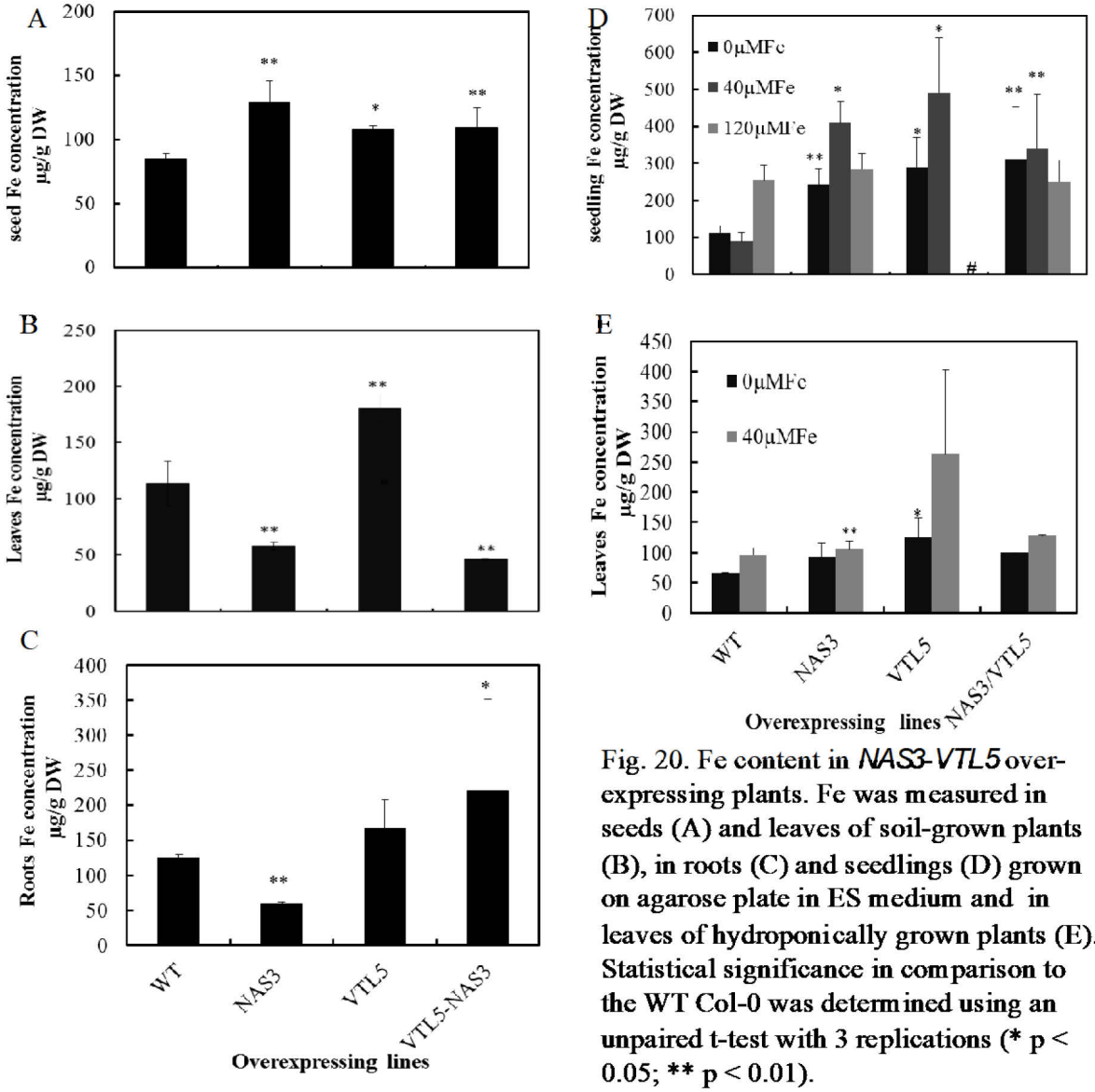

Fig. 20. Fe content in *NAS3-VTL5* over-expressing plants. Fe was measured in seeds (A) and leaves of soil-grown plants (B), in roots (C) and seedlings (D) grown on agarose plate in ES medium and in leaves of hydroponically grown plants (E). Statistical significance in comparison to the WT Col-0 was determined using an unpaired t-test with 3 replications (* $p < 0.05$; ** $p < 0.01$).

In further analyses the Fe content of leaves harvested from soil- (Fig. 20B) or hydroponically grown plants (Fig. 20C) was determined. Fe content in *NAS3* OE leaves that were harvested from soil had in tendency less Fe compared to WT. However, in these cases the Fe content in the double over-expressing lines was not increased over the WT. In fact, *NAS3* OE and *NAS-VTL5* OE lines had a decreased Fe content compared to the WT. Interestingly in the *VTL5* OE

line the Fe content in leaves was increased 3-fold compared to the WT (Fig. 20B and C). It appeared that over-expression of *NAS3* counteracted the *VTL5*-dependent increase in leaf Fe content.

The Fe content was also measured in seedlings that were grown for 2 weeks on agarose plates in ES medium and then transferred for 1 week to 0, 40 or 120 µM Fe. Subsequently the Fe content was measured. In *NAS3* OE seedlings grown on sufficient Fe (40 µM), the Fe content was higher than in the WT, and under Fe deficiency the Fe content in NAS3 OE seedlings was also higher than the WT (Fig. 20D). The Fe content in *VTL5* OE was also increased compared to the WT; although, the data were variability in relationship to all other lines. (Fig. 21 D). In 120 µM Fe no significant changes were observed. Fe content in roots of *NAS3* was lower in comparison to the WT and showed in general a relatively small increase in Fe in 40 µM, which was significant in the *NAS3*-*VTL5* OE lines (Fig. 20E).

4.3.2 Fe^{3+}-Chelate Reductase Activity in NAS3-VTL5 Double Over-Expressing Lines

The Fe^{3+}-chelate reductase (FCR) reduces Fe^{3+} to Fe^{2+} at the root epidermis to increase Fe availability in strategy I plants. In plants growing under Fe deficiency, FCR activity is increased, proportional to the degree of deficiency (Connolly et al. 2003). FCR activity was

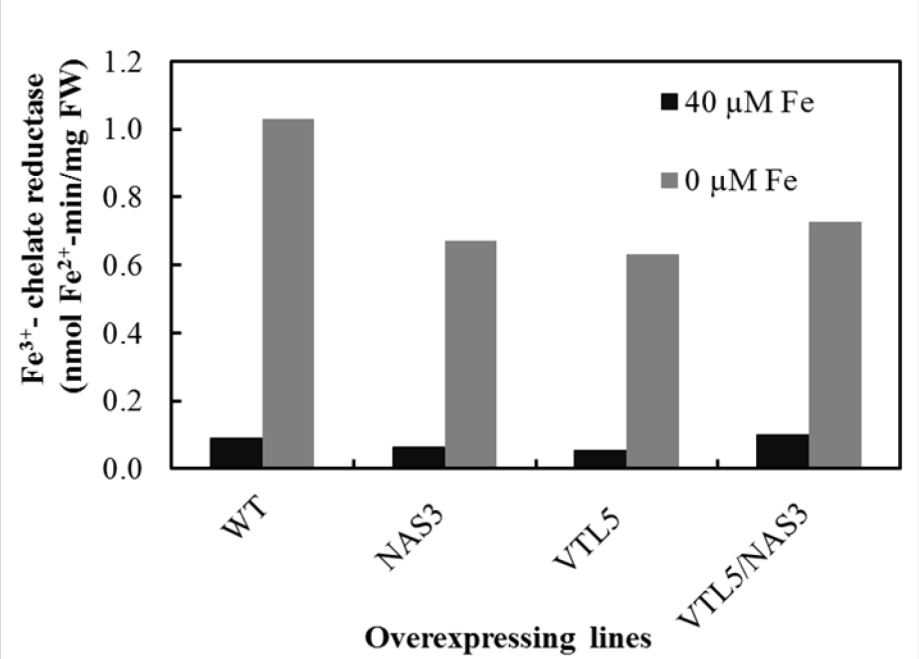

Fig. 21. Fe^{3+}-chelate reductase activity in the WT, *NAS3* OE(A), *VTL5* OE and *NAS3-VTL5* double over-expressing lines. Reduction of Fe was determined after 10, 20 and 40 min, and the activity was calculated by linear regression analysis with the Pearson correlation coefficient $r^2 > 0.9$ for all measurements. Values are the average of three plants.

determined in plants that were grown for 4 weeks in hydroponic medium (40 µM Fe) and then transferred to Fe-deficient (0 µM Fe) or -sufficient medium (40 µM Fe) for 2 days prior to analysis. The rate of Fe^{3+} reduction was calculated as nmoles Fe^{2+}-BPDS formed per mg fresh weight and min and determined as the slope of the line at 10, 20 and 40 min. The FCR activity in WT was approximately 1 nmole Fe^{2+}-BPDS/min/mg FW and in the NAS3 line was 0.67 nmole Fe^{2+}-BPDS/min/mg FW (Fig. 21). Activity staining of FCR, in which Fe^{2+} is chelated by Ferrozine®, showed a stronger color development in Fe deficient roots compared to WT control (Data not shown). Fe content in roots of *NAS3* plants was lower than WT and in parallel the reductase activity was decreased compare to the WT. Although, the increase in root Fe in the *NAS3* over-expressing plants was not greatly increased over control roots (Fig. 21). Taken as a whole, the single and double over-expressing plants appeared to be resistant to Fe deficiency.

4.3.3 Chlorophyll Content in NAS3 and VTL5 Single and NAS3-VTL5 Double Over-Expressing Lines

Fe has an important role in biosynthesis of chlorophyll, and Fe deficiency also affects the ultrastructure of chloroplasts (Briat et al., 1995). Therefore, the chlorophyll content in leaves might reveal the impact of Fe deficiency on photosynthesis. To test the over-expression of

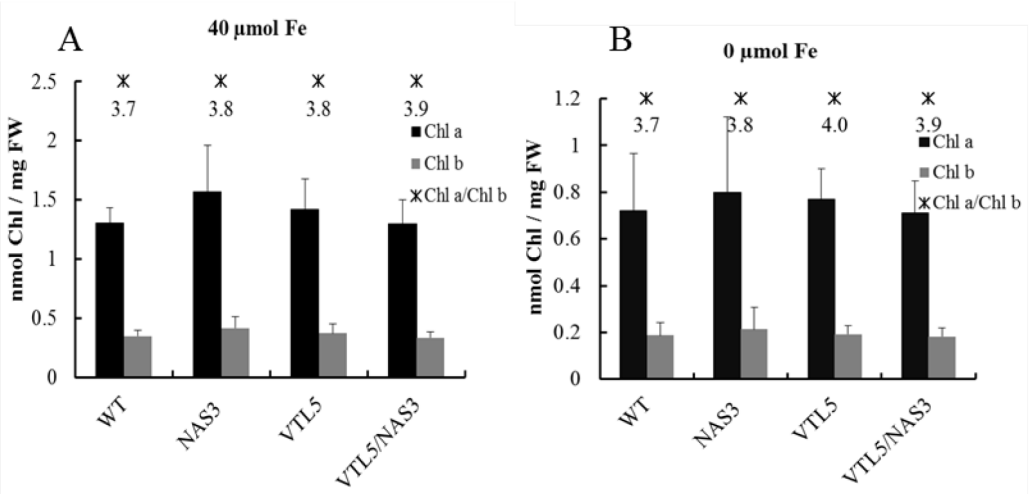

Fig.22. Chlorophyll a and b content and the Chla/Chlb ratio in WT, *NAS3* OE, *VTL5* OE and *VTL5-NAS3* double over-expressed lines.

NAS3, *VTL5* and *NAS3-VTL5* on chlorophyll content, plants were grown in hydroponic culture in Fe sufficient media for 4 weeks and were then transferred for 1 week to 40 or 0 µM Fe. As expected plants grown in the absence of Fe had both lower chlorophyll a and b content compared to plants grown in sufficient Fe, but chlorophyll content in the over-expression plants was not significantly different from the WT. Also, the ratio of chlorophyll a/b in the over-expressed lines comparison to the WT was not affected (Fig. 22).

4.3.4 Analysis of Root Growth in NAS3 and VTL5 Single and NAS3-VTL5 Double Over-Expressing Lines

Root growth can be influenced by the nutrients in the medium, and the genotype can determine the root structure and morphology (Gruber et al., 2013). Root hair patterning can alter the root shape depending on the Fe concentration (Schmidt et al., 2000). Plants require approximately 100 µg Fe/g dry weight for optimal growth (Marscher, 2012). Arabidopsis grown in 5-10 µM Fe showed symptoms of moderate Fe deficiency that included a stimulation in primary root growth (Gruber et al., 2013). Severe Fe deficiency (0 µM Fe) dramatically inhibited primary root growth (Gruber et al., 2013). Using root growth as a measure for Fe deficiency, the over-expressing lines were grown on agarose media containing 0 or 40 µM Fe growth in 0 µM Fe

was determined after 7 and 14 days. Whereas the root growth was not affected by *NAS3-VTL5* double OE compared to the WT, *VTL5* over-expression inhibited root growth both after 7 and 14 d of growth (Fig. 23).

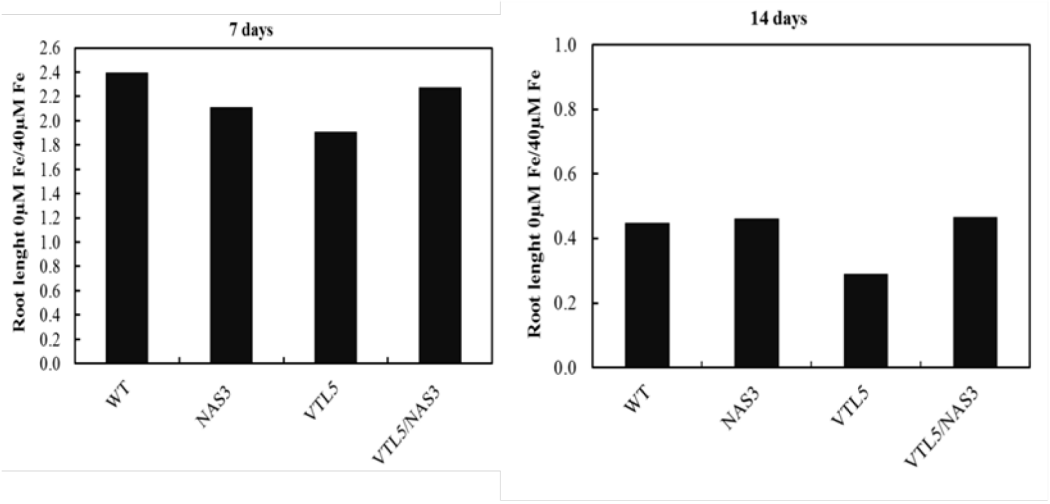

Fig. 23. Analysis of root length in the over-expression plants. Presented are the root length as a ratio between 0 µM/40 µM Fe. Root length was determined after 7 and 14 days of growth in the light on agarose with ES medium containing 0 or 40 µM Fe.

The root length at 0 µM Fe after 7 days in *NAS3* and *NAS3-VTL5* was same as the WT plants. After 14 days of growth the general pattern of the ratio of root length remained the same; however, the ratio decrease in the *VTL5* line, likely indicating a decrease in root growth in the absence of Fe (Fig. 23).

4.3.5 Gene expression of Fe Homeostasis Genes in the NAS3-VTL5 Double Over-Expressing Plants

Seed Fe content in single and double over-expressing lines showed a tendency to accumulate Fe compared to the WT (Fig. 20A). Although, Fe content in roots and seedlings increased (Fig. 20E), leaf Fe was decreased relative to the WT (Fig. 20B and C). Therefore, an expression analysis was conducted of genes that were known to be regulated by the Fe supply. Genes for acquisition of Fe as well as transcription factors were chosen to analyze the activity of the FIT-regulated and PYE-regulated pathways among other processes. *NAS3* OE, *VTL5* OE and NAS3-VTL5 OE lines as well as the WT were grown in ES medium containing 40 µM Fe and after 2 weeks seedlings were transferred to 0 µM or 40 µM Fe. Expression of each line was compared to the WT as a control.

4.3.5.1 Fe^{3+}-Reduction Oxidase-2 (FRO2) and Iron-Regulated Transporter-1 (IRT1)

As reported in the literature, *FRO2* expression in plants grown under Fe deficiency was greatly increased compared to Fe sufficient plants. Transcriptional analyses of FRO2 in over-expressing lines showed that in *NAS3* OE, *VTL5* OE and *NAS3* -*VTL5*-OE lines grown with or without Fe (40 vs. 0 µM Fe) were decreased compare to the WT (Fig. 24). These data were consistent with the FCR activity reported in Fig. 21 and likely indicated an increased resistance to Fe deficiency in the over-expressing plants.

Fe^{2+} is transported into the root epidermis via the IRT1 metal transporter. IRT1 is a high affinity transporter that is upregulated in response to Fe starvation (Vert et al., 2002). With the exception of the *NAS3*-*VTL5* OE line, the results for *IRT1* expression were similar to the results obtained for *FRO2* (Fig. 24). In general, a decrease in expression compare to the WT was observed (Fig. 24).

4.3.5.2 Expression of the Transcription Factors bHLH38, MYB72, PYE and ILR3

The current understanding of regulation of the Fe-deficiency response implicates two transcription-regulated networks. In Arabidopsis and presumably in all strategy I plants, all steps in Fe acquisition are regulated by FIT (bHLH29), including Fe^{3+}-chelate reduction, Fe^{2+} uptake, H^+ extrusion and coumarin production (Ivanov et al., 2012; Colangelo and Guerinot, 2004). For regulatory activity FIT must form a heterodimer with bHLH38, bHLH39, bHLH100 or bHLH101 (Yuan et al. 2008; Sivitz et al., 2012; Wang et al., 2013), and upon dimerization control downstream pathways (Hindt et al. 2017).

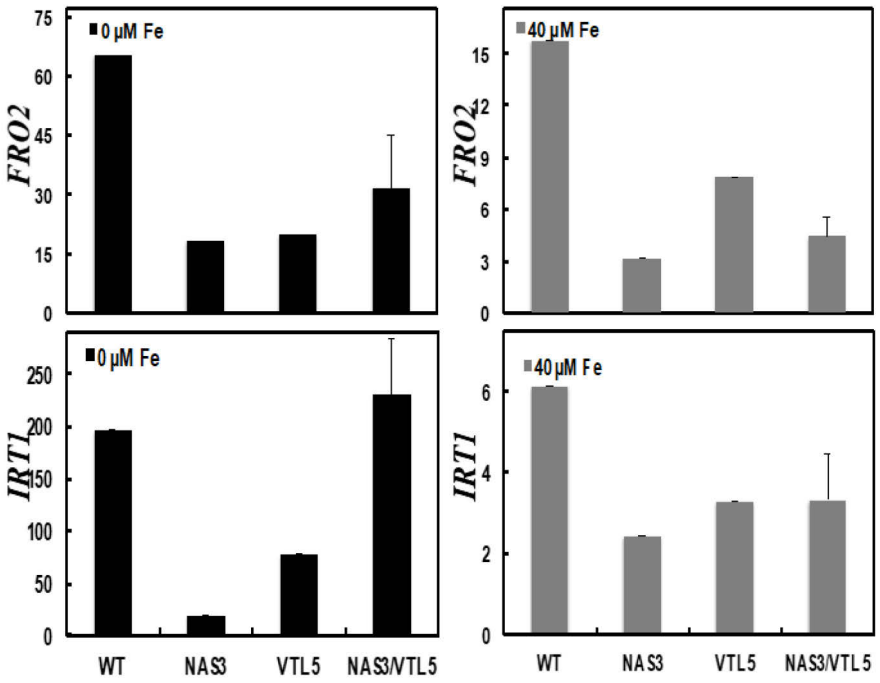

Fig. 24. qRT-PCR analysis of *FRO2* und *IRT1* expression in NAS3/VTL5 over-expression lines. cDNA was synthesized from four week-old soil-grown plants. *ACTIN2* was used for standardization. The relative expression values are presented as $2^{-\Delta C(t)}$.

Recent research has shown that MYB72 was directly regulated by FIT (Sivitz et al., 2012). MYB10 and MYB72 are both necessary to induce *NAS4* expression under Fe-deficient conditions (Palmer et al., 2013). *POPEYE* (*PYE*) is as a bHLH transcription factor involved in the Fe deficiency response, and it can bind directly to the *NAS4* promoter (Long et al. 2010). Previous studies showed that PYE expression was induced under Fe deficiency. Three PYE-like (PYEL) transcription factors, bHLH34, bHLH104 and bHLH105 (ILR3; Li et al., 2016; Zhang et al. 2015) activate the expression of *PYE*, a negative regulator of the Fe deficiency response (Long et al., 2010). The PYE regulon does not non-overlap with the FIT regulon.

For the analysis of expression for the genes mentioned above, differences of greater than 2-fold with respect to the WT were considered to be significant. Using this criterion, expression of all genes tested in Fig. 25 in Fe-sufficient and –deficient plants showed with only few exceptions no changes in all over-expressing lines compared to the WT (Fig. 25).

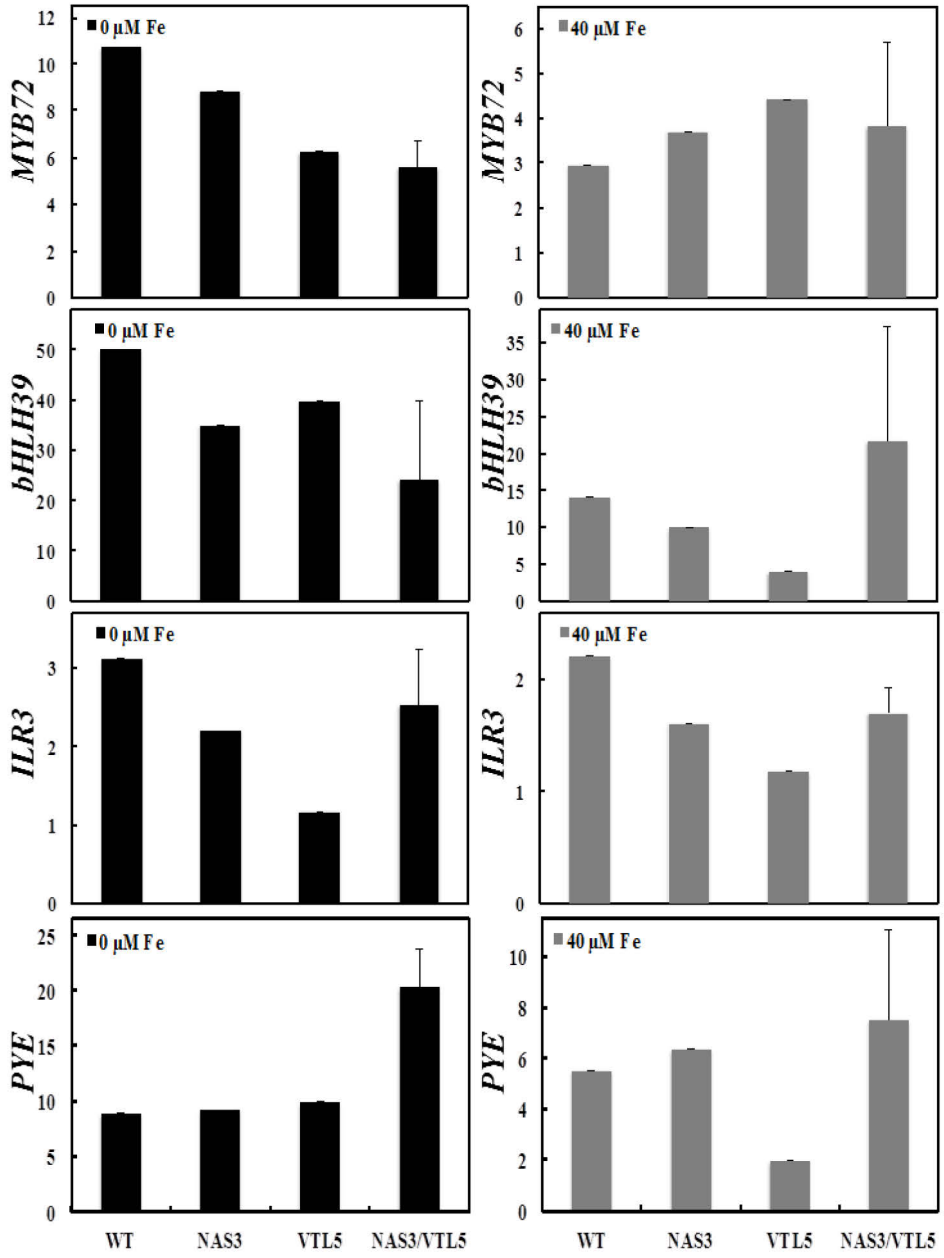

Fig. 25. qRT-PCR analysis of the Fe-deficiency regulated transcription factors, *MYB72*, *bHLH39*, *ILR3* and *PYE* in NAS3/VTL5 over-expression lines. cDNA was synthesized from four week-old soil-grown plants. *ACTIN2* was used for standardization. The relative expression values are presented as $2^{-\Delta C(t)}$.

4.3.5.3 Expression of BRUTUS (BTS), NEET (At5g51720), Ferritin1 (FER1) and Ascorbate Peroxidase1 (APX1)

BTS encodes an E3 ligase and is a negative regulator of the Fe deficiency response. Under Fe deficiency, BTS is degraded and Fe deficiency regulated genes are express (Hindt et al., 2017).

PYE interacts with PYE-like (PYEL) proteins, which also bind to BTS and are

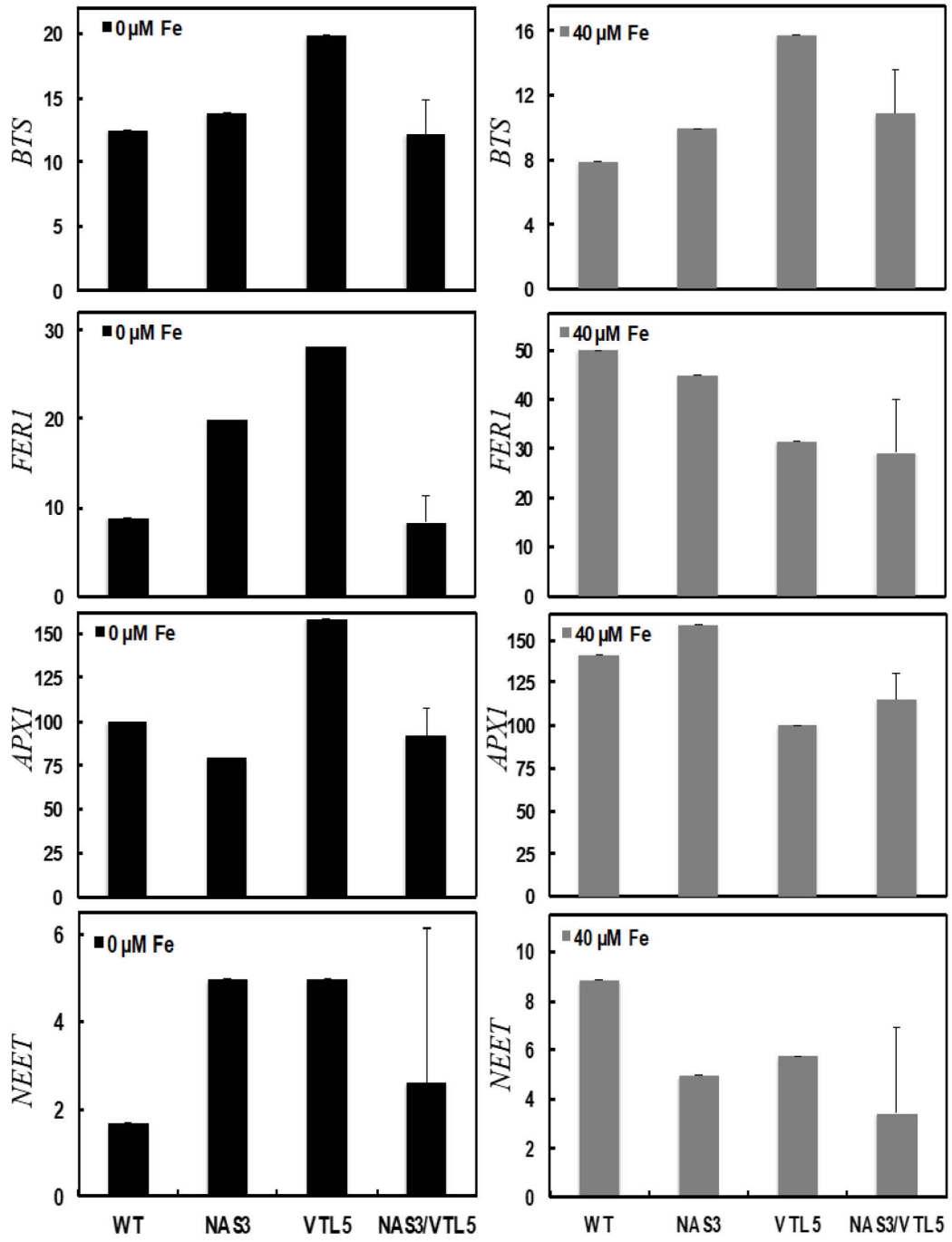

Fig. 26. qRT-PCR analysis of the Fe-deficiency regulated transcription factors, *BTS*, *FER1*, *APX1* and *NEET* in NAS3/VTL5 over-expression lines. cDNA was synthesized from four week-old soil-grown plants. *ACTIN2* was used for standardization. The relative expression values are presented as $2^{-\Delta C(t)}$.

degraded in a proteosomal-dependent manner (Mathiadi and Long, 2016). NEET is a chloroplast protein that plays a role in Fe metabolism and regulation (Su et al., 2013). Its expression is regulated by the bHLH transcription factor ILR3 (Aparicio and Pallas, 2016).

Ferritins are ubiquitous proteins in plants; *FER1* is the only ferritin gene expressed in roots and induced under excess Fe (Petit et al., 2001). Finally to determine if the over-expression plants suffered under oxidative stress due to Fe toxicity, *APX1* expression was investigated. *APX1* and *FER1* gene are co-regulated when plants were grown with excess Fe (Fourcroy et al., 2004). Ascorbate peroxidase is a key enzyme that is activated during oxidative stress and Fe toxicity.

The expression of all genes described above was largely unchanged in the double expression lines in plants grown under Fe-sufficient or –deficient conditions (Fig. 26). In NAS3 OE and VTL5 OE lines, *NEET* expression was increased compared to the WT under conditions of Fe sufficiency; however, no difference in expression was observed in the double over-expressing line (Fig. 26).

4.4 Determination of NA contents in *NAS3-VTL5* Double Over-Expressing Lines and the Effect of NAS3 Over-Expression on *VTL 5* Expression

For determination of NA content in the NAS3-VTL5 double over-expressing line. The NA analysis was conducted at the IPK-Gaterleben in the lab. of Prof. Nicolas von Wiren using Ultra Pressure Liquid Chromatography. NA content of single and double over-expressing plants was 2 fold that of the WT. This analysis resulted in on difference in the NA content in the double over expressed lines (Fig. 27A).

Previous results in Fig. 20 indicated that Fe content in double overexpressing *NAS3-VTL5* lines did not change compare with *NAS3* overexpressing plants. To understand the effect of *NAS3* on VTL5 expression, WT and *NAS3* OE seeds were grown on agarose in Fe sufficient and Fe deficiency medium and the expression of *VTL5* was determined by qPCR (Fig. 27B). The result showed that in Fe sufficient medium *VTL5* expression was up-regulated. Thus, the lack of effect of *NAS3*/*VTL5* over-expression was most likely due to the unchanged NA content in the transgenic plants, in spite of the over-expression of *NAS3*, and to the increased *VTL5* expression in *NAS3* over-expressing plants.

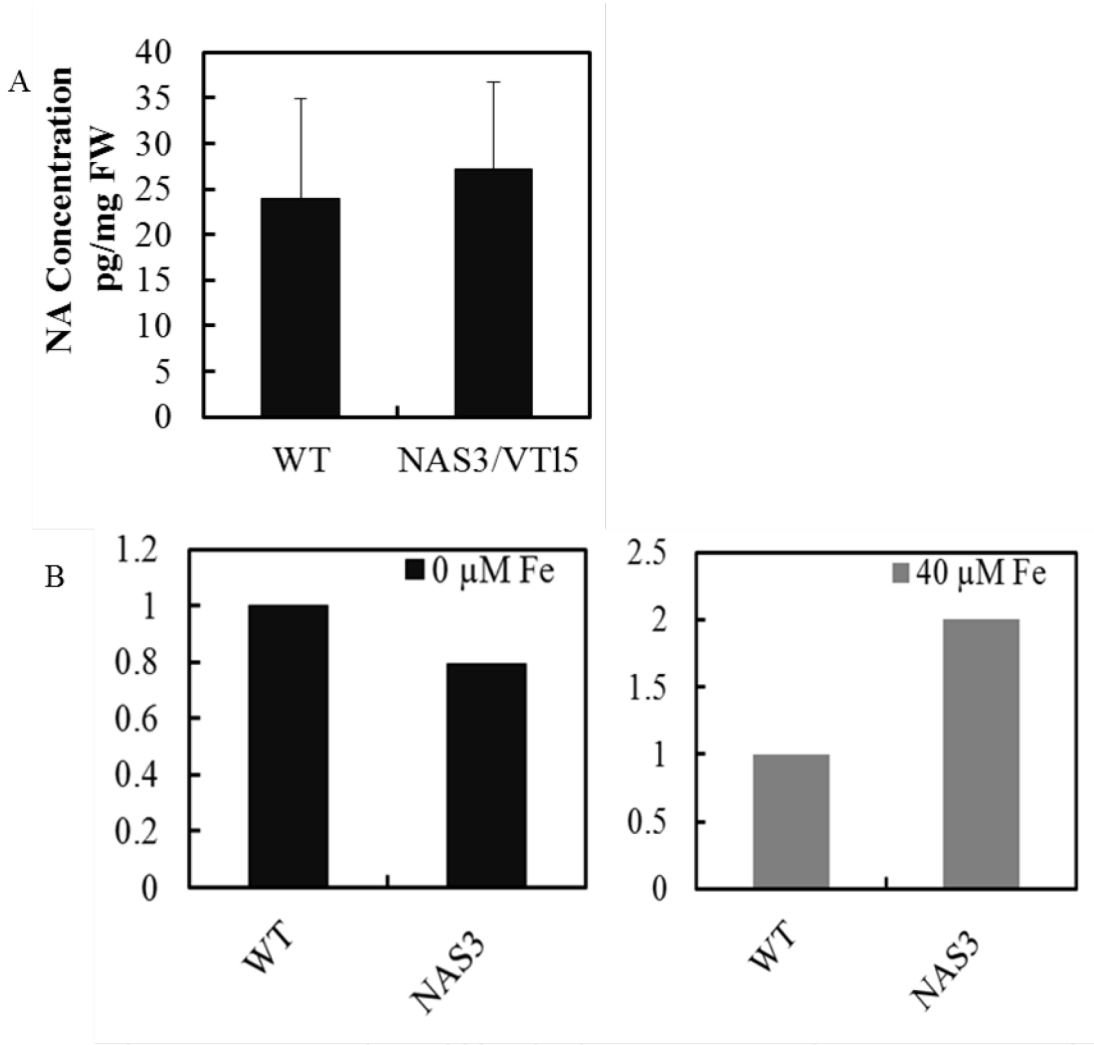

Fig.27. NA content in Arabidopsis plants over-expressing *NAS3*, *VTL5* and *NAs3-VTL5* . NA was measured in leaves from plants grown for 3 weeks in the presence of 40 µM Fe (A). Effect of *NAS3* on expression of *VTL5*. The expression of *VTL5* was determined by qRT-PCR analysis in *NAS3* over-expressing plants. cDNA was synthesized from two week-old plants grown on agarose with ES medium. *Actin2* was used for standardization. The relative expression values ($2^{-\Delta\Delta C(t)}$) are shown (B).

5 Discussion

Several sustainable agricultural approaches have been attempted to reduce Fe malnutrition in humans by increasing the Fe storage capacity through overexpressing of ferritin or Fe availability by decreasing phytic acid content in plants. In this work, we have used new strategies for increasing the Fe content by overexpressing *VTL*, *NAS3* and *IMA1* genes in Arabidopsis in order to identify transgenic Arabidopsis lines that have increased Fe content, especially in seeds.

5.1 Biofortification by Over-expression of VTL Genes

Recent studies have investigated VTL proteins as Fe transporters in plants. Microarray analysis reveals that *VTL*s (*VTL1*, *2* and *5*) are down-regulated under iron deficiency (Buckhout et al. 2009; Yang et al. 2010). These proteins exist in mono- and dicotyledon plants and also in *Chlamydomonas*, *Physcomitrella* and prokaryotes, but not in animals (Gollhofer et al. 2011b). Analysis of the VTL proteins in *Arabidopsis* showed a 61-88% similarity to each other and a 30% homology to VIT1 (Gollhofer et al. 2011). As was described before, VIT1 was responsible for transporting Fe into the seed vacuole. Slavic et al. (2016) showed that *PVIT*s in *Plasmodium* played a critical role Fe detoxification and the development of malaria parasites in their mammalian host. A recent investigation showed that VTL1 and 2 were localized on the vacuolar membrane in onion cells (Gollhofer et al. 2014). In addition, the Fe content in isolated vacuoles from yeast cells transformed with *VTL1*, *2* or *5* had increased Fe compare to the Δccc1 mutant (Gollhofer et al. 2014). Our current investigations showed that GFP-VTL fluorescence in Saccharomyces was detected on the vacuolar membrane and in some cases in the ER/Golgi network (Timofeev and Buckhout, unpublished). These data indicated the function of VTLs was in vacuolar Fe transporter. For this reason, we overexpressed *VTL* genes to increase vacuolar Fe storage.

The function of VTL proteins in Fe homeostasis under different developmental conditions is still poorly understood. Their functions have been inferred from published results and from new data reported in this thesis. To identify the organs and tissues where *VTL*s were expressed, promoter-β-glucuronidase (GUS) assays were used. The results showed that *VTL1* was expressed in roots in association with the root stele and seed cotyledons and seedling shoot (Gollhofer et al. 2011). On the other hand, *VTL5* was only expressed in the root stele, and was absent under Fe deficiency (Fig. S6). Although GUS analysis showed that *VTL1* and *VTL5* were expressed in roots, the root Fe content in the 35S::*VTL1* and *2* OE lines showed only small but insignificant changes in Fe content compared to the WT. *VTL3*, *4* and *5* OE lines also had only

a marginal increase in root Fe content. With regard to root length, one would have expected that under Fe deficiency longer roots would have correlated with increased Fe content. However, the results were inconclusive. There was no clear correlation between Fe content and root length in either Fe sufficient or deficient seedlings (Fig. 6). Fe concentration in leaves of *VTL* OE lines was higher in the over-expressing plants compared to the WT but only in *VTL2* and 3 was the increase significant, and under Fe sufficient conditions the increases in Fe were not significant (Fig. 5). Although for all organs the OE lines had a tendency for increased Fe, only in a few cases was this increase statistically significant.

Fe content in seeds, however, showed that all *VTL* OE lines had increased Fe compared to the WT. Whereas the Fe content in seeds of the knockout mutants *vtl2*, *vtl3* and *vtl5* were insignificantly less than the WT (Fig. 3). Therefore, these genes when acting alone had no discernable function in WT seed Fe storage and might have indicated a redundancy in VTL function. Perls' staining was used to detect Fe localization in the VTLs OE lines. Fe was localized in the provascular system in both the WT and the OE lines, but the cytoplasm in the OE lines was more intensely stained than in the WT. The Fe staining in embryo cross-sections was concentrated in the endodermal layer surrounding the provascular bundle in cotyledons and hypocotyls and predominantly in vacuoles of both WT and VTL OE lines. In VTL OE lines staining was notably heavier than in the WT (Fig. 4). It has already been shown that VIT1 is involved in the storage of embryonic Fe in the provascular cells (Kim et al., 2006). In contrast in the *vit1-1* mutant, Fe was clearly visible in sub-endodermal cells of cotyledons and the hypocotyl. The endodermis has been shown to be critical for proper distribution of Fe in roots. Studies with the *shr-1* mutant, which lacks an endodermis, showed that the endodermis, in embryos was essential for proper Fe distribution by forming a barrier that controlled Fe access to the stele. The cortical cells could not compensate for the loss of an endodermis. Although the data show that over-expression of VTL genes correlated with increased seed Fe, the VIT1 transporter likely determined the localization of Fe in the endodermal cells. Thus, the activity of the VIT1 transporter was dominant over the VTL transporters in determining storage of embryo Fe.

The efflux of Fe from the vacuole has been shown to be catalyzed 2 NRAMP transporters, AtNRAMP3 and AtNRAMP4 (Bastow et al., 2018). The double mutant *nramp3*/*nramp4* was unable to mobilize Fe and showed a short-root phenotype in germinating seeds (Roschzttardtz et al. 2009). Complementary studies by Mary et al. (2015) showed that AtVIT1, AtNRAMP3, and AtNRAMP4 function in the same pathway. In the wild-type embryo, about 50% of stored Fe is localized in endodermal cells where *AtVIT*, *AtNRAMP3* and *AtNRAMP4* are expressed. In

further investigations, Gollhofer et al. (2014) showed that the root growth phenotype of the *nramp3/nramp4* double mutant could be complemented by over-expression of *AtVTL1*, *2* or *5*; the Fe content in seeds was also increased by 40 and 60% compared to the WT and the *nramp3/nramp4* double mutant. Altogether, these findings demonstrated a functional link between VIT1, NRAMP3 and NRAMP4 and VTLs, only VIT1 and the NRAMPs defined a functional module surrounding the vasculature in the embryo. Both VIT1 and VTLs could transfer Fe into vacuoles, but a role for VTLs in seed Fe storage *in vivo* remained to be determined.

To elucidate the intercellular function and physiological role of VTL proteins, the expression of the Fe responsive genes was analyzed in all *VTL* OE lines. FRO2 is one of the first proteins that were directly involved in Fe deficiency response. The *FRO2* and *IRT1* expression under Fe limitation was decreased in *VTL 1*, *2*, *3* and *5* OE lines. Similarly, the activity of the Fe^{3+}-chelate reductase in all VTL OE lines was also lower compared to the WT under Fe deficient conditions. In contrast, under Fe sufficiency expression of *FRO2* and *IRT1* was increased (Fig. 7). We concluded that during Fe starvation, due to the increased supply of Fe in the VTL lines, *FRO2* and *IRT1* expression was lower in comparison to the WT, and under Fe sufficiency, because of increased sink demand for Fe in the transgenic lines compare to the WT, *FRO2* and *IRT1* expression was increased due to enhance Fe storage in the vacuole (Fig. 7).

The expression of transcription factors was analyzed that were involved in Fe homeostasis. These include both FIT-dependent and -independent genes. MYB10 and MYB72 are required for plant resistance to Fe deficiency. They are important in the regulatory cascade of the Fe-deficiency response, which includes *NAS4* expression (Palmer et al. 2013). Our results showed that *MYB72* expression was not altered under Fe deficient in the *VTL* OE lines, but that under Fe sufficiency transcript abundance was significantly increased (i.e. greater than 2-fold). Transcript analyses of *bHLH39* in the *VTL* OE lines showed the similar pattern to *MYB72*. In the presence of Fe, *bHLH39* expression was significantly increased, while in the absence of Fe expression was unchanged (Fig. 8). The expression of PYE and ILR3 was also investigated. Since PYE forms a dimer with ILR3 and represses Fe storage as a reaction to Fe deficiency, an increased *PYE* expression would be consistent with an increased Fe storage in VTL OE plants (Fig. 8; Long et al. 2010). Consistent with this interpretation, Rampey et al. (2006) observed that in the *ilr3* loss of function mutant, expression of *VTL1*, *2* and *5* were increased. The expression of *PYE* and *ILR3* in all Fe sufficient VTL OE lines was significantly increased compare to the WT. Whereas the expression of *PYE* and *ILR3* in the Fe-deficient VTL OE lines was in most cases unchanged compared to the WT. However, *PYE* expression under Fe

deficiency was increased for *VTL2* and *3* OE lines and *ILR3* expression was decreased for *VTL3* OE (Fig. 8). We conclude that during Fe sufficient growth, *ILR3* transcription was induced in the over-expressing plants in order to act as a negative control to prevent VTL gene expression and Fe storage (Fig. 8).

Arabidopsis has four ferritin genes (*FER1 – 4*). FER1, 2 and 3 are localized in plastids and FER4 in the mitochondria or in both organelles. *AtFer1* is the only ferritin gene in Arabidopsis that is expressed in roots (Petit et al. 2001b). Gene expression analyses of *FER1* in VTL OE lines growing without Fe was increased compared to the WT. In contrast in Fe sufficient plants, the expression of *FER1* was decreased or unchanged in VTL OE lines compared to the WT (Fig. 8). VTL proteins are presumably vacuolar Fe transporters and FER1 is localized in plastids. Under Fe starvation, the Fe content remained higher in over-expressing lines and expression of FER1 was increased, with the exception of *VTL1*, in compare to the WT, supporting the finding that *VTL* OE lines were enriched in Fe.

Altogether, the results showed that in *VTL1*, *2*, *3*, 4 and *5* OE lines seed Fe was increased. Perls' staining confirmed increased Fe content in the pro-vascular system of embryos and in embryo longitudinal sections. Due to Fe accumulation in *VTL* OE lines, expression of Fe responsive genes was altered and reflected an increased Fe availability under Fe deficiency due to the increased Fe stores and a decreased Fe availability in Fe sufficient growth due to an increased sink straight for Fe, again compared to the WT. These results have been summarized in Fig. 28.

5.2 Biofortification by Over-expression of *IronMan1* (*IMA1*)

IMA1 is a 50 amino acid polypeptide containing a 17 amino acid C-terminal consensus sequence that is present in all angiosperms. IMA1 is synonymous with FE-UPTAKE-INDUCING PEPTIDE1 (FEP1; Hirayama et al. 2018). *IMA1* was shown to belong to a gene family with 8 members in Arabidopsis and to be essential for Fe acquisition and for cellular Fe homeostasis (Grillet et al., 2018). It was predominantly expressed in the phloem and leaf mesophyll cells in Fe-deficient Arabidopsis, and the downstream proteins FIT and bHLH039 repressed its expression. Fe acquisition was increased by overexpression of *IMA1*, and Fe and Mn accumulated in seeds in over-expressing lines (Grillet et al., 2018). By silencing of all 8 *IMA* genes, Fe uptake was decreased and plants appeared chlorotic. It was suggested that IMAs were phloem-mobile signals controlling Fe uptake in Arabidopsis.

Fe^{2+} bound to IMA and controlled the stability of the peptide. It was hypothesized that the instability of IMAs constituted a negative feedback for Fe uptake, which was triggered by

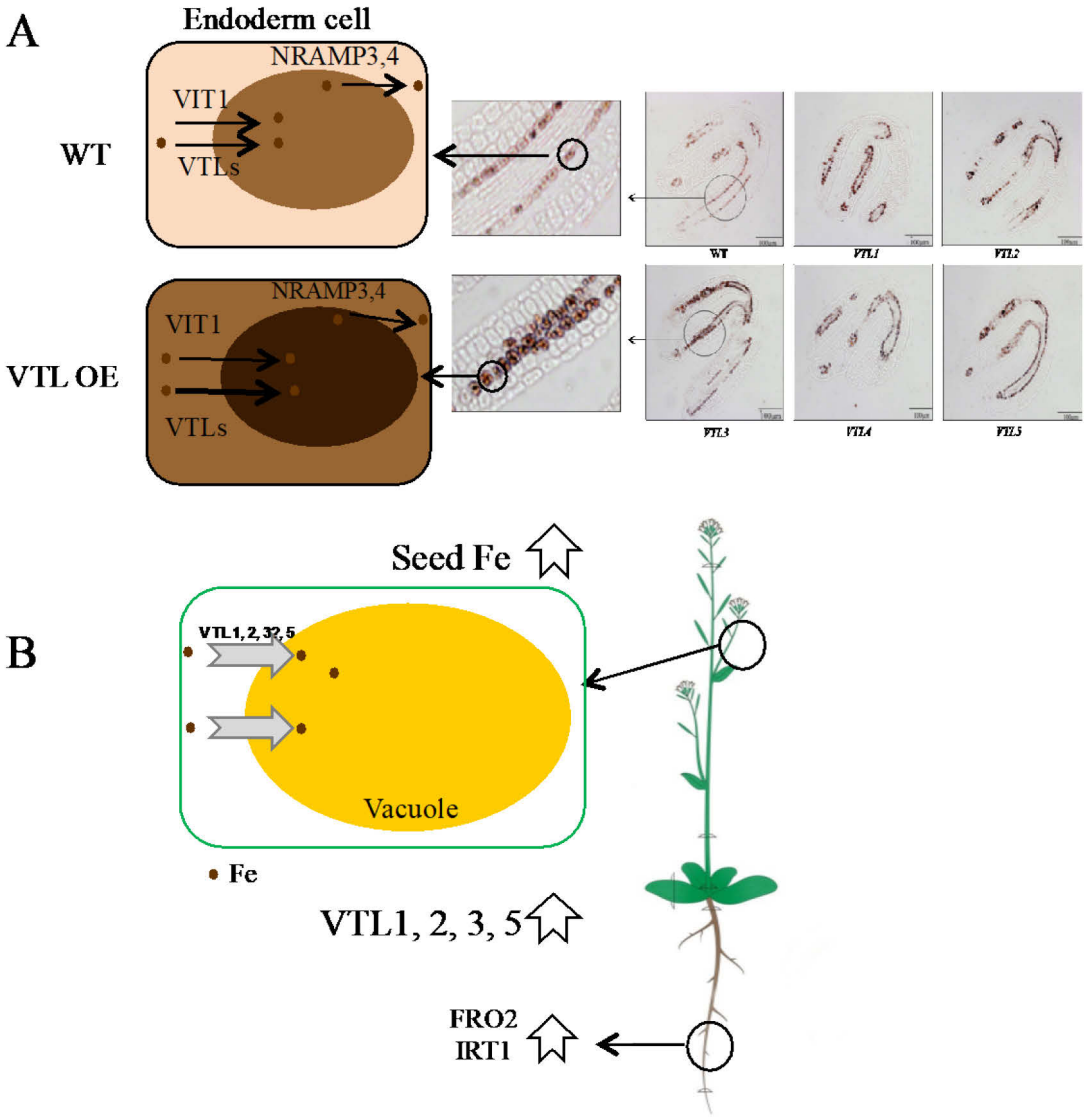

Fig. 28. Schematic illustration of the effects of *VTL1*, *2*, *3*, 4 and *5* OE in Arabidopsis. A. Over-expression of the VTLs resulted in an increased vacuolar seed Fe as demonstrated by Perls' staining. The Fe presence in pro-vascular cells of embryos is shown in longitudinal section. (B) Due to Fe accumulation in *VTL* OE lines, the expression of Fe responsive genes was altered. FCR activity and *IRT1* and *FRO2* expression were increased compared to the WT, presumably in response to an increased sink strength for Fe.

phloem Fe under Fe-replete conditions. Previous investigations showed that under Fe-sufficient conditions, the *ima1* mutants had lower Fe content in shoots but similar Fe content in roots compared with the WT (Hirayama et al. 2018). Using Perls' staining, Fe was detected in cross-sections of leaf nuclei and plastids in both WT and *IMA1* OE lines (Grillet et al. 2018). Therefore, we speculated that by overexpressing *IMA1* and *VTL*s, Fe might accumulate synergistically in seeds.

Our results showed in agreement with Grillet et al. (2018) that in *IMA1* OE lines Fe was increased 2- fold or greater compared to the WT (Fig. 10) and that Fe in the *IMA1* OE line was

detected on chloroplasts presumably associated with ferritin. Large precipitates were also observed in the vacuole (Fig. 11). Analysis of the Fe content in *IMA1* OE roots was greater compared to WT. In WT plants grown in the absence of Fe, root length was decreased compared to the controls, but in the *IMA1* OE line root length was longer under Fe limitation compared to the WT. This observation implies that *IMA1* OE plants are more resistant to Fe deficiency than the WT (Fig. 12).

To investigate the *IMA1* OE line in more detail, Fe^{3+}-chelate reductase activity was measured. The reductase activity in *IMA1* OE plants in the presence of Fe was higher than in the WT; however, under Fe deficiency the reductase activity was little changed. The expression of *FRO2* and *IRT1* in both Fe sufficient and deficient plants was notably increased with respect to the WT (Fig. 13). Further analyses were conducted on other Fe responsive genes. In the *IMA1* OE line, the expression of *bHLH39*, *MYB72*, *PYE* and *ILR3* were higher compared to the WT when grown under Fe-deficient conditions and were greatly increased under Fe sufficient conditions compared to the WT (Fig. 13). Grillet et al. (2018) and Hirayama et al. (2018) have also reported that in the *IMA1* OE line, Fe deficiency responsive genes in the bHLH subgroup Ib (e.g. *bHLH38*, *bHLH39*, *bHLH100* and *bHLH101*) were up-regulated. Gene expression in the FIT-independent pathway, *ILR3* and *PYE*, was increased in the IMA1 OE line, as was the expression of the Fe storage gene *FER1*, again as compared to WT.

In Arabidopsis eight IMA homologues have been identified (Grillet et al., 2018). The C-terminus of IMA homologous contained a consensus motif rich in aspartic acid residues that was necessary and sufficient for IMA function. The IMA1 peptide bound divalent cations but under reducing conditions only Fe^{2+}, Cu^{+} and Zn^{2+} were bound (Grillet et al., 2018). Based on results presented here and elsewhere, IMA1 functions as a phloem-mobile signal that coordinates information of the Fe status of the plant to Fe uptake from the soil. These results are summarized in Fig. 29.

5.3 Bio-fortification by Double Over-Expression of *IMA1* and *VTL*s

With the goal to test for a synergistic effect between over-expression of *IMA1* and *VTL2, 3, 4,* and *5*, we measured Fe content in plants over-expressing both *IMA1* and each of the *VTL* genes. Surprisingly, our results showed that the Fe content in seeds of the *VTL-IMA1* double over-expressing lines resulted in no synergistic increase in seed Fe content (Fig. 16). Similar results were observed in seedlings, leaves and roots (Fig. 16). In fact, the double-expressing

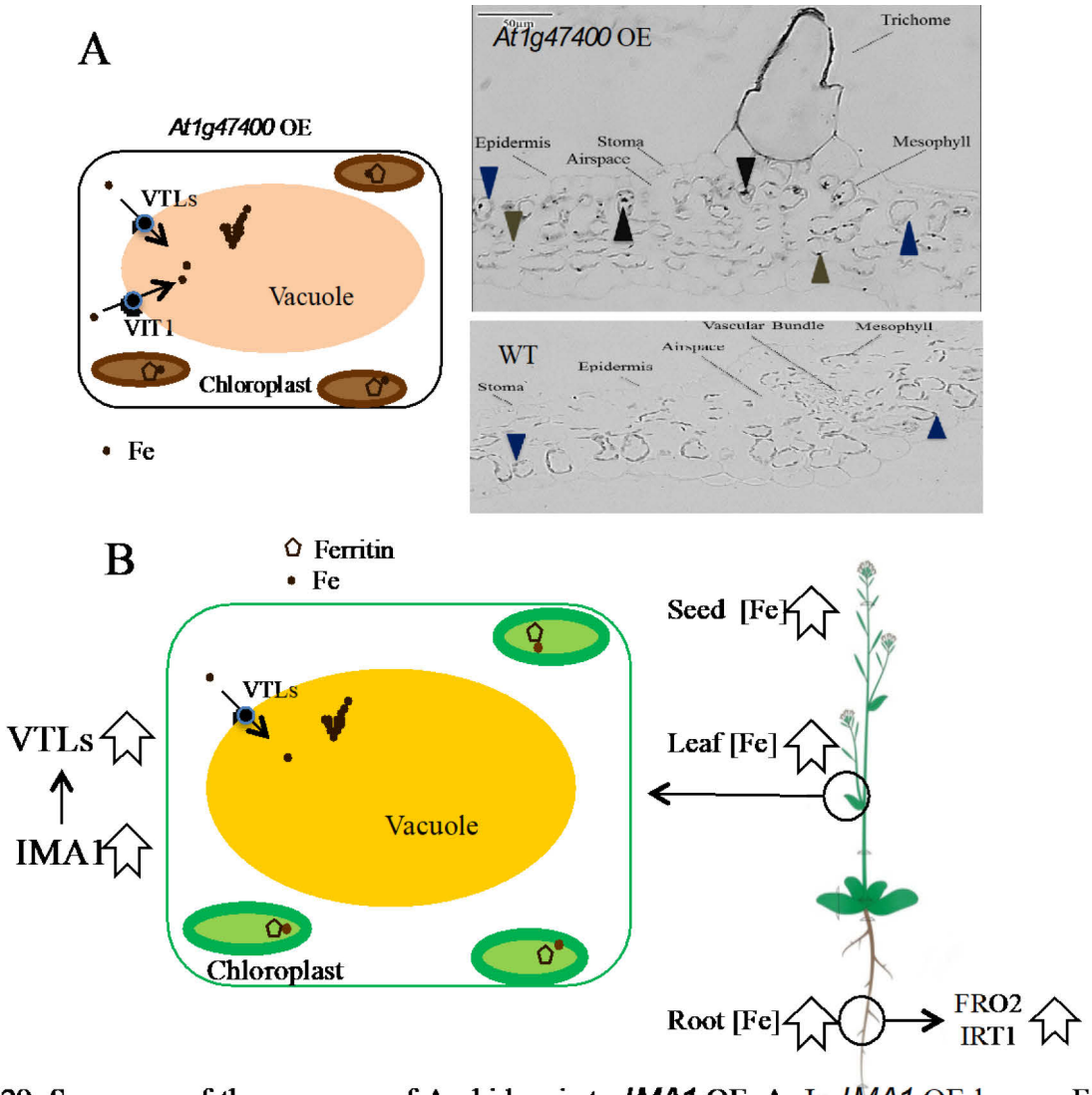

Fig. 29. Summary of the response of Arabidopsis to *IMA1* OE. A. In *IMA1* OE leaves, Fe deposits were localized by Perls' staining in mesophyll cells as dark blue particles located on the periphery of cells at a location occupied by chloroplasts. B. In *IMA1* OE seedlings, the expression of Fe responsive genes was altered. FCR activity under sufficient Fe supply was increased relative to the WT as was the expression the Fe acquisition genes *IRT1* and *FRO2*. This response resulted in increased Fe uptake. The over-expression of IMA1 was also correlated with increased expression of the VTL genes, likely resulting in increased Fe in vacuoles.

plants showed in many cases a decreased Fe content compared to the *IMA1* OE plants. In complementary studies, the effect of *IMA1* expression on the expression of *VTL* genes was analyzed. These results revealed that *IMA1* expression with the exception of *VTL4* enhanced the expression of VTLs. The increased expression of the VTL genes was most pronounced in plants grown under sufficient Fe (Fig. 17). We speculated that the over-expression of *IMA1* led to an increased expression of VTL genes, so that, in the double overexpressing lines no further effect of VTL expression in seed Fe content was observed. The cause of the reduced Fe content in seedlings, leaves and roots of the double over-expression compared to IMA1 OE plants is at present enigmatic. IMA1 has been reported to be unstable (Grillet et al. 2018). This instability

of IMA1 might be part of a negative feedback regulation of Fe uptake initiated by phloem Fe in plants growing under Fe sufficient conditions. The over-expression of VTL genes might have disrupted this regulation.

5.4 Bio-Fortification by Double Over-Expression of *NAS3* and *VTL5*

NA is an important component for Fe hemostasis in plants. In monocotyledon plants, NA is a precursor for phytosiderophores. Phytosiderophores are important for Fe uptake in strategy II plants. In both strategy I and II plants, NA plays an important role as Fe chelate in phloem and as a sensor for Fe availability (Koen et al. 2013). NA is synthesized from three S-adenosyl-methionine molecules by the enzyme NA synthase (Zhou et al. 2013). Genome analyses show that there are 3 NAS genes in rice, 4 in Arabidopsis, 9 in barley and 5 in maize (Zhou et al. 2013). *NAS1* and *NAS2* are located on chromosome 5, while *NAS3* and *NAS4* are located on chromosome 1 (Bauer and Schuler, 2011). With three amino and three carboxyl groups, the NA molecule forms a hexadentate chelate to a metal ion with an affinity series of $Mn > Fe^{2+} > Co > Zn > Ni > Cu > Fe^{3+}$. However, depending on the pH in for example the phloem and xylem the affinity series can change. For example in xylem, NA is a Cu chelator and can translocate Cu from the root to the shoot. In the phloem sap NA is a candidate for loading and unloading of Cu, Fe and Zn (Curie et al., 2009). The over-expression of ZINC-INDUCED FACILITATOR 1 (ZIF1) in Arabidopsis increased the amount of NA in the roots and shoots and led to Fe deficiency. ZIF1 is a vacuolar-localized putative transporter required for Zn tolerance that is hypothesized to transport NA from the cytoplasm into the vacuole. ENA is a member of the MFS family and is a homologue of ZIF1 in rice. Both transport NA into the vacuole (Haydon et al. 2012; Nozoye et al. 2011).

In transgenic rice the triple over-expression of bean ferritin, Arabidopsis *NAS1* and *Aspergillus* phytase genes led to a 6-fold increase in seed Fe (Wirth et al. 2009). We proposed that by double over-expressing *VTL5* and *NAS3*, the Fe content might be increased in seeds by storage in the vacuole (Fig. 29). As shown in Fig. 3 the *VTL5* OE lines contained significantly greater Fe content compared to the WT. Therefore, for further investigations a *VTL5* OE was selected and crossed with *NAS3* OE lines. These double overexpressing plants were analyzed for Fe content.

The results revealed that in the *NAS3* OE lines, the NA content was increased by approximately 40%. The Fe content in seeds of *NAS3* OE lines and the *VTL5* OE line was significantly increased by approximately 50% compared to the WT. However, in the double over-expressing *VTL5*-*NAS3* lines there was no improvement in seed Fe content above the single over-expression (Fig. 20). Leaves of the *VTL5* OE line contained notably greater Fe, but in the *NAS3*

OE and *VTL5-NAS* double over-expressing lines, Fe content was lower compared to the WT (Fig. 20). Regardless of the Fe concentration in the growth medium or the organ selected for analysis, a synergistic effect of double over-expression was not observed.

An analysis of FCR activity as well as the Fe homeostasis genes was conducted to identify potential effects of the over-expression of *NAS3* and *VTL5*. In general, we observed no consistent effect of *VTL5-NAS3* double over-expressing lines in addition to the effect observed in single over-expression of these genes. The lack of a synergistic effect could be explained by two observations. Firstly, over-expression of *NAS3* under Fe sufficiency was correlated with an increase expression of *VTL5*. Thus, as with the over-expression of *IMA1* discussed above, single over-expression of *NAS3* may have resulted in increased expression of all VTLs. Secondly, although NA content was increase in *NAS3* single over-expression plants, the NA content was unchanged compared to the WT in the double over-expressing plants. This observation was in spite of the fact, that the *NAS3* expression was greatly increased in double over-expression plants. Thus, the question of a synergistic effect between *VTL5* and *NAS3* over-expression on Fe accumulation remained unanswered.

5.5 Conclusions

Our work has shown that the over-expression of the genes in the VTL family resulted in increased Fe content in Arabidopsis seeds. The increased Fe was visualized primarily in the pro-vascular cells in the embryo and corresponded to the same location as has been attributed to Fe storage by the VIT1 Fe transporter. Although over-expression of the VTL genes resulted in increased Fe storage, the primary regulator of the storage location was the VIT1 transporter. The expression of genes encoding proteins involved in the Fe deficiency response in strategy I plants was reduced when grown under Fe deficiency and increased under Fe sufficiency compared to the WT. These data were interpreted as an increased Fe sink strength in Fe-sufficient plants, which resulted in high demand and uptake of Fe. Under Fe deficient growth conditions, the increased Fe in the VTL over-expressing plants decreased the demand for Fe uptake, and thus resulted in lower expression of Fe-responsive genes.

An increase in Fe content in Arabidopsis was also achieved by over-expression of *IMA1*. *IMA1* encoded a Fe-binding regulatory protein and was found in all angiosperm plants. The expression of *IMA1* was greatly increased under Fe deficiency, and the Fe in the over-expressing plants was significantly increased over the WT. A transcriptional analysis showed that genes encoding components of the Fe-deficiency were greatly induced compared to the WT. This induction was present both under Fe-sufficient and –deficient growth condition; although, the difference

between the over-expressing plants and the WT was greatest in plants grown on sufficient Fe. Double over-expression the VTL genes and *IMA1* showed no synergistic effect. The likely cause of this observation was the induction of VTL expression in the *IMA1* OE line.

Finally, the over-expressing *NAS3* resulted in increased NA content Fe content in Arabidopsis seed, thus confirming reports in the literature. Attempts to further increase Fe content by double over-expression of *VTL5* and *NAS3* were unsuccessful. We found no synergetic effect on Fe content by *VTL5*-*NAS3* double over-expression. Although both genes were greatly over-expressed in the transgenic lines compared to the WT, the NA content showed no difference compared to the WT. Thus, the utility of combining VTL5 and NAS3 over-expression to increase Fe content remains an open question.

In this dissertation we have demonstrated that over-expression of the VTL gene provided an additional method for manipulation of the Fe content in plants that may have applications for biofortification in the future.

6 References

Adkins, S. & Burmeister, M., 1996. Visualization of DNA in agarose gels as migrating colored bands: applications for preparative gels and educational demonstrations. Analytical Biochemistry, 240(1), pp.17–23.

Aparicio, F., and V. Pallás. 2017. The coat protein of Alfalfa mosaic virus interacts and interferes with the transcriptional activity of the bHLH transcription factor ILR3 promoting salicylic acid-dependent defence signalling response. Molecular Plant Pathology 18:173–186.

Bastow, E. L., V. S. Garcia de la Torre, A. E. Maclean, R. T. Green, S. Merlot, S. Thomine, and J. Balk. 2018. Vacuolar Iron Stores Gated by NRAMP3 and NRAMP4 Are the Primary Source of Iron in Germinating Seeds. Plant Physiology 177:1267–1276.

Bauer, P., and M. Schuler. 2011. Heavy Metals Need Assistance: The Contribution of Nicotianamine to Metal Circulation Throughout the Plant and the Arabidopsis NAS Gene Family. Frontiers in Plant Science 2.

Becker, D., E. Kemper, J. Schell, and R. Masterson. 1992. "New Plant Binary Vectors with Selectable Markers Located Proximal to the Left T-DNA Border." Plant Molecular Biology 20 (6): 1195–97.

Blancquaert, D., H. Steur, X. Gellynck, and D. Der Straeten. 2017. Metabolic engineering of micronutrients in crop plants. Annals of the New York Academy of Sciences 1390:59–73.

Briat, JF, I Fobis-Loisy, N Grignon, S Lobréaux, N Pascal, G Savino, S Thoiron, N Wirèn, and O Van Wuytswinkel. 1995. "Cellular and Molecular Aspects of Iron Metabolism in Plants.," no. 84: 69–81.

Briat, J.-F., C. Dubos, and F. Gaymard. 2015. Iron nutrition, biomass production, and plant product quality. Trends in Plant Science 20:33–40.

Buckhout, T. J., and W. Schmidt. 2013. Iron in Plants. Page Encyclopedia of Life Science (eLS). John Wiley & Sons, Ltd.

Buckhout, T. J., T. J. Yang, and W. Schmidt. 2009. Early iron-deficiency-induced transcriptional changes in Arabidopsis roots as revealed by microarray analyses. BMC Genomics 10:147.

Cassin, G., S. Mari, C. Curie, J.-F. Briat, and P. Czernic. 2009. Increased sensitivity to iron deficiency in Arabidopsis thaliana overaccumulating nicotianamine. Journal of Experimental Botany 60:1249–1259.

Chaney, R. L., J. C. Brown, and L. O. Tiffin. 1972. Obligatory reduction of ferric chelates in iron uptake by soybeans. Plant Physiology 50:208–213.

Chang S., Kim B., Kang B., Kim D., and Nam H. 1994. “Stable Genetic Transformation of Arabidopsis Thaliana by Agrobacterium Inoculation in Planta,” 5(4), , 551–58.

Clemens, S., and M. Weber. 2016. The essential role of coumarin secretion for Fe acquisition from alkaline soil. Plant Signaling & Behavior 11:e1114197.

Colangelo, E. P., and M. L. Guerinot. 2004. The essential basic helix-loop-helix protein FIT1 is required for the iron deficiency response. The Plant Cell 16:3400–3412.

Connorton, J. M., J. Balk, and J. Rodríguez-Celma. 2017. Iron homeostasis in plants - a brief overview. Metallomics: Integrated Biometal Science 9:813–823.

Conte, S. S., H. H. Chu, D. C. Rodriguez, T. Punshon, K. A. Vasques, D. E. Salt, and E. L. Walker. 2013. Arabidopsis thaliana Yellow Stripe1-Like4 and Yellow Stripe1-Like6 localize to internal cellular membranes and are involved in metal ion homeostasis. Frontiers in Plant Science 4:283.

Curie, C., and J.-F. Briat. 2003. Iron Transport and Signaling in Plants. Annual Review of Plant Biology 54:183–206.

Curie, C., G. Cassin, D. Couch, F. Divol, K. Higuchi, M. Le Jean, J. Misson, A. Schikora, P. Czernic, and S. Mari. 2009. Metal movement within the plant: contribution of nicotianamine and yellow stripe 1-like transporters. Annals of Botany 103:1–11.

Curie, C., Z. Panaviene, C. Loulergue, S. L. Dellaporta, J. F. Briat, and E. L. Walker. 2001. Maize yellow stripe1 encodes a membrane protein directly involved in Fe(III) uptake. Nature 409:346–349.

De Benoist, B., World Health Organization, and Centers for Disease Control and Prevention (U.S.). 2008. Worldwide prevalence of anaemia 1993-2005 of: WHO Global Database of anaemia. World Health Organization, Geneva.

Dell'Orto, M., S. Santi, P. De Nisi, S. Cesco, Z. Varanini, G. Zocchi, and R. Pinton. 2000. Development of Fe-deficiency responses in cucumber (Cucumis sativus L.) roots: involvement of plasma membrane H(+)-ATPase activity. Journal of Experimental Botany 51:695–701.

Douchkov, D., C. Gryczka, U. W. Stephan, R. Hell, and H. Bäumlein. 2005. Ectopic expression of nicotianamine synthase genes results in improved iron accumulation and increased nickel tolerance in transgenic tobacco. Plant, Cell & Environment 28:365–374.

Drakakaki, G., P. Christou, and E. Stöger. 2000. Constitutive expression of soybean ferritin cDNA in transgenic wheat and rice results in increased iron levels in vegetative tissues but not in seeds. Transgenic Research 9:445–452.

Eide, D., M. Broderius, J. Fett, and M. L. Guerinot. 1996. A novel iron-regulated metal transporter from plants identified by functional expression in yeast. Proceedings of the National Academy of Sciences of the United States of America 93:5624–5628.

Estelle & Somerville. (1987). Auxin-resistant mutants of *Arabidopsis thaliana* with an altered morphology. Mol. & General Gen , 200 - 206.

Fourcroy, P., N. Tissot, F. Gaymard, J.-F. Briat, and C. Dubos. 2016. Facilitated Fe Nutrition by Phenolic Compounds Excreted by the Arabidopsis ABCG37/PDR9 Transporter Requires the IRT1/FRO2 High-Affinity Root Fe(2+) Transport System. Molecular Plant 9:485–488.

Gollhofer, J. 2015. Identifizierung und Untersuchung der VTL Eisentransporter in Arabidopsis thaliana. Dissertation. Humboldt Universität zu Berlin.

Gollhofer, J., C. Schläwicke, N. Jungnick, W. Schmidt, and T. J. Buckhout. 2011. Members of a small family of nodulin-like genes are regulated under iron deficiency in roots of Arabidopsis thaliana. Plant physiology and biochemistry: PPB 49:557–564.

Gollhofer, J., R. Timofeev, P. Lan, W. Schmidt, and T. J. Buckhout. 2014. Vacuolar-Iron-Transporter1-Like proteins mediate iron homeostasis in Arabidopsis. PloS One 9:e110468.

Goto, F., T. Yoshihara, N. Shigemoto, S. Toki, and F. Takaiwa. 1999. Iron fortification of rice seed by the soybean ferritin gene. Nature Biotechnology 17:282–286.

Grillet, L., P. Lan, W. Li, G. Mokkapati, and W. Schmidt. 2018. IRON MAN is a ubiquitous family of peptides that control iron transport in plants. Nature Plants.

Gruber, B. D., R. F. H. Giehl, S. Friedel, and N. von Wirén. 2013. Plasticity of the Arabidopsis root system under nutrient deficiencies. Plant Physiology 163:161–179.

Hakoyama, T., K. Niimi, T. Yamamoto, S. Isobe, S. Sato, Y. Nakamura, S. Tabata, H. Kumagai, Y. Umehara, K. Brossuleit, T. R. Petersen, N. Sandal, J. Stougaard, M. K. Udvardi, M. Tamaoki, M. Kawaguchi, H. Kouchi, and N. Suganuma. 2012. The Integral Membrane

Protein SEN1 is Required for Symbiotic Nitrogen Fixation in Lotus japonicus Nodules. Plant and Cell Physiology 53:225–236.

Hanahan, D. 1983. “Studies on Transformation of Escherichia Coli with Plasmids.” Journal of Molecular Biology 166 (4): 557–80.

Haydon, M. J., M. Kawachi, M. Wirtz, S. Hillmer, R. Hell, and U. Krämer. 2012a. Vacuolar nicotianamine has critical and distinct roles under iron deficiency and for zinc sequestration in Arabidopsis. The Plant Cell 24:724–737.

Herbik, A., G. Koch, H. P. Mock, D. Dushkov, A. Czihal, J. Thielmann, U. W. Stephan, and H. Bäumlein. 1999. Isolation, characterization and cDNA cloning of nicotianamine synthase from barley. A key enzyme for iron homeostasis in plants. European Journal of Biochemistry 265:231–239.

Hindt, M. N., G. Z. Akmakjian, K. L. Pivarski, T. Punshon, I. Baxter, D. E. Salt, and M. L. Guerinot. 2017. BRUTUS and its paralogs, BTS LIKE1 and BTS LIKE2, encode important negative regulators of the iron deficiency response in Arabidopsis thaliana. Metallomics: Integrated Biometal Science 9:876–890.

Hirayama, T., G. J. Lei, N. Yamaji, N. Nakagawa, and J. F. Ma. 2018. The Putative Peptide Gene FEP1 Regulates Iron Deficiency Response in Arabidopsis. Plant and Cell Physiology 59:1739–1752.

Ivanov, R., T. Brumbarova, and P. Bauer. 2012. Fitting into the harsh reality: regulation of iron-deficiency responses in dicotyledonous plants. Molecular Plant 5:27–42.

Jeong, J., A. Merkovich, M. Clyne, and E. L. Connolly. 2017. Directing iron transport in dicots: regulation of iron acquisition and translocation. Current Opinion in Plant Biology 39:106–113.

Jin, C. W., G. Y. You, Y. F. He, C. Tang, P. Wu, and S. J. Zheng. 2007. Iron deficiency-induced secretion of phenolics facilitates the reutilization of root apoplastic iron in red clover. Plant Physiology 144:278–285.

Jin C. W., Du S. T., Zhang Y. S., Lin X. Y., Tang C. X. (2009). Differential regulatory role of nitric oxide in mediating nitrate reductase activity in roots of tomato (Solanum lycocarpum). Ann. Bot. 104 9–17. 10.1093/aob/mcp087

Kim, S. A., and M. L. Guerinot. 2007. Mining iron: iron uptake and transport in plants. FEBS letters 581:2273–2280.

Kim, S. A., T. Punshon, A. Lanzirotti, L. Li, J. M. Alonso, J. R. Ecker, J. Kaplan, and M. L. Guerinot. 2006. Localization of Iron in Arabidopsis Seed Requires the Vacuolar Membrane Transporter VIT1. Science 314:1295–1298.

Klatte, M., M. Schuler, M. Wirtz, C. Fink-Straube, R. Hell, and P. Bauer. 2009. The Analysis of Arabidopsis Nicotianamine Synthase Mutants Reveals Functions for Nicotianamine in Seed Iron Loading and Iron Deficiency Responses. Plant Physiology 150:257–271.

Kobayashi, T., R. N. Itai, M. S. Aung, T. Senoura, H. Nakanishi, and N. K. Nishizawa. 2012. The rice transcription factor IDEF1 directly binds to iron and other divalent metals for sensing cellular iron status. The Plant Journal: For Cell and Molecular Biology 69:81–91.

Kobayashi, T., S. Nagasaka, T. Senoura, R. N. Itai, H. Nakanishi, and N. K. Nishizawa. 2013. Iron-binding haemerythrin RING ubiquitin ligases regulate plant iron responses and accumulation. Nature Communications 4:2792.

Kobayashi, T., and N. K. Nishizawa. 2012. Iron uptake, translocation, and regulation in higher plants. Annual Review of Plant Biology 63:131–152.

Kobayashi, T., M. Suzuki, H. Inoue, R. N. Itai, M. Takahashi, H. Nakanishi, S. Mori, and N. K. Nishizawa. 2005. Expression of iron-acquisition-related genes in iron-deficient rice is co-ordinately induced by partially conserved iron-deficiency-responsive elements. Journal of Experimental Botany 56:1305–1316.

Koen, E., A. Besson-Bard, C. Duc, J. Astier, A. Gravot, P. Richaud, O. Lamotte, J. Boucherez, F. Gaymard, and D. Wendehenne. 2013. Arabidopsis thaliana nicotianamine synthase 4 is required for proper response to iron deficiency and to cadmium exposure. Plant Science: An International Journal of Experimental Plant Biology 209:1–11.

Lanquar, V., F. Lelièvre, S. Bolte, C. Hamès, C. Alcon, D. Neumann, G. Vansuyt, C. Curie, A. Schröder, U. Krämer, H. Barbier-Brygoo, and S. Thomine. 2005. Mobilization of vacuolar iron by AtNRAMP3 and AtNRAMP4 is essential for seed germination on low iron. The EMBO journal 24:4041–4051.

Lee, H.-J., N. Mochizuki, T. Masuda, and T. J. Buckhout. 2012a. Disrupting the bimolecular binding of the haem-binding protein 5 (AtHBP5) to haem oxygenase 1 (HY1) leads to oxidative stress in Arabidopsis. Journal of Experimental Botany 63:5967–5978.

Lee, S., U. S. Jeon, S. J. Lee, Y.-K. Kim, D. P. Persson, S. Husted, J. K. Schjorring, Y. Kakei, H. Masuda, N. K. Nishizawa, and G. An. 2009. Iron fortification of rice seeds through activation of the nicotianamine synthase gene. Proceedings of the National Academy of Sciences 106:22014–22019.

Lee, S., Y.-S. Kim, U. S. Jeon, Y.-K. Kim, J. K. Schjoerring, and G. An. 2012. Activation of Rice nicotianamine synthase 2 (OsNAS2) enhances iron availability for biofortification. Molecules and Cells 33:269–275.

Lei, X. G., J. D. Weaver, E. Mullaney, A. H. Ullah, and M. J. Azain. 2013. Phytase, a new life for an “old” enzyme. Annual Review of Animal Biosciences 1:283–309.

Li, L., O. S. Chen, D. McVey Ward, and J. Kaplan. 2001. CCC1 is a transporter that mediates vacuolar iron storage in yeast. The Journal of Biological Chemistry 276:29515–29519.

Li, X., H. Zhang, Q. Ai, G. Liang, and D. Yu. 2016. Two bHLH Transcription Factors, bHLH34 and bHLH104, Regulate Iron Homeostasis in *Arabidopsis thaliana*. Plant Physiology 170:2478–2493.

Lingam, S., Mohrbacher, J., Brumbarova, T., Potuschak, T, and Fin, C. 2011. Interaction between the bHLH Transcription Factor FIT and ETHYLENE INSENSITIVE3/ETHYLENE INSENSITIVE3-LIKE1 Reveals Molecular Linkage between the Regulation of Iron Acquisition and Ethylene Signaling in *Arabidopsis*. The Plant Cell, Vol. 23: 1815–1829.

Long, T. A., H. Tsukagoshi, W. Busch, B. Lahner, D. E. Salt, and P. N. Benfey. 2010. The bHLH transcription factor POPEYE regulates response to iron deficiency in Arabidopsis roots. The Plant Cell 22:2219–2236.

Marschner, H., V. Römheld, and M. Kissel. 1986. Different strategies in higher plants in mobilization and uptake of iron. Journal of Plant Nutrition 9:695–713.

Mary, V., M. Schnell Ramos, C. Gillet, A. L. Socha, J. Giraudat, A. Agorio, S. Merlot, C. Clairet, S. A. Kim, T. Punshon, M. L. Guerinot, and S. Thomine. 2015. Bypassing Iron Storage in Endodermal Vacuoles Rescues the Iron Mobilization Defect in the natural resistance associated-macrophage protein3natural resistance associated-macrophage protein4 Double Mutant. Plant Physiology 169:748–759.

Meiser, J., S. Lingam, and P. Bauer. 2011. Posttranslational regulation of the iron deficiency basic helix-loop-helix transcription factor FIT is affected by iron and nitric oxide. Plant Physiology 157:2154–2166.

Milner, M. J., J. Seamon, E. Craft, and L. V. Kochian. 2013. Transport properties of members of the ZIP family in plants and their role in Zn and Mn homeostasis. Journal of Experimental Botany 64:369–381.

Mita S, Hirano H, Nakamura K. 1997. Negative regulation in the expression of a sugar-inducible gene in Arabidopsis thaliana. Plant Physiol 114: 575–582

Momonoi, K., K. Yoshida, S. Mano, H. Takahashi, C. Nakamori, K. Shoji, A. Nitta, and M. Nishimura. 2009. A vacuolar iron transporter in tulip, TgVit1, is responsible for blue coloration in petal cells through iron accumulation. The Plant Journal: For Cell and Molecular Biology 59:437–447.

Moog et al. 1995. Responses to iron deficiency in Arabidopsis thaliana:The Turbo iron reductase does not depend on the formation of root hairs and transfer cells. Planta , 505 - 513.

Morrissey, J., I. R. Baxter, J. Lee, L. Li, B. Lahner, N. Grotz, J. Kaplan, D. E. Salt, and M. L. Guerinot. 2009. The ferroportin metal efflux proteins function in iron and cobalt homeostasis in Arabidopsis. The Plant Cell 21:3326–3338.

Naranjo-Arcos, M. A., F. Maurer, J. Meiser, S. Pateyron, C. Fink-Straube, and P. Bauer. 2017. Dissection of iron signaling and iron accumulation by overexpression of subgroup Ib bHLH039 protein. Scientific Reports 7.

Narayanan, N., G. Beyene, R. D. Chauhan, E. Gaitán-Solis, M. A. Grusak, N. Taylor, and P. Anderson. 2015. Overexpression of Arabidopsis VIT1 increases accumulation of iron in cassava roots and stems. Plant Science: An International Journal of Experimental Plant Biology 240:170–181.

Nechushtai, R., A. R. Conlan, Y. Harir, L. Song, O. Yogev, Y. Eisenberg-Domovich, O. Livnah, D. Michaeli, R. Rosen, V. Ma, Y. Luo, J. A. Zuris, M. L. Paddock, Z. I. Cabantchik, P.

A. Jennings, and R. Mittler. 2012. Characterization of Arabidopsis NEET Reveals an Ancient Role for NEET Proteins in Iron Metabolism. The Plant Cell 24:2139–2154.

Nozoye, T., S. Nagasaka, T. Kobayashi, M. Takahashi, Y. Sato, Y. Sato, N. Uozumi, H. Nakanishi, and N. K. Nishizawa. 2011. Phytosiderophore efflux transporters are crucial for iron acquisition in graminaceous plants. The Journal of Biological Chemistry 286:5446–5454.

Oliva, N., P. Chadha-Mohanty, S. Poletti, E. Abrigo, G. Atienza, L. Torrizo, R. Garcia, C. Dueñas, M. A. Poncio, J. Balindong, M. Manzanilla, F. Montecillo, M. Zaidem, G. Barry, P. Hervé, H. Shou, and I. H. Slamet-Loedin. 2014. Large-scale production and evaluation of marker-free indica rice IR64 expressing phytoferritin genes. Molecular Breeding: New Strategies in Plant Improvement 33:23–37.

Palmer, C. M., M. N. Hindt, H. Schmidt, S. Clemens, and M. L. Guerinot. 2013a. MYB10 and MYB72 are required for growth under iron-limiting conditions. PLoS genetics 9:e1003953.

Perera, I., S. Seneweera, and N. Hirotsu. 2018. Manipulating the Phytic Acid Content of Rice Grain Toward Improving Micronutrient Bioavailability. Rice11:4, 11-13.

Petit, J. M., J. F. Briat, and S. Lobréaux. 2001. Structure and differential expression of the four members of the Arabidopsis thaliana ferritin gene family. Biochemical Journal 359:575–582.

Pich, A., and G. Scholz. 1996. Translocation of copper and other micronutrients in tomato plants (Lycopersicon esculentum Mill.): nicotianamine-stimulated copper transport in the xylem. Journal of Experimental Botany 47:41–47.

Porra et al. (1989). Determination of accurate extinction coefficients and simultaneous equations for assaying chlorophylls a and b extracted with four different solvents:

verification of the concentration of chlorophyll standards by atomic absorption spectroscopy. Biochimica et BiophysicaActa , 975, pp. 384 - 394.

Qu, L. Q., T. Yoshihara, A. Ooyama, F. Goto, and F. Takaiwa. 2005. Iron accumulation does not parallel the high expression level of ferritin in transgenic rice seeds. Planta 222:225–233.

Raboy, V. 2001. Seeds for a better future: 'low phytate' grains help to overcome malnutrition and reduce pollution. Trends in Plant Science 6:458–462.

Rajniak, J., R. F. H. Giehl, E. Chang, I. Murgia, N. von Wirén, and E. S. Sattely. 2018. Biosynthesis of redox-active metabolites in response to iron deficiency in plants. Nature Chemical Biology 14:442–450.

Rampey, R. A., A. W. Woodward, B. N. Hobbs, M. P. Tierney, B. Lahner, D. E. Salt, and B. Bartel. 2006. An Arabidopsis basic helix-loop-helix leucine zipper protein modulates metal homeostasis and auxin conjugate responsiveness. Genetics 174:1841–1857.

Rauch, C., G. Christa, J. de Vries, C. Woehle, and S. B. Gould. 2017. Mitochondrial Genome Assemblies of Elysia timida and Elysia cornigera and the Response of Mitochondrion-Associated Metabolism during Starvation. Genome biology and evolution 9:1873–1879.

Reyt, G., S. Boudouf, J. Boucherez, F. Gaymard, and J.-F. Briat. 2015. Iron- and Ferritin-Dependent Reactive Oxygen Species Distribution: Impact on Arabidopsis Root System Architecture. Molecular Plant 8:439–453.

Robinson, N. J., C. M. Procter, E. L. Connolly, and M. L. Guerinot. 1999. A ferric-chelate reductase for iron uptake from soils. Nature 397:694–697.

Rodríguez-Celma, J., I. C. Pan, W. Li, P. Lan, T. J. Buckhout, and W. Schmidt. 2013. The transcriptional response of Arabidopsis leaves to Fe deficiency. Frontiers in Plant Science 4:276.

Römheld, V., and H. Marschner. 1986. Evidence for a specific uptake system for iron phytosiderophores in roots of grasses. Plant Physiology 80:175–180.

Roschzttardtz, H., G. Conéjéro, C. Curie, and S. Mari. 2009. Identification of the endodermal vacuole as the iron storage compartment in the Arabidopsis embryo. Plant Physiology 151:1329–1338.

Santi, S., and W. Schmidt. 2009. Dissecting iron deficiency-induced proton extrusion in Arabidopsis roots. The New Phytologist 183:1072–1084.

Schmidt, W., 1994. Root-mediated ferric reduction - responses to iron deficiency, exogenously induced changes in hormonal balance and inhibition of protein synthesis. Journal of Experimental Botany, 45(275), pp.725–731.

Schmidt, W., 1996. Influence of chromium(III) on root-associated Fe(III) reductase in Plantago lanceolata L. , 47(299), pp.805–810.

Schmidt W., Tittel J., Schikora A. (2000). Role of hormones in the induction of iron deficiency responses in Arabidopsis roots. Plant Physiol. 122 1109–1118. 10.1104/pp.122.4.1109.

Schmidt, W., and T. J. Buckhout. 2011. A hitchhiker's guide to the Arabidopsis ferrome. Plant physiology and biochemistry: PPB 49:462–470.

Schuler, M., R. Rellán-Álvarez, C. Fink-Straube, J. Abadía, and P. Bauer. 2012. Nicotianamine Functions in the Phloem-Based Transport of Iron to Sink Organs, in Pollen Development and Pollen Tube Growth in Arabidopsis. The Plant Cell 24:2380–2400

Selote, D., R. Samira, A. Matthiadis, J. W. Gillikin, and T. A. Long. 2015. Iron-Binding E3 Ligase Mediates Iron Response in Plants by Targeting Basic Helix-Loop-Helix Transcription Factors1[OPEN]. Plant Physiology 167:273–286.

Sivitz, A. B., V. Hermand, C. Curie, and G. Vert. 2012. Arabidopsis bHLH100 and bHLH101 control iron homeostasis via a FIT-independent pathway. PloS One 7:e44843.

Socha, A. L., and M. L. Guerinot. 2014. Mn-euvering manganese: the role of transporter gene family members in manganese uptake and mobilization in plants. Frontiers in Plant Science 5. 106.

Stevenson-Paulik, J., R. J. Bastidas, S.-T. Chiou, R. A. Frye, and J. D. York. 2005. Generation of phytate-free seeds in Arabidopsis through disruption of inositol polyphosphate kinases. Proceedings of the National Academy of Sciences of the United States of America 102:12612–12617.

Stringlis, I. A., K. Yu, K. Feussner, R. de Jonge, S. Van Bentum, M. C. Van Verk, R. L. Berendsen, P. A. H. M. Bakker, I. Feussner, and C. M. J. Pieterse. 2018. MYB72-dependent coumarin exudation shapes root microbiome assembly to promote plant health. Proceedings of the National Academy of Sciences of the United States of America 115:E5213–E5222.

Su, L.-W., S. H. Chang, M.-Y. Li, H.-Y. Huang, W.-N. Jane, and J.-Y. Yang. 2013. Purification and biochemical characterization of Arabidopsis At-NEET, an ancient iron-sulfur protein, reveals a conserved cleavage motif for subcellular localization. Plant Science: An International Journal of Experimental Plant Biology 213:46–54.

Suzuki, M., M. Takahashi, T. Tsukamoto, S. Watanabe, S. Matsuhashi, J. Yazaki, N. Kishimoto, S. Kikuchi, H. Nakanishi, S. Mori, and N. K. Nishizawa. 2006. Biosynthesis

and secretion of mugineic acid family phytosiderophores in zinc-deficient barley. The Plant Journal 48:85–97.

Takagi, S., K. Nomoto, and T. Takemoto. 1984. Physiological aspect of mugineic acid, a possible phytosiderophore of graminaceous plants. Journal of Plant Nutrition 7:469–477.

Takemoto, T., K. Nomoto, S. Fushiya, R. Ouchi, G. Kusano, H. Hikino, S. Takagi, Y. Matsuura, and M. Kakudo. 1978. Structure of Mugineic Acid, a New Amino Acid Possessing an Iron-Chelating Activity from Roots Washings of Water-Cultured Hordeum vulgare L. Proceedings of the Japan Academy, Series B 54:469–473.

Tsai, H. H., and W. Schmidt. 2017. Mobilization of Iron by Plant-Borne Coumarins. Trends in Plant Science 22:538–548.

Van der Ent, S., S. C. M. Van Wees, and C. M. J. Pieterse. 2009. Jasmonate signaling in plant interactions with resistance-inducing beneficial microbes. Phytochemistry 70:1581–1588.

Vert, G., N. Grotz, F. Dédaldéchamp, F. Gaymard, M. L. Guerinot, J.-F. Briat, and C. Curie. 2002. IRT1, an Arabidopsis transporter essential for iron uptake from the soil and for plant growth. The Plant Cell 14:1223–1233.

Von Wiren, N., S. Mori, H. Marschner, and V. Romheld. 1994. Iron Inefficiency in Maize Mutant ys1 (Zea mays L. cv Yellow-Stripe) Is Caused by a Defect in Uptake of Iron Phytosiderophores. Plant Physiology 106:71–77.

Wang, N., Y. Cui, Y. Liu, H. Fan, J. Du, Z. Huang, Y. Yuan, H. Wu, and H.-Q. Ling. 2013. Requirement and functional redundancy of Ib subgroup bHLH proteins for iron deficiency responses and uptake in Arabidopsis thaliana. Molecular Plant 6:503–513.

Waters, B. M., H.-H. Chu, R. J. DiDonato, L. A. Roberts, R. B. Eisley, B. Lahner, D. E. Salt, and E. L. Walker. 2006. Mutations in Arabidopsis Yellow Stripe-Like1 and Yellow Stripe-Like3 Reveal Their Roles in Metal Ion Homeostasis and Loading of Metal Ions in Seeds. Plant Physiology 141:1446–1458.

Wu, T.-Y., W. Gruissem, and N. K. Bhullar. 2018. Targeting intracellular transport combined with efficient uptake and storage significantly increases grain iron and zinc levels in rice. Plant Biotechnology Journal.

Yan, J. Y., C. X. Li, L. Sun, J. Y. Ren, G. X. Li, Z. J. Ding, and S. J. Zheng. 2016. A WRKY Transcription Factor Regulates Fe Translocation under Fe Deficiency. Plant Physiology 171:2017–2027.

Yang, A., and W.-H. Zhang. 2016. A Small GTPase, OsRab6a, is Involved in the Regulation of Iron Homeostasis in Rice. Plant & Cell Physiology 57:1271–1280.

Yang, T. J. W., W.-D. Lin, and W. Schmidt. 2010. Transcriptional Profiling of the Arabidopsis Iron Deficiency Response Reveals Conserved Transition Metal Homeostasis Networks. Plant Physiology 152:2130–2141.

Yuan, Y., H. Wu, N. Wang, J. Li, W. Zhao, J. Du, D. Wang, and H.-Q. Ling. 2008. FIT interacts with AtbHLH38 and AtbHLH39 in regulating iron uptake gene expression for iron homeostasis in *Arabidopsis*. Cell Research 18:385–397.

Zhang, J., B. Liu, M. Li, D. Feng, H. Jin, P. Wang, J. Liu, F. Xiong, J. Wang, and H.-B. Wang. 2015. The bHLH Transcription Factor bHLH104 Interacts with IAA-LEUCINE RESISTANT3 and Modulates Iron Homeostasis in Arabidopsis. The Plant Cell 27:787–805.

Zhang, Y., Y.-H. Xu, H.-Y. Yi, and J.-M. Gong. 2012. Vacuolar membrane transporters OsVIT1 and OsVIT2 modulate iron translocation between flag leaves and seeds in rice. The Plant Journal: For Cell and Molecular Biology 72:400–410.

Zheng, L., Z. Cheng, C. Ai, X. Jiang, X. Bei, Y. Zheng, R. P. Glahn, R. M. Welch, D. D. Miller, X. G. Lei, and H. Shou. 2010. Nicotianamine, a Novel Enhancer of Rice Iron Bioavailability to Humans. PLoS ONE 5.

Zhou, X., S. Li, Q. Zhao, X. Liu, S. Zhang, C. Sun, Y. Fan, C. Zhang, and R. Chen. 2013. Genome-wide identification, classification and expression profiling of nicotianamine synthase (NAS) gene family in maize. BMC genomics 14:238.

Zimmermann, M. B., and R. F. Hurrell. 2007. Nutritional iron deficiency. Lancet (London, England) 370:511–520.

7 Supplement

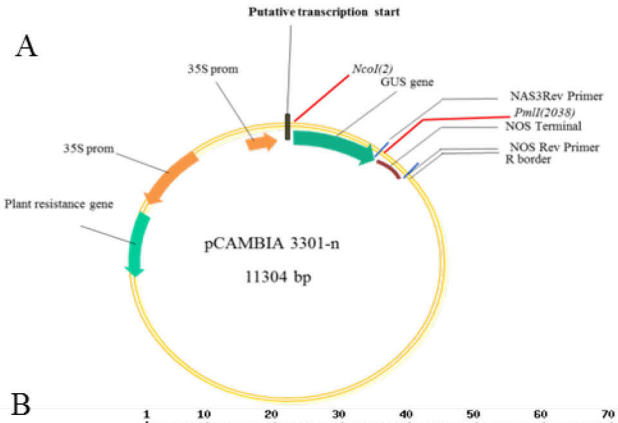

Fig.S1. Schematic illustration of the pCAMBIA 3301-n vector (A) and the nucleotide sequences of the cloned *AtNAS3* gene (B).

B

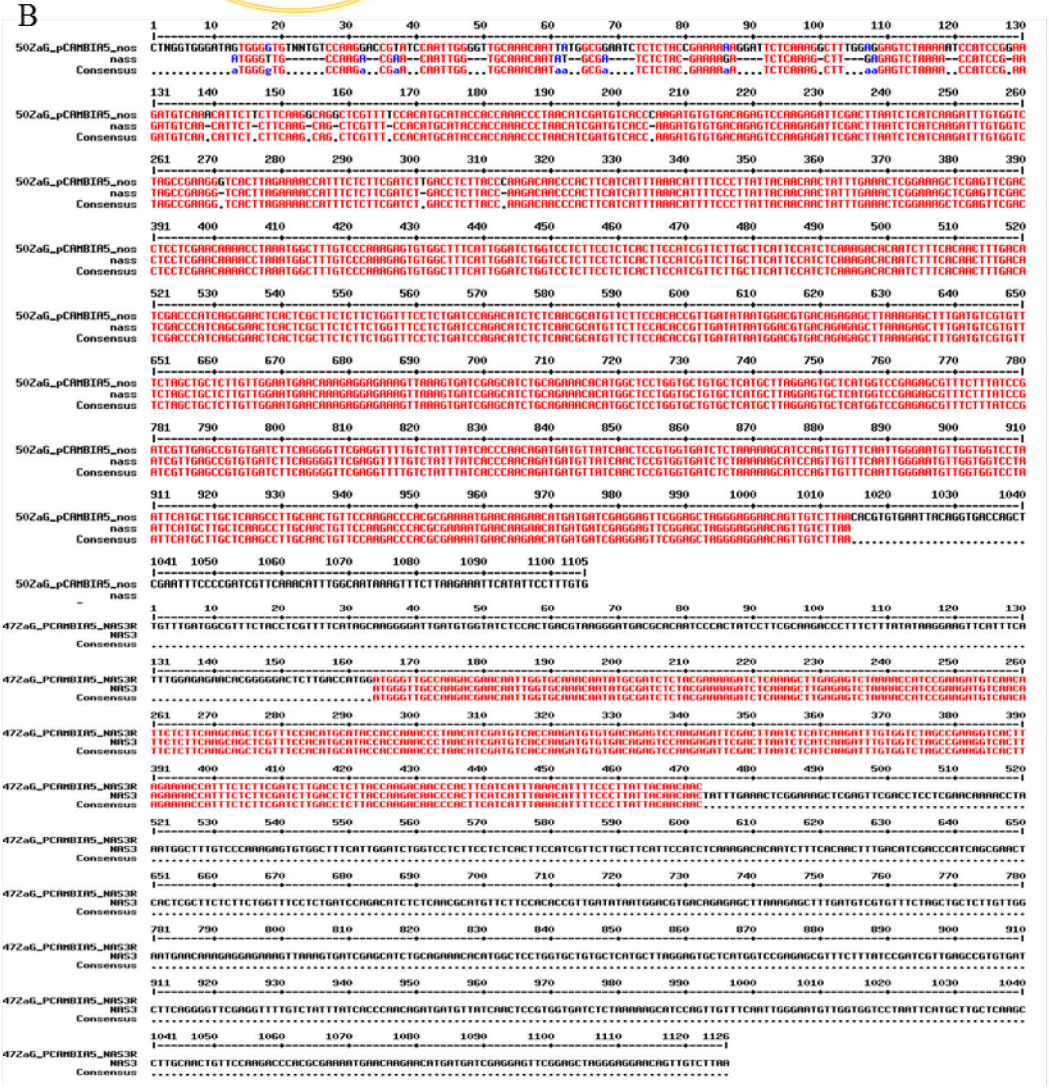

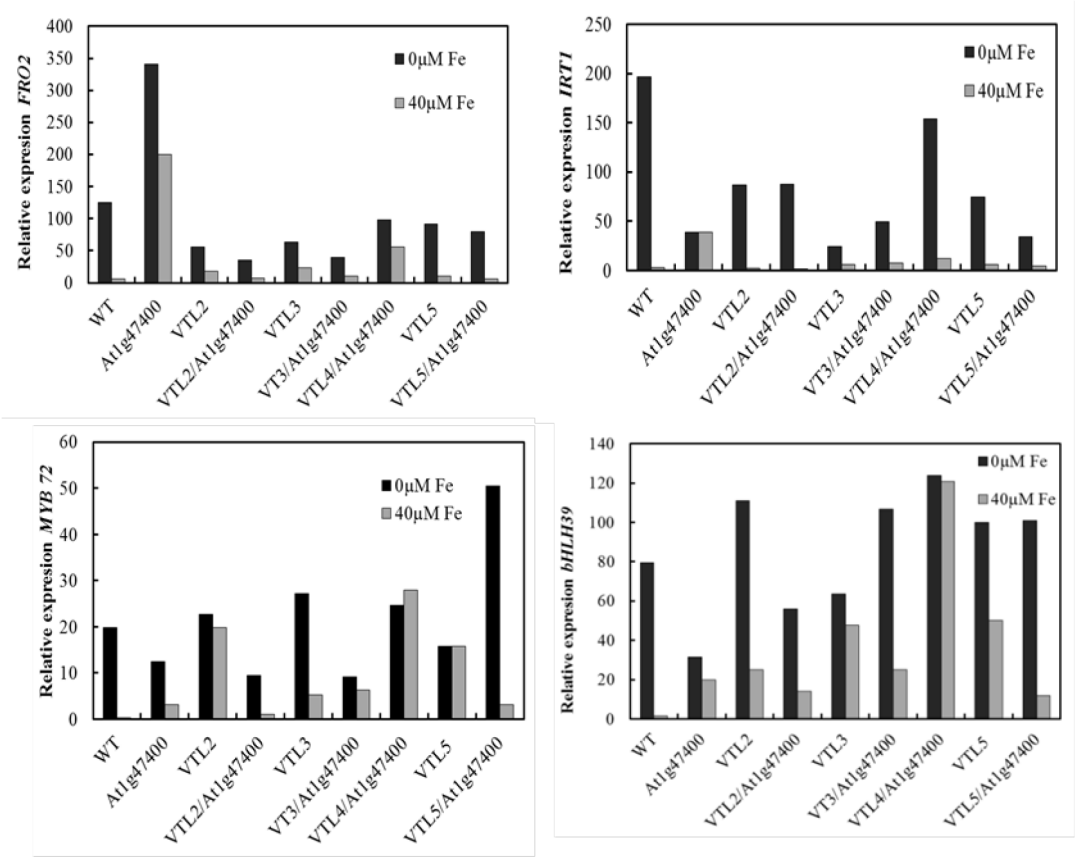

Fig. S2. qRT-PCR analysis of the Fe-deficiency regulated transcription factors, *FRO2*, *IRT1*, *MYB72* and *bHLH39* in At1g47400/VTL 2, 3, 4 and 5 over-expression lines. cDNA was synthesized from four week-old soil-grown plants. *ACTIN2* was used for standardization. The relative expression values are presented as $2^{-\Delta C(t)}$.

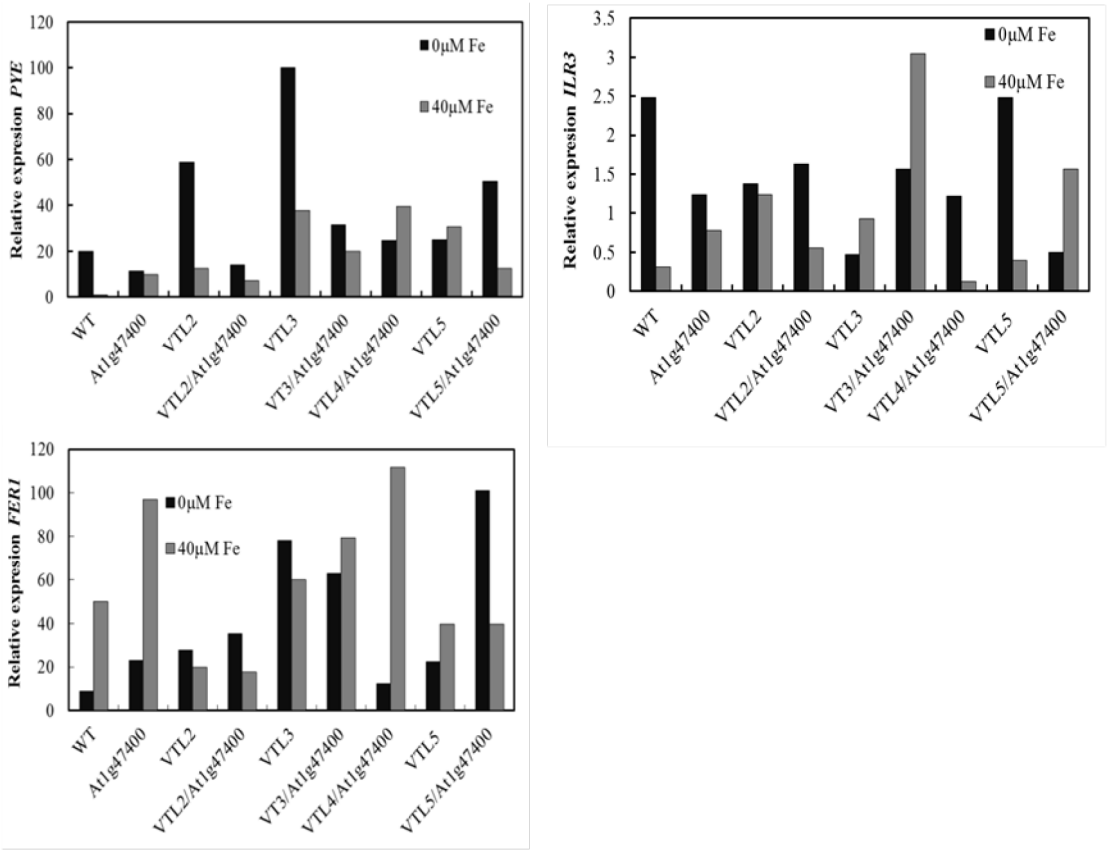

Fig. S3. qRT-PCR analysis of the Fe-deficiency regulated transcription factors, *PYE*, *ILR3* and *FER1* in At1g47400/VTL1, 2, 3, 4 and 5 over-expression lines. cDNA was synthesized from four week-old soil-grown plants. *ACTIN2* was used for standardization. The relative expression values are presented as $2^{-\Delta C(t)}$.

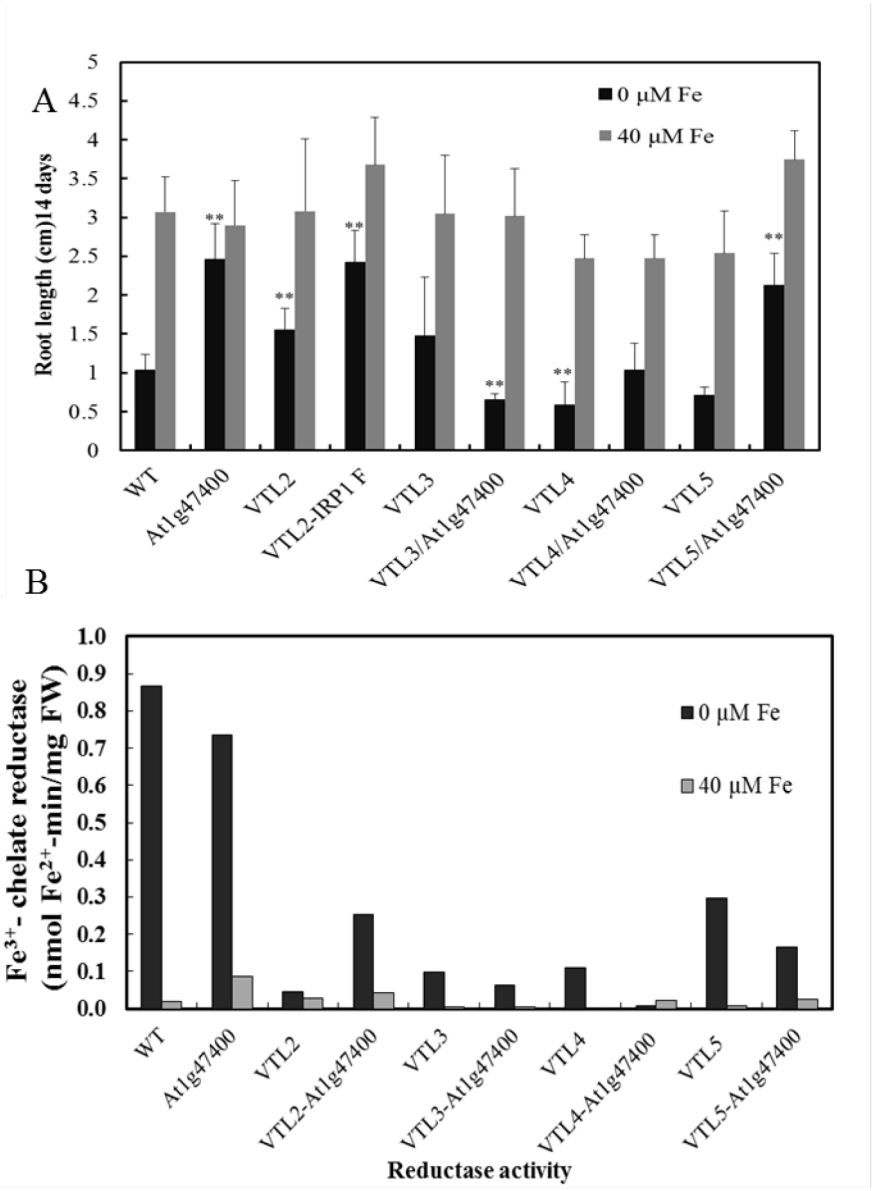

Fig. S4. The primary root length of over-expressing plants grown in 0 or 40 μM Fe determined after 14 d of growth (A). Reduction of Fe was determined after 10, 20 and 40 min. The activity was calculated by linear regression analysis with the Pearson correlation coefficient r2 > 0.9 for all measurements (B).

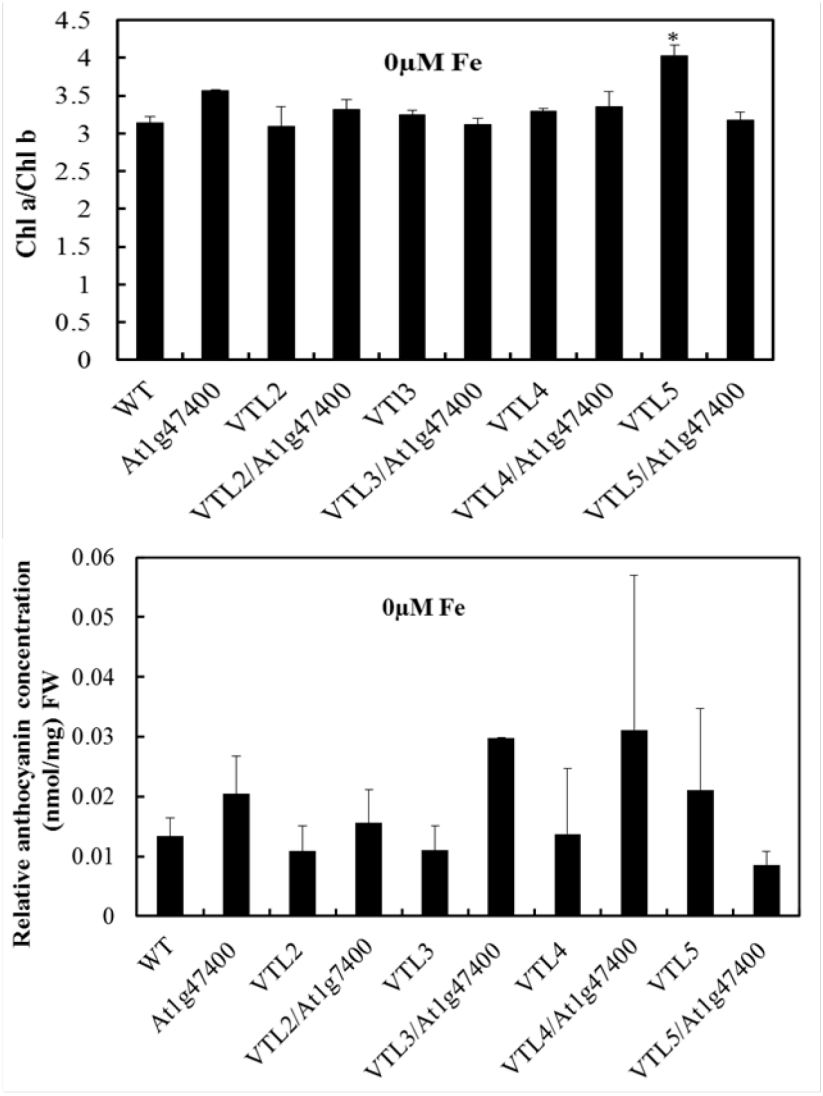

Fig. S5. Chlorophyll a/b ratio in WT and *VTL1*, *2*, *3*, *4* and *5-At1g47400* double over-expressed lines. Statistical significance in comparison to the WT was determined using an unpaired t-test with 3 replications (* $p < 0.05$) (A). (B) Relative anthocyanin expression in WT and VTL1, 2, 3, 4 and 5-At1g47400 double over-expressed lines.

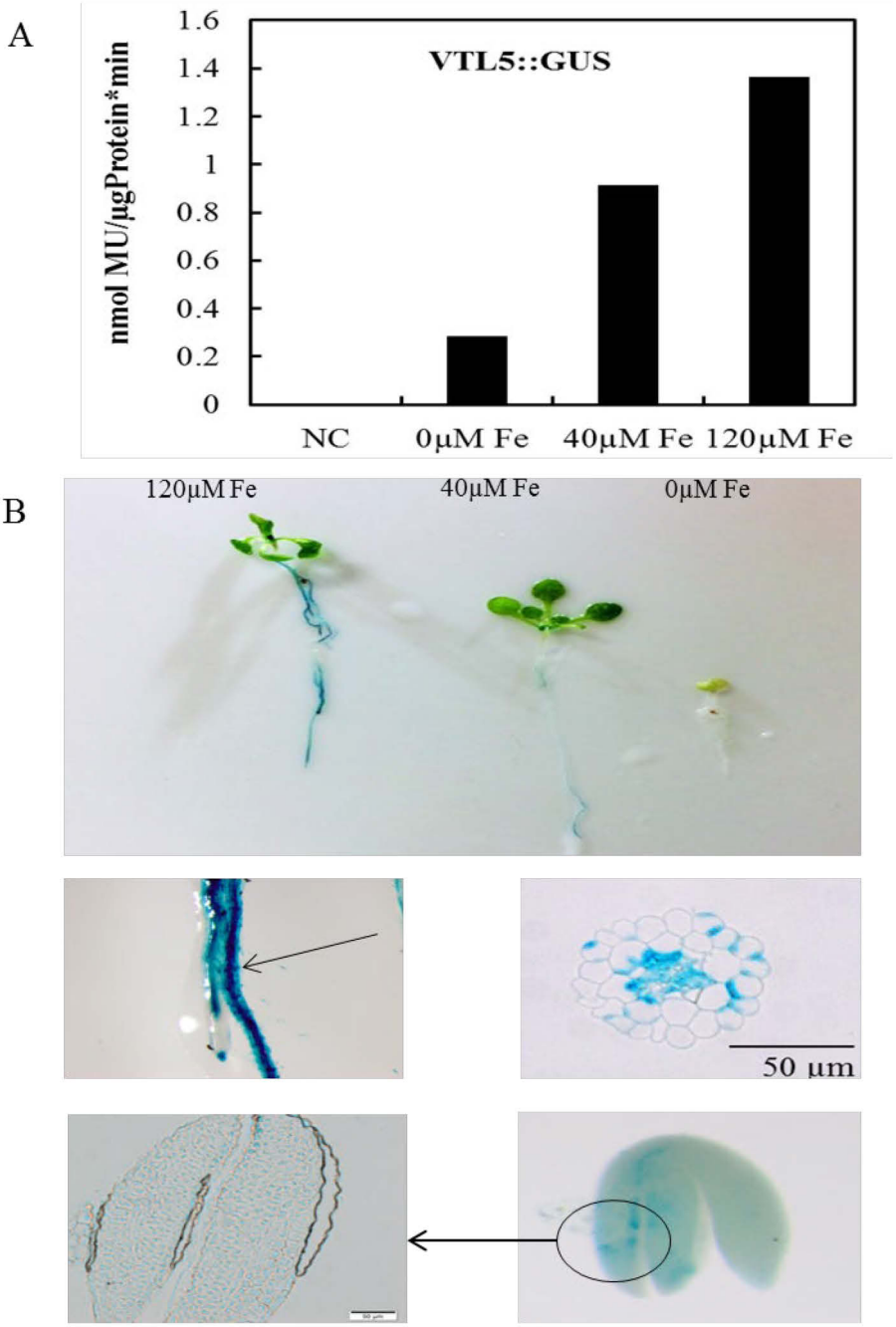

Fig.S6. GUS activity in Arabidopsis in of 0, 40 and 120 μM Fe (A), histochemical staining of GUS activity (B).

8 Acknowledgments

Firstly, I would like to express my sincere gratitude to my Supervisor Prof. Dr. Thomas Buckhout for the continuous support of my Ph.D study and related research, for his patience, motivation, and immense knowledge. His guidance helped me in all the time of research and writing of this thesis.

Besides my Supervisor, I would like to thank the rest of my thesis committee: Prof. Dr. Kurt Zoglauer, Prof. Dr. Simonette Santi for their insightful comments and encouragement, but also for the hard question which incented me to widen my research from various perspectives and my special thanks to Prof. Dr. Kerstin Kaufmann and PD Dr. Christina Kühn to accept my request to be committee member in my examination.

My sincere thanks also go to the Yousef Jameel Foundation and Biology institute (Kommission für Frauenförderung) that financially supported my Ph.D. Research, and appreciate Prof. Dr. von Wiren and Dr. Mohammadreza Hahirezaei at IPK and Prof. Dr. Carsten Lüter, Ms. Jutta Zeller and Ms. Anke Sänger in Naturkundemusem, who gave access to the laboratory and research facilities. Without they precious support it would not be possible to conduct this research. I appreciate Dr. Boris Hedtke for his valuable comment in cloning part of my work.

I thank our group member, In particular Mona Fechler for her kind role during my research and be a best friend, also thank Marion Dewender with her kind help as well as other students Helena Tran and Titus Hinze to help me doing my research. In addition, I thank my friends in the Botanik and Arboretum, Juliane Raschke and Dr. Andrea Rupps, for being the kind neighbor.

Finally, I would like to thank my family: my parents and to my brother and sisters and my omi for supporting me and encourage me to achieve my goals in my life and my omi and friends to support me in every situation of my education in Germany and especially their spiritually support throughout writing this thesis

9 EIGENSTÄNDIGKEITSERKLÄRUNG

Hiermit versichere ich, dass ich die vorliegende Masterarbeit erstmalig einreiche, selbständig verfasst und keine anderen als die angegebenen Quellen und Hilfsmittel verwendet habe.

Berlin, den 08.02.2019